Wax Characterisation by Instrumental Analysis

by

Glenda Vanessa Webber

B.Sc. (Hons) (*Potchefstroom University for C.H.E.)*

Thesis presented in partial fulfilment of the requirements for the degree of

Master of Science

at the

University of Stellenbosch

Study leader: Prof RD Sanderson

Institute for Polymer Science
Department of Chemistry

December 2000

DECLARATION

I, the undersigned, hereby declare that the work contained in this thesis is my own original work and has not previously, in its entirety or in part, been submitted at any university for a degree.

ABSTRACT

Various companies produce waxes, which are used extensively in various applications, either as produced or as chemically or physically modified value-added products. They are used in the traditional candle industry and applications including hot melt adhesives, inks, plastics, polishes and emulsions for rust prevention or fruit coating. Insight into the properties of these waxes is required to assist the applications chemist in understanding the role of the wax component in a specific formulation.

Analytical techniques such as differential scanning calorimetry (DSC), thermogravimetry (TG), rheometry, gel permeation chromatography (GPC), high temperature gas chromatography (HTGC) and infra-red spectroscopy (IR) were used to characterise Fischer Tropsch, polyethylene, natural and petroleum waxes. Property profiles were formulated by integrating the results from the various techniques. The results of traditional wax analyses (e.g. congealing point, melting point, penetration, density and viscosity) were also correlated to relevant analytical results obtained from the instrumental techniques. Structure-property relationships have been proposed.

OPSOMMING

Verskeie maatskappye vervaardig wasse, wat in menige toepassings gebruik word – of direk, of as chemies- of fisies- veranderde produkte van hoër waarde. Benewens die tradisionele kersbedryf, word die wasse in toepassings soos warmsmeltkleefmiddels, ink, plastiek, roeswerende- en vrugtebedekkings- emulsies en politoere gebruik. Wetenskaplikes betrokke by die formuleering van wasse vir verskillende toepassings sal baat vind by beter inligting van waseienskappe en die rol van waskomponente in formulasies.

Tegnieke, bv. differensialeskandeerkalorimetrie (DSC), termogravimetrie (TG), reologie, gelpermeasiechromotografie (GPC), hoëtemperatuurgaschromatografie (HTGC) en infra-rooispektroskopie (IR), is gebruik om Fischer Tropsch-, polietileen-, petroleum- en natuurlike-wasse te karakteriseer. Profile van waseienskappe is geformuleer deur die integrasie van die data verkry van die verskillende analitiese tegnieke. Die resultate van tradisionële wasanalises (bv. stolpunt, smeltpunt, penetrasie, digtheid, viskositeit en olie-inhoud) word ook in verband gebring met die resultate van die instrumentele analises. Verbande tussen struktuur en waseienskappe word ook voorgestel.

DEDICATION

To

Angus, Daniel and Luke

ACKNOWLEDGEMENTS

John Beigley, my colleague at Schümann Sasol, for his friendship, support and much respected advice.

Norman Dowler, formerly of Schümann Sasol, for the privilege of learning from him.

Prof. Ron Sanderson, my promoter, for allowing me the freedom to face the challenge of recording my many years of experience.

Dr. Margie Hurndall, of the Institute of Polymer Science, University of Stellenbosch, for her advice and encouragement.

Neeloshini Naidoo, Nirusha Gurupersaad, Ena Murray, Laetitia Michau, Carel Broekman, René Engelbrecht, Vesna Hrestak and Minette Roux, for assistance with analyses.

Table of Contents

List of Tables

List of Figures

List of Abbreviations

ARES	Advanced Rheometric Expansion system
DMA	dynamic mechanical analysis
DRI	differential refractive index
DSC	differential scanning calorimetry
DTG	differential thermogravimetry
FCO	forced convection oven
FID	flame ionisation detector
GLC	gas liquid chromatography
GPC	gel permeation chromatography
HDPE	high density polyethylene
HMA	hot melt adhesive
HPLC	high performance liquid chromatography
HTGC	high temperature gas chromatography
IR	infra-red spectroscopy
LC	liquid chromatography
LDPE	low density polyethylene
MEK	methyl ethyl ketone
MIBK	methyl iso-butyl ketone
MMD	molecular mass distribution
PE	polyethylene
TG	thermogravimetry/ thermogravimetric
TGA	thermogravimetric analysis/ analyser
TMA	thermomechanical analysis
XRD	X-ray diffraction

CHAPTER 1

INTRODUCTION

1.1 OVERVIEW OF WAX ORIGIN

Wax is as old as man. Beeswax was used by the ancient Egyptians to preserve mummies. Artists have sculpted with wax from very early times. It was customary to model in wax what they later desired to cut from stone or cast in bronze. The use of beeswax for anatomical studies was first practiced in Florence. Permanent wax models are found in the exhibition of wax works of Marie Tussaud in London. The term *wax* is derived from the Anglo-Saxon word *weax*, which refers to beeswax. Similar substances later found in plants became known as *weax* or *wachs*, and later *wax*. Today, the term is applied to all wax-like substances, regardless of their origin or method of preparation. [1]

There are two major classes, viz. natural and synthetic waxes. The natural waxes may be sub-classified as animal (e.g. beeswax, lanolin, shellac wax, Chinese insect wax); vegetable (carnauba, candelilla, bayberry, sugar cane); or mineral (e.g. fossil or earth waxes, such as ozocerite, ceresin or montan; or petroleum, such as paraffin, microcrystalline or slack wax). Animal and vegetable waxes are complex mixtures of compounds such as fatty non-glyceride esters of carboxylic acids and hydroxyacids, hydrocarbons and long chain paraffinic alcohols. The mineral waxes are mixtures of straight chain and branched aliphatic hydrocarbons and cycloparaffinic compounds. Synthetic waxes are either ethylene or propylene polymers or hydrocarbon type waxes. Fischer Tropsch waxes fall into the latter category. They are mostly long chain, saturated hydrocarbons with very few branched molecules. Polyethylene waxes are produced by the controlled polymerisation of ethylene to yield relatively low molecular mass polymers which are waxy in nature and which may have either a low or a high degree of branching, depending on the conditions employed during polymerisation. Alternatively, they may be produced by thermal degradation of a high molecular mass polyethylene to yield a lower molecular mass wax. Polypropylene waxes are long chain hydrocarbons having regularly spaced methyl side groups. Synthetic waxes are often chemically modified by introducing, for example, oxygenate, halogenate or amide functionalities, in order to manipulate their properties for certain specialised uses. [2]

1.2 OVERVIEW OF WAX APPLICATIONS

The most obvious and well-known use of wax today is for the manufacture of functional and decorative candles. However, waxes are also used extensively as additives in various applications, such as in hot melt adhesives (HMAs), inks, paints and coatings, plastics, emulsions for rust prevention and fruit coating, and polishes. Their importance lies in the unique properties that they impart to these formulations. For example, the correct waxes will reduce the viscosity of a hot melt adhesive, impart gloss to an ink or fruit coating emulsion, behave as a lubricant during the manufacture of PVC pipes or lend desirable buffability, gloss and hardness properties to a solvent or emulsion paste polish.

1.3 OVERVIEW OF INSTRUMENTAL TECHNIQUES FOR WAX CHARACTERISATION

The characterisation of wax properties is of great importance to the wax applications chemist. The correct information considerably simplifies the task of formulating the correct product for a specific application. It is also always useful to determine the composition of commercial wax-containing formulations, in order to keep abreast of commercial developments. The traditional wax analyses, such as congealing point, melting point, penetration, viscosity, density, and acid and saponification values often do not provide adequate information. They are single point analyses, which provide limited, albeit valuable, information. It is therefore useful to employ complementary instrumental techniques, such as differential scanning calorimetry (DSC), thermogravimetry (TG), rheology, gel permeation chromatography (GPC), high temperature gas chromatography (HTGC) and infra-red spectroscopy (IR), to analyse the waxes in greater detail. Each of these techniques characterises a different wax property. Integrating, or inter-relating, the data obtained from this combination of analyses allows an analysis profile of each wax to be formed.

Over the years, the most popular and useful analytical instrument for wax analysis has been the DSC. DSC generates a melting or crystallisation profile of the sample being analysed. Since the 1960s, DSC melting curves have been cited as a method to "fingerprint" or distinguish waxes.[3,4,5,6,7,8] It is a rapid, highly discriminating technique and requires very small quantities of sample. The technique has, however, been somewhat less successful for the qualitative and quantitative evaluation of wax blends.[7,9,10,11,12] This is due to overlapping melting ranges which do not allow the wax blend components or their ratios to be determined easily. Various authors have

correlated certain DSC parameters, such as the melting peak temperature, to the results of other traditional wax analyses, such as melting or congealing point. [3,5,6,9,13] This proved successful, but could not be applied to wax blends. DSC has also been used in conjunction with other instrumental techniques, such as GPC, [14] refractometry, [3] X-ray diffraction (XRD), [15,16] thermomechanical analysis (TMA), [15] and IR. [5,7,15] In general this has been to attempt to arrive at a combination of techniques that allows the user to classify waxes unambiguously. It has also been used as a tool for the formulation of wax blends for dentistry applications, [10] and as an aid to predicting the performance of HMAs containing different wax components. [17,18,19] The combination of DSC and GPC to qualitatively identify alternative feedstocks for the rubber processing industry has also been investigated. [14]

TG is used to examine a mass loss profile of the sample as a function of temperature. There were only a few references to the use of TG as a means of characterising waxes and wax blends. [20,21] The authors reported little success with either the qualitative or the quantitative application of this technique.

No literature references were found pertaining to the use of rheology to characterise waxes. Rheology is an analytical technique used to measure the mechanical properties of a sample. The use of dynamic mechanical analysis (DMA) to predict the performance of HMA formulations has received considerable interest in recent years. [22,23,24]

GPC is a technique historically used to characterise the molecular mass distributions of high molecular mass polymeric materials. The technique gives a molecular size distribution, which is converted, by way of calibration, to a molecular mass distribution. Its application in the field of wax analysis is fairly novel. It has been shown that it is possible to "fingerprint" natural waxes using GPC. [25,26] The technique has also been used to assess the presence of n-alkane fractions within the range C_{20}-C_{160} in crude oils. [27]

HTGC separates the components of a sample by their boiling point differences. This data is then converted, by calibration, to a carbon number distribution. HTGC analyses are useful for determining the carbon number distribution of waxes containing chain lengths $<C_{80}$. [28] The carbon distributions of the higher melting Fischer Tropsch waxes, polyethylene and polypropylene

waxes can therefore not be accurately quantified using this instrumental technique. It is also possible to determine the percentage isomer content up to C_{50}. [28, 29]

Different chemical species or molecules interact in a characteristic manner with energy in the infra-red region of the electromagnetic spectrum. This phenomenon is used in IR analysis to identify the chemical nature of the molecules present in a sample. IR analyses have been correlated to various wax properties, such as crystallinity and branching. [30,31,32] The structure elucidation of oxidised, microcrystalline and paraffin waxes by IR analysis, has also been described. [33,34]

1.4 OBJECTIVES

The objectives of this work were:

(1) to characterise a number of waxes by various instrumental techniques, and where the procedures were not obvious, to develop analytical methods to provide reliable and accurate results;

(2) integrate the data gleaned from each type of analysis to formulate a complete profile of wax properties, for various classes of waxes;

(3) illustrate how these wax profiles could be used by the wax applications chemist, using practical examples.

The task of a wax applications chemist is: (a) to understand the influence of wax properties on a final application formulation; (b) to be able to optimise the ratio of components in this formulation in order to ensure optimal performance of the application; and (c) to be able to apply his/ her insight into the combination of wax properties and application performance requirements to be able to supply innovative solutions to meet the end user's specific needs.

The types of waxes to be examined in this study are Fischer Tropsch, polyethylene, petroleum and natural. The analytical techniques to be used to characterise the waxes are DSC, TG, rheology, GPC, HTGC and IR.

1.5 REFERENCES

(1) A. H. Warth, The Chemistry and Technology of Waxes, 2nd Ed., Reinhold Publishing Corporation, New York, 1956.

(2) N. I. Sax, R. Lewis Sr., Hawley's Condensed Chemical Dictionary, 11th Ed., Van Nostrand Reinhold Company, New York, 1987.

(3) R. Miller, G. Dawson, Thermochim. Acta, 1980, 41, 93-105.

(4) B. R. Currell, B. Robinson, Talanta, 1967, 14, 421-424.

(5) B. Flaherty, J. Appl. Chem. Biotechnol., 1971, 21, 144-148.

(6) H. R. Faust, Thermochim. Acta, 1978, 26, 383-398.

(7) R. G. Craig et al, Analytical Calorimetry, Proc. Am. Chem. Soc. Symp. On Analytical Calorimetry, San Francisco, California, April 1968, 158-166.

(8) J. M. Powers, R. G. Craig, J. Dent. Res., 1978, 57, 37-41.

(9) R. G. Craig et al, J. Dent. Res., 1967, 46 (5), 1090-1097.

(10) J. M. Powers et al, J. Dent. Res., 1969, 48 (6), 1165-1170.

(11) M de Jong, Schümann Sasol Internal Report, 1994.

(12) M. Wesolowski, Thermochim. Acta, 1981, 46 (8), 21-45.

(13) A. P. Gray, Instrument News, date unknown, 17(1), 6-7.

(14) D. J. Harmon, J. Liq. Chromatogr. 1978, 1(2), 231-240.

(15) R. J. Howes, Proceedings of the 2nd European Symposium on Thermal Analysis, date unknown, 277-280.

(16) D. S. Barmby et al, Proceedings 6th World Petroleum Congress, 1963, VI (21), 1-17.

(17) T. R. Graves, J. G. McCormick, Adhesives Age, June 1988, 22-26.

(18) E. F. Eastman, Proc. Hot Melt TAPPI Symposium, 1988, 45-50.

(19) J. Komornicki et al, J. Adhesion Sci. Technol., 1992, 6(2), 293-305.

(20) J. Boelter, Fette, Seifen, Anstrichm, 1973, 75, 593-597.

(21) R. G. Craig et al, J. Dent. Res., 1971, 50 (2), 450-454.

(22) D. W. Bamborough and P. M. Dunckley, Adhesives Age, November 1990, 20-26.

(23) W. J. Honiball, TAPPI Hot Melt Symposium Notes, TAPPI Press, Atlanta, 1983.

(24) Hot Melt Adhesives, http://www.rheosci.com/app1.htm, 1997.

(25) D. E. Hillman, Analytical Chemistry, 1971, 43 (8), 1007-1013.

(26) L. Carbognani, J. High Resol. Chromatogr., 1996, 19, 549-558.

(27) L Carbognani, J. Chromatogr. A, 1997, 788, 63-73.

(28) E. R. Adlard (Ed.), Chromatography in the Petroleum Industry, Journal of Chromatography Library Series, Elsevier Science, 1995, Volume 56, Chapter 3.

(29) A. K. Gupta and D. Severin, Petroleum Science and Technology, 1997, 15 (9&10), 943-957.

(30) J. H. le Roux, J. Appl. Chem., February 1969, 19, 39-42.

(31) J. H. le Roux, J. Appl. Chem., July 1970, 20, 203-207.

(32) J. H. le Roux, J. Appl. Chem., August 1969, 19, 230-234.

(33) J. H. le Roux, South African J. Sci., August 1979, 75, 356-361.

(34) F. J. Ludwig, Anal. Chem., December 1965, 37(13), 1737-1741.

CHAPTER 2

THE WAXES AND THEIR APPLICATIONS

2.1 INTRODUCTION

The waxes examined by the analytical techniques in this study are varied in origin. Each type of wax has its own specific composition, peculiar to its origin, and therefore specific physical properties.

Analysis is important in formulation, especially if a wax analysis profile allows prediction of the properties of the final product. It is therefore necessary to introduce the wax applications in order to understand the need for wax analysis by the various analytical techniques.

Waxes impart desirable properties to many applications, the most important of which are hot melt adhesives (HMAs), polishes, inks, plastics and candles. An understanding of the basic requirements of each industry or market, and the ability to integrate the knowledge of wax properties with these, is the basis of the work of a wax applications chemist. Please note that many of the observations relating wax properties to its performance in the end application, as described in the following chapters, are of a general nature, as no attempt has been made to relate the analysis results shown in this work to actual applications testing data.

2.2 THE WAXES

The waxes examined in this study are classified in Table 2.1. The most economically significant wax types are included, viz. Fischer Tropsch, polyethylene (PE), petroleum-based and natural.

Table 2.1: Classification of waxes examined in this study

Class of wax	Specific wax	Manufacturer
Fischer Tropsch	Paraflint H1, Paraflint C80 and Paraflint C105	Schümann Sasol SA (Pty) Ltd
	SX 30, SX 50, SX 70 and SX 100	Shell MDS
Oxidised Fischer Tropsch	Paraflint A1, Paraflint A975 and Paraflint A28	Schümann Sasol SA (Pty) Ltd
High-density polyethylene (HDPE) wax	Polywax 1000, Polywax 2000 and Polywax C4040	Petrolite
Low-density polyethylene (LDPE) copolymer wax	Escomer H101*	Exxon
Degradation PE wax	Epolene N-21	Eastman
Medium-melting, narrow MMD, petroleum-based wax	HNP 3, HNP 9 and HNP 10	Nippon Wax Co.
Low melting, fully-refined paraffin wax	Ter Hell 6039	Schümann Sasol KG
	Grade 58/60°C	Chinese origin
Microwax	Mobil 2360	Mobil
	Be Square 195	Petrolite
Natural wax	Carnauba	
	Candelilla	

* No longer produced

2.3 THE APPLICATIONS

2.3.1 HOT MELT ADHESIVES

A HMA is a thermoplastic material. It is applied in its molten form, and on cooling forms a bond by way of adhesion of the solid HMA to the bonded surfaces. HMAs are used in various applications, which include packaging, bookbinding, furniture and shoe manufacture, and the production of diapers and cigarettes. Each application demands specific properties from the HMA used. A HMA is a blend of a polymer, a tackifying resin and a wax. The polymer is the adhesive backbone and contributes to the HMA's strength and toughness. The resin provides specific adhesion and substrate wetting. Waxes are used in HMAs for several reasons. They decrease the viscosity of the polymer used and thereby facilitate processing (mixing, pumping and application) of the HMA. This also aids surface wetting. Waxes increase the blocking point of the solid HMA. The blocking

point is the temperature at which the solid HMA pellets or chicklets will adhere to each other. The wax increases the blocking temperature due to the fact that its surface tension is low. This imparts slip to the HMA pellets or chicklets, preventing them from sticking together. The high temperature properties of a HMA are controlled by the addition of a wax having decomposition behaviour appropriate to the temperature of use of a HMA. Waxes are the most crystalline component of the HMA, and they modify the crystallinity of the system, thereby controlling its open and set times, flexibility and elongation. [1,2]

2.3.2 POLISHES

Paste polishes are used to protect, enhance and clean surfaces, such as floors, vehicle surfaces, wood furniture and leather. In general, they are gelled mixtures of 25% solids, consisting of wax, emulsifiers, pigments and dyes, and 75% solvent or water. The wax fraction is usually a blend of waxes having different properties, with each component performing a specific function in the formulation. [3]

Hard, high molecular mass waxes provide gloss and durability. Ease of application is promoted by the incorporation of softer, lower molecular mass waxes. The ability of a polish to gel may also be introduced by oxidation of the wax. This allows the formation of network structures, by way of saponification of the carboxylic acid functionalities during the preparation of the polish. These waxes may also be saponifed prior to the manufacture of the polish. Branched waxes are also often used to impart gelling characteristics. [3]

2.3.3 INKS

A wax is incorporated into an ink in a micronised form. Grinding and spraying are the two most common methods employed to micronise waxes for this application. Spraying produces spherical wax particles. The discrete, dispersed particles form a protective barrier that protrudes above the surface of the ink film, improving surface slip and reducing damage due to scuffing and rubbing. Performance is optimal when the wax particle diameter is similar to the thickness of the printed film. [4]

Waxes generally serve several functions as printing ink additives. Harder, higher molecular mass waxes improve the resistance of the ink film to rubbing and scuffing. Waxes with high melting points are more resistant to the heat treatment required for baked coatings. Low-viscosity waxes with a highly linear structure and suitable surface tension allow the overprinting of ink films with a varnish, to further improve the gloss of the film. This also contributes to anti-blocking and low slip of the film. The waxes used in water-based inks require a degree of polar functionality in order to improve their compatibility with the system. The performance of a wax in a printing ink depends on several parameters, such type of wax, wax particle size and shape, and final ink application. [4]

The final application determines certain criteria for the performance of the printing ink. Packaging applications require ink films which have excellent rub and scuff resistance, to prevent damage during transportation and storage. High quality magazines need to have excellent gloss of the printed film. If varnish overprinting of the film is required, such as for magazine covers, the varnish should adhere well to the ink film. Good anti-blocking performance and low slip are required where printed sheets are to be stacked.

2.3.4 PLASTICS

Lubricants for the processing of polymers such as PVC are classified as internal or external. Internal lubricants shorten processing times by increasing inter-particle friction due to higher compatibility. For this reason, internal lubricants contain polar functional groups which render them more compatible with PVC. External lubricants retard fusion time and improve lubrication between the PVC and metal surfaces. Waxes may be used as either internal or external lubricants during PVC processing. Internal lubricants require polar functionalities, which promote their compatibility with PVC. Low molecular mass material, which will volatilise and eventually char at a typical PVC processing temperature (200°C), is undesirable in a lubricant. [5]

2.3.5 CANDLES

The secret to the manufacture of candles is to use a combination of the correct wax, wick and conditions for the specific type of manufacturing process employed. When producing moulded candles, the wax should contract sufficiently on cooling to enable the candle to be removed from the mould. Waxes which undergo a volume change on solidification are therefore desirable.

Balanced wax hardness properties are required, as waxes that are too soft or too hard will, respectively, not release well from the mould, or be brittle and crack. However, wax contraction is not desirable when producing jar candles, as the wax should adhere to the sides of the container. A wax oil content that is too high is undesirable as the oil will bleed out onto the surface of the candle during storage and soil the packaging. Candles produced from such a wax can also not be overdipped, as blisters will form between the base wax and the overdipped layer, due to oil bleeding. Higher molecular mass waxes are often used as additives to the softer candle base wax in order to promote surface gloss. [6]

2.4 REFERENCES

(1) www.schuemann-sasol.co.za/hotmelt/H105/H105.htm

(2) www.schuemann-sasol.co.za/hotmelt/C80/C80.htm

(3) www.schuemann-sasol.ca.za/polishes/polishes.htm

(4) www.schuemann-sasol.co.za/Inks/Spra30/Spray30.htm

(5) www.schuemann-sasol.co.za/pvc/pvc.htm

(6) www.schuemann-sasol.co.za/candles/decorati.htm

CHAPTER 3

THE ANALYTICAL TECHNIQUES

3.1 DIFFERENTIAL SCANNING CALORIMETRY (DSC)

3.1.1 THEORY

DSC measures the heat flow to or from a sample in a controlled atmosphere as a function of temperature or time. A sample may absorb heat as the result of melting or evaporation, or heat may be evolved as a result of crystallisation or condensation. Various types of DSC equipment, which operate on slightly differing principles, are commercially available. The Perkin Elmer Pyris 1 used for this work is an example of a power-compensation DSC. Adding or subtracting an equivalent amount of electrical energy to a heater located in the reference furnace holder compensates for the heat flow to or from the sample. This measurement is made directly in differential power units (milliwatts, mW). Thermal events in the sample appear as upward or downward deviations from the baseline. The convention used here is that upward peaks describe endothermic processes. The signal may be described by the equation $\Delta(dq/dt) = (dT/dt)(C_s-C_r)$, where $\Delta(dq/dt)$ is the measured heat flow signal, dT/dt is the heating rate, C_s is the sample heat capacity and C_r is the heat capacity of the reference (calibration) material. [1]

3.1.1.1 DSC MAXIMUM AND MELTING RANGE

The most frequent application of DSC is to measure transition heats and temperatures. The vertex of the endotherm (or exotherm) usually most accurately reflects the temperature of the transition, referred to here as the DSC maximum (or minimum). Greatest accuracy in temperature measurements is obtained by observing the following considerations: (1) instrument calibration; (2) small sample size; (3) proper sample encapsulation; (4) slow scanning rates; (5) and the elimination of thermal history. Temperature calibration is performed using a high purity material with a known melting point, such as indium. The material should ideally melt in, or close to, the melting range of the sample to be analysed.

In wax samples, the melting range is just as important as the DSC maximum. This is because wax samples contain a distribution of material that melts over a wide range of overlapping temperatures. The components of this distribution act as impurities towards each other, and therefore, the wider the distribution of material, the broader and flatter the DSC melting peak. This is due to the melting point depression of components by other lower melting components. This is sometimes referred to as the solubility effect. Therefore, only tentative information regarding the relative molecular mass distributions of the wax samples may be deduced from the DSC melting ranges. The lower and upper limits of the DSC melting range are usually referred to as the beginning and end of melt, respectively.

3.1.1.2 HEATS OF TRANSITION

The area underneath a DSC peak is proportional to the enthalpy change, ΔH, of the thermal event. It may be represented as $\Delta H = A \times K/m$, where A is the area under the peak, K is a calibration factor and m is the mass of the sample. The K factor is determined by relating a known enthalpy change to the measured peak area. Indium is again used to perform this calibration. The calibration is specific to a certain instrument under a certain set of operating conditions. The precautions given above for the accurate determination of transition temperatures also apply to the measurement of heats of transition. Two further concerns may be added, viz. precise weighing of the sample and accurate determination of the area underneath the curve.

The energy consumed by a wax sample on melting, i.e. fusion enthalpy, is dependent on a number of factors, such as the molecular mass distribution, the average molecular mass, and the crystallinity of the sample. The latter factor is dependent on the chemical composition of the sample. Branched or oxidised hydrocarbons have lower crystallinities than their n-alkane homologues, due to the inability of the chains of the former to undergo optimal crystal packing. [2]

3.1.2 WAX ANALYSIS BY DSC

The ASTM methods for the DSC analysis of polymers and petroleum waxes were adapted here for the analysis of waxes, mainly to optimise analysis time. [3,4,5]

The melting behaviour of a wax sample is highly dependent on its thermal history. Unless the thermal history is standardised, this will reduce the usefulness of DSC both to fingerprint waxes and to examine batch variations in a specific type of wax. Standardisation of wax thermal history is done by means of melting the wax sample and cooling it at a controlled, reproducible rate to a temperature below its beginning of melt. It is far easier to standardise the thermal histories of waxes than of polymers, due to their lower molecular masses. For this reason, it is possible to use a fairly short residence time at the wax melting temperature and a relatively fast cooling rate. The result is a relatively short analysis time (ca. 20 min), which allows for the high sample throughput required by a technical support laboratory.

To produce reproducible DSC analyses one must ensure that the contact between the sample and the base of the pan is optimal. This is a further advantage of melting the wax to eliminate its thermal history, as it will flow out and cover the bottom of the sample pan, due to its low viscosity, thereby optimising thermal contact with the pan.

It has been established by the author that it is possible to analyse most waxes over the temperature range of 0-130 °C. This takes the guesswork out of choosing the temperature limits for DSC analysis. This temperature range may be optimised to 0-80 °C for the softer, lower molecular mass waxes. Certain polymeric waxes may require a higher upper temperature limit, viz. 150-170 °C, in order to obtain a complete melting profile with a good baseline on the high-temperature side of the peak.

In order to accurately determine the area underneath a peak, it is necessary to construct a baseline. This calls for a degree of analyst subjectivity. For the purpose of this work, the baseline was considered to be flat, due to the fact that its flatness had been optimised and a baseline subtraction performed for each analysis. The baseline was chosen by extrapolating the flat portion of the baseline backward from the high temperature side of the peak to where it sensibly intersected the baseline at the low temperature end of the peak.

The reproducibility and repeatability of the DSC analyses of waxes has been found to be within the limits stipulated by the ASTM methods previously mentioned. [3,4,5]

3.1.3 EXPERIMENTAL

DSC analyses were performed on a Perkin Elmer Pyris 1 power-compensated DSC, equipped with an Intracooler II sub-ambient accessory and controlled by Perkin Elmer Pyris software. The sub-ambient accessory is a gas-type refrigeration unit which permits operation from –60 °C. Standard aluminium sample pans and lids were used. An empty sample pan and lid were placed in the reference furnace to balance the specific heat consumption of the sample's pan and lid. The analyses were performed in a nitrogen atmosphere. The instrument was calibrated on the melting peak maximum, using an indium standard obtained from Perkin Elmer. Sample sizes were between 2 and 3 mg. A standard sample pan press was used to seal the sample into the sample pan. Samples were loaded at 130 °C, held for 0.5 min, cooled at 20 °C/min to 0 °C, held for 1 min at 0°C, and then heated at 10 °C/min to 130 °C. This program was performed with baseline subtraction. The first three steps of the program ensure that all samples analysed have identical thermal histories. A further advantage of this temperature program is that the sample's crystallisation curve is also readily available. The last step of the program gives the sample's DSC melting curve. The method is based on various ASTM methods. [3, 4, 5]

3.2 THERMOGRAVIMETRY (TG)

3.2.1 THEORY

Changes in sample mass with temperature can be measured using a thermobalance. This consists of a suitable electronic microbalance and a furnace with an associated temperature programmer. The balance is contained in a suitably enclosed system, so that the atmosphere can be controlled. A sample will lose mass as it evaporates or decomposes, or may gain mass, for example, if it is oxidised in an air atmosphere.

Various types of balance mechanisms are available commercially. The Perkin Elmer TGA-7 used for the analyses in this work is an example of a top loading balance based on the null point mechanism of weighing. An optical sensor detects the deviation of the balance beam from the null position. The amplified output from the sensor is used to restore the balance to its null point by means of an electromagnetic mechanism, and serves as a measure of mass change. The advantage of this type of mechanism is that the position of the sample pan in the furnace remains

constant, thereby eliminating the influence of temperature gradient within the furnace on the sample. [1]

Calibration of the small furnaces used for TG is performed by means of the measurement of the Curie points of a selection of metals and alloys. A ferromagnetic material loses this property at a certain temperature, which is known as its Curie point. If a sample of such a material is placed in the pan of a TGA, and a magnet is positioned below, then the total downward force on the sample at a temperature below the Curie point is the sum of its mass and the magnetic force. At the Curie point the magnetic force is reduced to zero, and an apparent mass loss is observed. By using several ferromagnetic materials, a multi-point temperature calibration is obtained. [1]

3.2.1.1 QUALITATIVE THERMOGRAVIMETRY

Different waxes have characteristic mass loss profiles, depending on their physical properties, such as average molecular mass, molecular mass distribution and chemical composition. It is therefore possible to produce a wax mass loss fingerprint, which is characteristic of that type of wax, by analysing it using TG. In general, lower molecular mass waxes display mass losses at lower temperatures than higher molecular mass waxes. Waxes with narrow MMDs will have narrower decomposition ranges than waxes with broader MMDs. The maximum temperature of the derivative mass loss (DTG) curve also serves as a general indication of the type of wax analysed.

(A) TG ONSET TEMPERATURE

The point of intersection of a tangent to the TG curve drawn through the temperature of the maximum rate of decomposition, and an extrapolation of the initial part of the curve where zero mass loss occurs, is the TG onset temperature. The temperature of the maximum rate of decomposition is the peak maximum of the differential TG (DTG) curve. Comparison of the TG onsets of various waxes gives an indication of their relative thermal stabilities. This may sometimes yield misleading results, however, as it does not account for any low boiling material that may be present.

(B) TEMPERATURE AT 0.5% MASS LOSS

This parameter gives an indication of the thermal stability of a wax sample in terms of its initial mass loss. This is often a more useful and appropriate parameter than the TG onset temperature, as it gives an indication of the expected relatively high temperature performance of waxes as they are processed in the applications.

(C) DTG MAXIMUM

The mass loss signal may be differentiated to give a derivative thermogravimetric (DTG) curve. This curve represents the rate of mass change of the sample. The position of the DTG maximum is characteristic of the type of wax sample. Reproducible DTG temperatures may be achieved by consideration of the following: (1) regular and precise instrument calibration; (2) small sample size, with optimum surface area to volume ratio; (3) slow scanning rates; and (4) reproducible gas flow rates. The packing of the sample in the TG sample pan is not a factor influencing the accuracy of the analysis, as the wax at its melting point will melt and flow out over the bottom of the pan.

3.2.1.2 QUANTITATIVE THERMOGRAVIMETRY

It was mentioned in section 3.2.1.1 that the physical properties of a wax dictate its mass loss behaviour and that its TG analysis serves as a fingerprint which assists in identifying the type of wax. It is possible to estimate the composition of a wax blend, and the identity of its components, provided that the temperature ranges over which mass loss occurs are sufficiently separated. Some wax-based formulations contain components that do not display mass losses below the upper temperature limit of the TG analysis. It is possible to accurately assess the concentrations of these components. Examples of such additives are metals used to saponify oxygenate functionalities, inorganic pigments and fillers such as calcium carbonate or carbon black. It is also sometimes possible to identify the nature of such components. For example, carbon black and calcium carbonate both show characteristic mass loss behaviour at elevated temperatures.

3.2.2 WAX ANALYSIS BY TG

Waxes degrade within the temperature range 50-800 °C, which is fairly wide. The choice of heating rate is a trade-off between the resolution of the decomposition steps and analysis time. The former is not a consideration when analysing waxes. Experience has also shown that slower heating rates do not have an appreciable influence on the resolution of components with overlapping degradation ranges in a wax blend. For these reasons a heating rate of 20 °C/min, which is academically considered to be very rapid, is recommended for wax TG analysis. Even so, the analysis time is in the order of 45 min, including the time required for the furnace to cool back down to 50 °C after a run.

The higher molecular mass and fuctionalised waxes leave a very small percentage of carbonaceous residue which does not degrade in a nitrogen atmosphere below 800°C. For this reason, oxygen is introduced into the system at 550 °C in order to volatilise this as carbon dioxide. Failure to do this results in a build-up of carbon on the sample pan and furnace. This shortens the lifetime of the furnace.

The packing of the sample in the sample pan is critical for particulate samples such as catalyst, where the surface area to volume ratio will have a great influence on the TG analysis result. Wax samples will melt and flow out over the bottom of the sample pan. By controlling sample weight, the sample surface area to volume ratio, and therefore the degree of interaction with the atmosphere, may be considered constant.

TG analysis repeatability and reproducibility can be achieved to be within 2 °C, provided that the instrument's calibration remains within the same limit.

3.2.3 EXPERIMENTAL

TG analyses were performed using a Perkin Elmer TGA-7 controlled by Perkin Elmer Pyris software. The instrument was calibrated using the Curie point method with Alumel, nickel, Perkalloy and iron standards obtained from Perkin Elmer. Sample sizes of 2-3 mg were used. The mass loss profiles were recorded from 50 to 850 °C at a heating rate of 20 °C/min. The

atmosphere was switched from nitrogen at 20 ml/min to oxygen at 20 ml/min at 500 °C in order to combust any remaining carbonaceous residue on the sample pan and/ or furnace.

3.3 RHEOMETRY

3.3.1 THEORY

Rheology is the science of the study of the deformation and flow of matter. The response (strain) generated in a sample when it is subjected to a deforming force (stress) is measured. The sample's mechanical properties govern the relationship between the applied stress and the resulting strain, and are characteristic of the physical structure and chemical composition of the sample. The stress which is required to attain a deformation is that which must overcome the internal forces in the material which resist this deformation. Materials of rheological interest range from highly rigid or elastic solids to very low-viscosity fluids. Of greatest interest are materials that are partly fluid and partly solid, and which therefore exhibit complex rheological behaviour. Waxes are such materials. Of specific interest to the applications chemist is the manner in which a wax-containing end product, such as a HMA, ink or emulsion, will behave in the field. The properties of the wax used in the final product will play a role in this.

The rheological character of a material may be characterised with reference to a simple deformation called simple shear. This is illustrated in Figure 3.1, where a material of thickness *y* is confined between two parallel plates. A force *F* is applied parallel to the lower plate, which may move in its own plane, while the upper plate is kept stationary. The shear stress is defined as the force divided by the area of the surface (A) on which it acts, $\sigma = F/A$. Since it is assumed that the material adheres to the plates, if it is deformable, the lower plate may be displaced by an amount Δy in response to the applied force. Since there is no displacement of the upper plate, a displacement gradient is established in the material, which is equivalent to the shear strain and may be represented by the equation $\gamma = \Delta y/y$.

The rheology of a material is defined in terms of the way in which the shear stress depends on the shear strain. Mechanical response may be broadly classified as elastic, viscous or viscoelastic. If, at equilibrium, the material reaches constant strain in response to a constant stress, and the ratio is directly proportional, the material is called a linear elastic solid, and the

proportionality constant is the shear modulus, G'. This may be represented as $G' = \sigma/\gamma$. Should the relationship be more complex and nonlinear, the ratio would not be constant, but would be represented by the equation $G'(\sigma \text{ or } \gamma) = \sigma/\gamma$. Elastic materials have the ability to return to their original dimensions once the applied stress is removed. If the material continues to deform, or flow, in response to an applied stress, the material is called a viscous fluid. The material undergoes irreversible deformation. A steady state will be reached in which the strain will be increasing at a constant rate, $\dot{\gamma}$. If the ratio of the shear rate to the shear strain is directly proportional, the material is linear viscous or Newtonian, and the proportionality constant may be represented by the equation $\eta = \sigma/\dot{\gamma}$, where η is the viscosity. Where a more complex relationship exists between the shear rate and the shear stress, the ratio is not a constant and the material is non-Newtonian. The apparent viscosity equation, $\eta(\sigma \text{ or } \dot{\gamma}) = \sigma/\dot{\gamma}$, describes this behaviour.

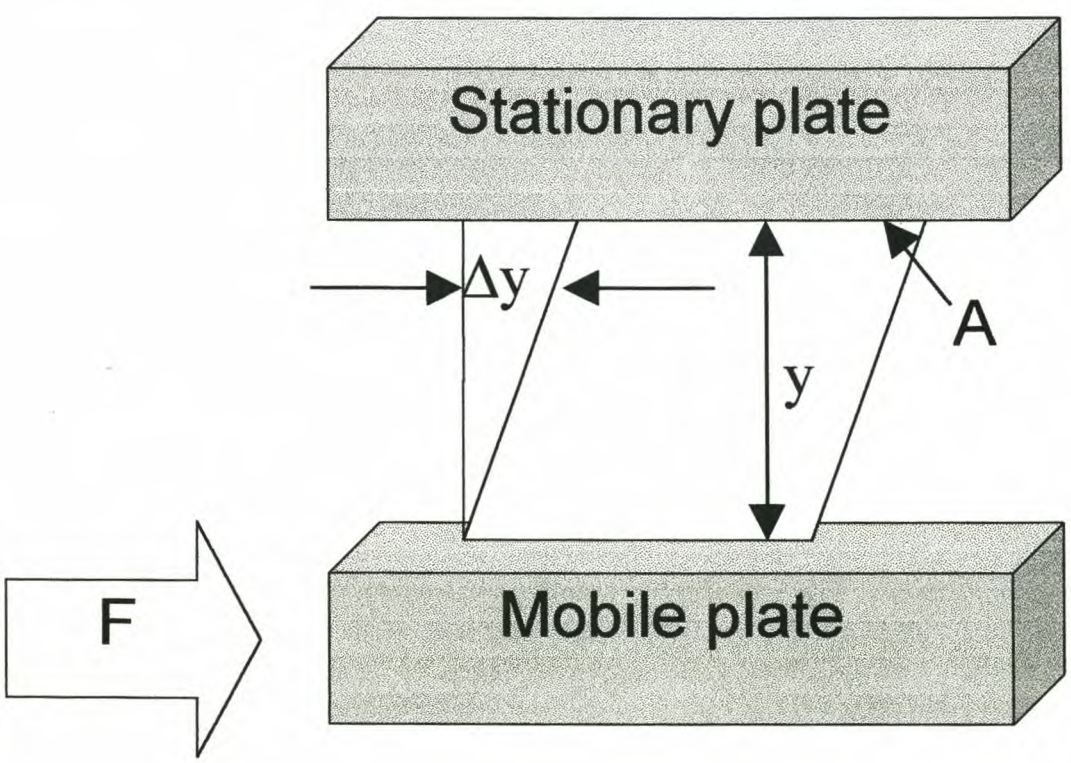

Figure 3.1: Response of a material to simple shear. F = deforming force; A = surface area upon which F acts; y = thickness of material; Δy = amount of displacement of plate, or deformation of material, by F.

The stress required to result in the deformation of an elastic material is therefore dependent only on the magnitude of the deformation, whereas for a viscous fluid it depends only on the rate of deformation. Many materials, however, exhibit properties that are characteristic of both elastic solids and viscous fluids, and are referred to as viscoelastic. This behaviour is commonly characterised by its response to an imposed oscillatory strain. This involves measuring the magnitude and the phase of the stress required to achieve a specific oscillatory strain. Figure 3.2 illustrates this for elastic, viscous and viscoelastic materials. The stress response of an elastic material is in phase with the imposed strain while that of a viscous material will lead the strain by 90°. The phase shift, δ, for viscoelastic materials will be less than 90°. The mechanical properties of a material may then be quantified in terms of storage modulus, loss modulus and tan δ.

3.3.1.1 STORAGE MODULUS

The storage modulus is the ratio of the oscillatory stress to the oscillatory strain, $G' = \sigma/\gamma$, and represents the in-phase component of the stress-strain relationship, characteristic of elastic behaviour. It can also be described as the amount of energy that is stored and recovered from an elastic deformation.

As the shear stress can be expressed as the ratio of the applied force to the area on which it acts, and the shear strain by the ratio of the deformation to the original dimension in that plane, the storage modulus may also be expressed in terms of $G' = (F/A)/(\Delta y/y)$. As the entities F, A and y are known, and Δy is measured, G' may therefore be derived.

Hardness is a measure of a sample's resistance to penetration, scratching, marring, etc., and is dependent on its crystallinity. A highly crystalline material is also strong, tough and stiff. Since there is a direct relationship between crystallinity and G', it can be expected that sample hardness will increase as G' increases. [6, 7] A decrease in flexibility is observed along with an increase in G'. It is also known that low sample flexibility is associated with a reduced molecular free volume, usually resulting from a lower degree of branching, which restricts molecular motion. [8] Therefore it is to be expected that branched samples will display lower G's than unbranched samples of similar molecular mass.

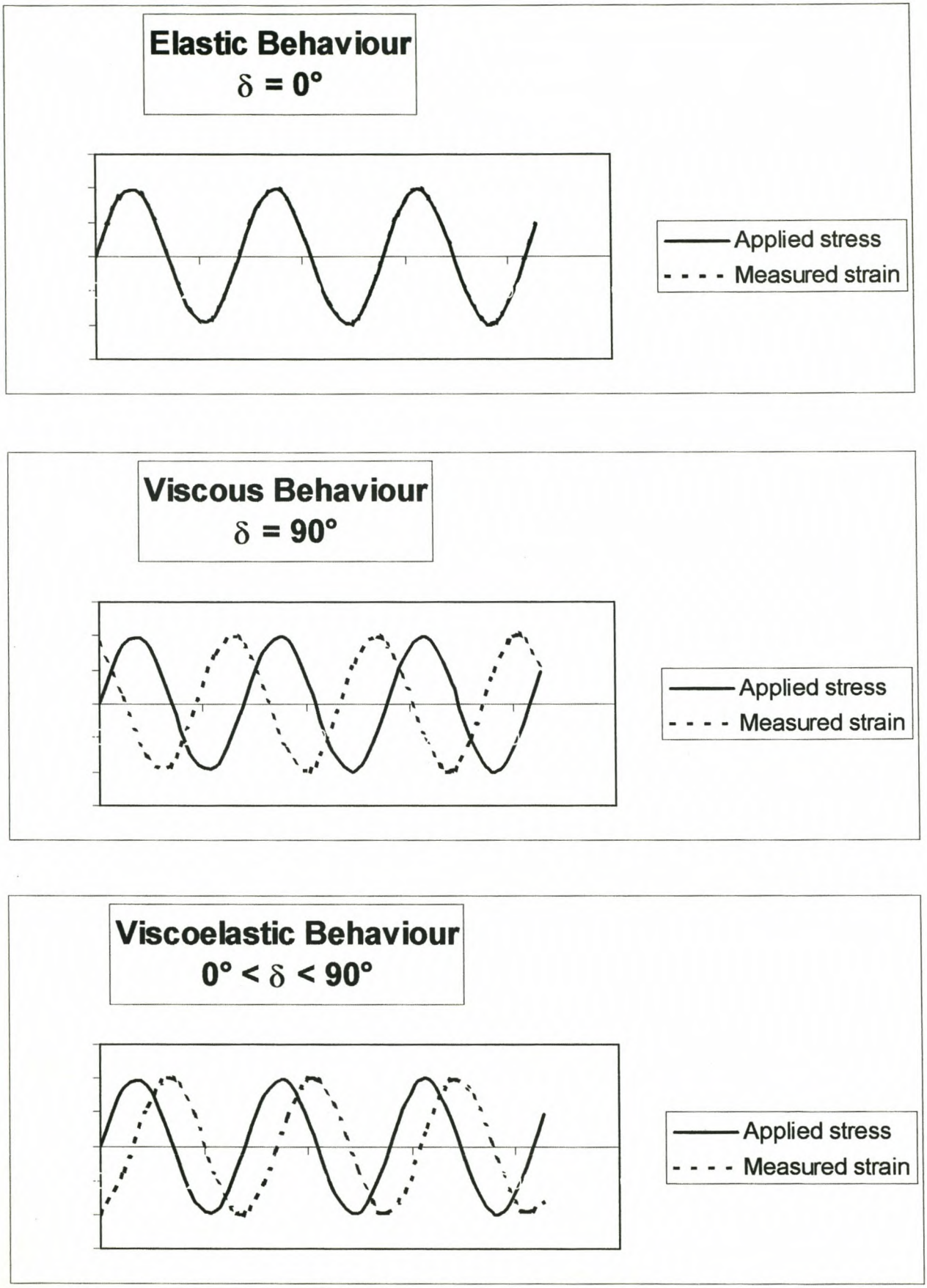

Figure 3.2: Responses of materials to an oscillatory (sinusoidal) stress of frequency ω

3.3.1.2 TAN δ

The phase angle, δ, between stress and strain is called the loss tangent, and is measured directly. Tan δ therefore indicates the balance of viscous and elastic properties of a material.

Brittleness is a measure of resistance to flexural fatigue or the flex life of a sample. It is the property of a material that results in its failure under conditions of low strain. Increasing M_n and decreasing crystallinity generally increase brittle strength, i.e. decrease sample brittleness. [6, 8, 9] A brittle sample is elastic, i.e. has a low tan δ and is hard, i.e. has a high G'. [6, 7] If the ratio of G' to tan δ decreases, the sample brittleness will therefore also decrease.

A sample is inherently cohesive when tan $\delta < 1$, with the degree of cohesive strength increasing as tan δ decreases, i.e. as the viscous properties of the sample decrease in relation to its elastic properties. The higher the cohesive strength of a sample, the lower its flexibility. Considering samples with the same hardness, but differing tan δ values, the sample with the lowest tan δ will have the greatest cohesive strength and lowest flexibility. [7]

3.3.1.3 LOSS MODULUS

G", the loss modulus, is the out-of-phase component of stress vs. strain, and represents the viscous behaviour component. Energy is dissipated by viscous deformations and lost. It is the multiple of the storage modulus and tan δ, G" = G'*tan δ. It is therefore also known as the imaginary component of the modulus, due to the fact that it is not measured, but calculated.

3.3.1.4 RELAXATION TRANSITIONS

Relaxation transitions are apparent as maxima on the tan δ curve. Their origins are due to the onset of various types of molecular motion. These transitions are labelled α, β, γ, in order of decreasing transition temperature. [6, 9, 10] They are generally referred to as second order transitions. The glass transition temperature, T_g, is defined for amorphous polymers as the highest temperature transition of a number of such possible transitions, i.e. T_α. The lowest

temperature transition, i.e. T_γ, observed in crystalline polymers, is defined as the T_g. [6] T_γ indicates the lowest temperature of use of the sample in terms of brittleness. [8, 9]

The α-transition is associated with the onset of molecular motion in the crystalline regions, the β-transition with the relaxation of molecular branch points, and the γ-transition with the onset of molecular motion in the amorphous regions of the sample. [6, 8, 10] HDPE undergoes α- and γ-transitions only, while LDPE exhibits α- (ca. 70°C), β- (ca. 0°C) and γ- (ca. -120°C) transitions [6, 10] The actual temperatures at which these transitions occur are influenced by the molecular mass of the sample. n-Alkanes exhibit only the α- and γ-transitions. [10, 11]

Factors affecting the positions of the transition temperatures are sample molecular mass, flexibility and polarity. The temperature of the α-transition, at a fixed frequency, increases with an increasing number (n) of CH_2 repeat units, and therefore increasing molecular mass, for the n-alkanes. [10, 11] The temperature increases rapidly for small values of n and levels off as n increases. For samples which display chain folding (i.e. carbon chain length > C_{150}), T_α increases as the fold length increases and the degree of branching decreases. [12] The intensity of the β-transition is directly proportional to the branch content and inversely proportional to sample crystallinity. [6] T_α will decrease with increasing sample flexibility, due to greater ease of rotation about the main bonds of the sample backbone. Polar groups will restrict this rotation due to mutual interaction, resulting in an increase in T_α. [8]

Highly crystalline (70-90%) materials are stiff, hard and brittle above and below their T_g, unlike amorphous materials which are brittle and rubbery below and above their T_g, respectively. For this reason, evaluation of the rheology results of wax samples are relative comparisons only, and may often not be verified empirically.

3.3.2 WAX ANALYSIS BY RHEOMETRY

The frequency, strain and heating rate parameters used to analyse wax samples using this technique were based on those recommended in the literature for the analysis of polyethylene and hot melt adhesives. [13]

Sample preparation was the most difficult and time consuming part of the analysis. Much trial and error led to the development of the sample preparation method. Bars of the required dimensions, viz. 50x10x2 mm, were machined from stainless steel and were used as templates to produce moulds from a curable silicon rubber. The moulds were heated to the same temperature as the molten waxes in an oven. Wax was carefully poured into the moulds, ensuring a small amount of overfill to compensate for the contraction of the wax surface that occurs. Once the wax reached the temperature at which it had congealed but was still soft, this overfill was carefully scraped off with a hot, flat, metal object. The samples were left to cool in the moulds. It was found that it was advisable to place a weight on top of these samples during the final stages of cooling, as they tended to "curl" upwards along their length. This made it difficult to load the sample into the rheometer.

The dimensions of the wax bars were accurately determined using a micrometer. The bars were loaded into the rheometer's torsion assembly by first clamping into the top fixture, then carefully lowering the top fixture and guiding the other end of the bar into the lower fixture. Offsetting the motor alignment in the appropriate direction, as indicated on the instrument's user interface, before tightening the bottom clamp, made compensation for any residual curvature of the sample bar. It is recommended that the clamps be fully tightened only at this stage, in order to prevent the sample bar from breaking during the loading process. The operator should develop a feel for the degree to which the clamps must be fastened. Overtightening will result in the sample breaking. Undertightening will result in the sample slipping during the analysis, and will manifest as excessive noise on the recorded data. At this stage, it was necessary to zero the torque and normal forces that may have developed in the sample as a result of clamping, by offsetting the motor alignment again and adjusting the height of the top torsion fixture in the appropriate direction, respectively. The next step was to cool the sample, by means of a forced convection oven (FCO), to –60 °C, the initial test temperature. Waxes contract on cooling and it was therefore necessary to compensate for this by continuously adjusting the height of the top fixture. This was achieved by setting an autotension sensitivity of 40 g.cm. This setting allows automatic adjustment of the height of the top fixture whenever the negative normal force that develops due

to sample contraction reaches 40 g.cm. Visual verification that the autotension sensitivity function was in operation also served to indicate whether the sample had been clamped correctly, and not broken during loading. Sample thickness is a crucial parameter, as it determines the ease with which a sample can be loaded. A sample which is too thin is difficult to clamp firmly, and a sample which is too thick will break easily.

The expected analysis reproducibility could not be established from the literature. The analyses were therefore performed in triplicate in order to develop a feel for the reproducibility. It was found that a reproducibility of <2% could be achieved. This also indicated that the sample preparation procedure sufficiently standardises thermal history.

3.3.3 EXPERIMENTAL

A Rheometric Scientific ARES strain controlled rheometer was used to determine the mechanical properties of the samples. Oscillatory measurements were performed using a transducer having a torque measurement range of 2-200 g.cm, a frequency of 10 rad/sec and a strain of 10 %. Solid state analyses were performed over a temperature range of –60 to 80 °C, using a heating rate of 2 °C/min. Temperature control was obtained using a forced convection oven fitted with a Polycold gas-type refrigeration accessory. Samples were moulded into bars of 50x10x2 mm dimensions and mounted using a torsion rectangular clamp.

3.4 GEL PERMEATION CHROMATOGRAPHY (GPC)

3.4.1 THEORY

GPC, or size exclusion chromatography (SEC), is a liquid chromatographic technique which separates molecules according to their sizes. The technique is widely used to characterise high molecular mass synthetic polymers, which are normally composed of a distribution of chain lengths. This technique gives information on the molecular mass distribution (MMD) of the sample. A sample solution is introduced onto a column which is filled with a rigid structure, porous particle packing and is carried by a mobile phase (solvent) through the column. Size separation takes place by repeated exchange of solute molecules between the bulk solvent of the mobile phase and the stagnant liquid phase within the pores of the packing. The packing pore size

determines the molecular size range within which separation occurs. [14] Smaller molecules diffuse into the pores of the packing matrix more easily than larger molecules do, and are therefore retained for longer. Thus a molecular size distribution is obtained from a GPC experiment with the elution order exhibiting large molecules first and small molecules last. The amount of material eluting from the column at any specific point in time is proportional to a signal obtained by continuously comparing the refractive index of the analyte dissolved in the mobile phase to that of the mobile phase. The system is calibrated by relating the retention time of a series of compounds of known molecular mass, and of chemical composition similar to that of the sample to be analysed, to molecular mass. [15]

The molecular mass of a sample may be expressed as a number of different averages. The significance of each of these averages lies in its relationship to other properties of the sample. These averages are explained in Table 3.1 and Figure 3.3. N_i is the number of molecules with molecular mass M_i. These averages do not give any information on the spread of the molecular mass distribution. The polydispersity, $P_d = M_w/M_n$, is a useful indication of whether this distribution is broad or narrow. It, however, gives no indication of the shape of the peak. The number average and z-average molecular masses are dependent on the low and high molecular mass materials in the distribution, respectively. [15]

Table 3.1: Mathematical definitions of molecular mass averages

Average	Mathematical definition
Number	$M_n = \Sigma(N_i.M_i) / \Sigma N_i$
Weight	$M_w = \Sigma(N_i.M_i^2) / \Sigma(N_i.M_i)$
Z-average	$M_z = \Sigma(N_i.M_i^3) / \Sigma(N_i.M_i)^2$

Polymer A

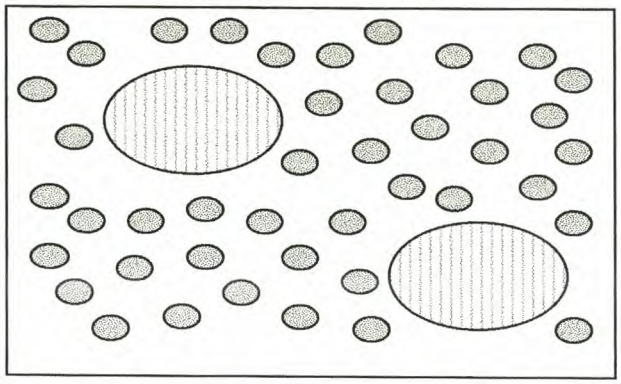

Assumptions:
500 molecules at 1 mg = 500 mg
2 molecules at 250 mg = 500 mg
Total mass = 1000 mg

$$M_n = \frac{(500x1) + (250x2)}{(500+2)} = \frac{1000}{502} = 1.99$$

$$M_w = \frac{(500x1^2) + (2x250^2)}{(500x1) + (2x250)} = \frac{125500}{1000} = 125.50$$

$$M_z = \frac{(500x1^3) + (2x250^3)}{(500x1^2) + (2x250^2)} = \frac{31250500}{12550} = 249.00$$

$$P_d = \frac{125.50}{1.99} = 63.07$$

Polymer B

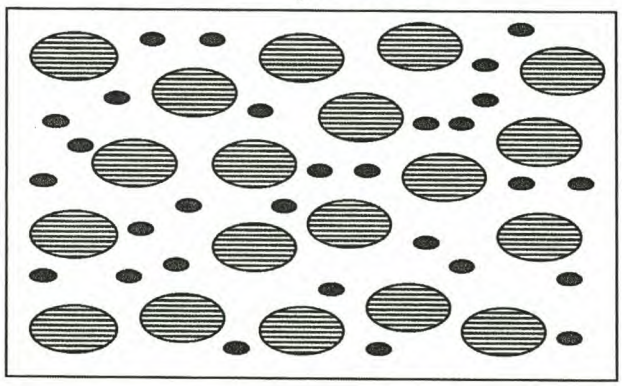

Assumptions:
400 molecules at 1 mg = 400 mg
100 molecules at 6 mg = 600 mg
Total mass = 1000 mg

$$M_n = \frac{(400x1) + (100x6)}{(400+100)} = \frac{1000}{500} = 2.00$$

$$M_w = \frac{(400x1^2) + (100x6^2)}{(400x1) + (100x6)} = \frac{4000}{1000} = 4.00$$

$$M_z = \frac{(400x1^3) + (100x6^3)}{(400x1^2) + (100x6^2)} = \frac{22000}{4000} = 5.50$$

$$P_d = \frac{4.00}{2.00} = 2.00$$

Figure 3.3: Schematic representation of calculation of molecular mass parameters

3.4.2 WAX ANALYSIS BY GPC

It is far easier to solubilse wax samples than polymers. Less aggressive solvents, agitation and time, and lower temperatures, may be employed. Toluene, xylene and o-dichlorobenzene are recommended as solvents for wax analysis by GPC. There is a greater refractive index difference between wax and xylene than between wax and toluene. This equates to a better detector response when using xylene.

GPC columns require careful handling in order to maximise their lifetimes. It is possible to extend the lifetimes to 18 months, which is 6 months longer than the supplier predicts, or other laboratories have experienced. The column life is influenced negatively by thermal or mechanical shock, a change in mobile phase without following the necessary precautions, overpressurising, reverse installation, or being allowed to dry out. The columns used here were only available with toluene as storage medium. It was therefore necessary to carefully introduce xylene into the columns. This was done by flushing the GPC with toluene prior to installation of the columns. The columns were connected and their temperature stabilised at the operating temperature. Xylene was gradually introduced into the mobile phase by pumping approximately 100 ml of toluene: xylene blends, of concentrations 90:10, 70:30, 50:50, 30:70, 10:90 and 0:100, consecutively, through the system.

The optimal wax solution concentration at 100 °C was ascertained by visually inspecting a number of solutions of different concentrations.

It was not possible to calibrate the system over its entire useful range, due to the unavailability of n-alkane standards $>C_{60}$. It was, however, possible to extrapolate the calibration curve to cover the entire range between the exclusion and permeation limits, provided that the resulting calibration curve displays a R^2 factor of at least 0.999. Experience has shown that a drop in R^2 below this value is indicative of either deterioration in the column plate count below the value specified by the manufacturer for minimum acceptable separation efficiency, signifying the end of column life, or that there may be outlying points on the calibration curve that require correction.

Sample to sample reproducibility should be in the order of 2-5% for calculated molecular mass averages. It has been shown for the system used here, that the analysis reproducibility is <2 carbon number units for the M_n parameter and <3 carbon number units for the M_w and M_z parameters. [16]

3.4.3 EXPERIMENTAL

GPC analysis was performed using a Waters 150-C GPC equipped with a differential refractive index (DRI) detector. Data acquisition was performed using Waters Millenium software. Separation was performed on two Waters HR 4E styragel columns (molecular separation range 50–100,000 Daltons). The mobile phase was HPLC grade o-xylene, obtained from Burdick and Jackson. The pump, injector and column compartments were programmed to 55 °C, 100 °C and 100 °C. A flow rate of 1 ml/min, scale factor of 10, sensitivity setting of 256 and run time of 35 min were employed.

Triplicate analyses of 200 μl volumes of a 0.05 % w/w wax in o-xylene solution were performed. Calibration was performed using n-alkanes from C_{12} to C_{50}. The calibration curve was extrapolated using a third order fit to enable quantification of peaks between the permeation and exclusion limits of the columns. The correlation factor for such an extrapolated curve was 0.9998.

3.5 HIGH TEMPERATURE GAS CHROMATOGRAPHY (HTGC)

3.5.1 THEORY

Gas chromatography, or more specifically gas liquid chromatography (GLC), is a technique that allows separation of components in a sample by virtue of their differing boiling points. Separation is accomplished by repeatedly partitioning the sample components between a mobile gas phase and a stationary liquid phase held on a solid support. A GLC system is composed of a sample inlet (injector), mobile phase (carrier gas), column (which contains the stationary phase), oven, detector and data handling system. Various factors require consideration in order to produce good, reproducible chromatographic results, viz. the type of carrier gas and control of its flow rate; sample preparation; type of injection and technique; oven temperature program and control; column specifications; and choice of detector. Wax samples are dissolved in a suitable solvent in

order to facilitate their introduction onto the column. The volume of sample injected should be optimised. This is determined by the amount and type of stationary phase, and the column temperature. The on-column injection technique is recommended for the generation of quantitative results, such as a carbon distribution. The sample is introduced directly onto the column. The choice of carrier gas is based on its efficiency, purity, reactivity and the detection method used. Nowadays, compensation for gas viscosity changes with increasing column temperature is effected using electronic pressure controllers. The choice of column and stationary phase is dependent on the type of sample to be analysed, the technique to be used and the required results. Column efficiency increases with a decrease in internal diameter and a decrease in film thickness. Overloading of the column results in peak fronting. This can be avoided by increasing the column temperature, decreasing the sample volume or using a column with a thicker stationary phase film. The oven temperature reproducibility and control are also critical to the quality of the analyses performed. A flame ionisation detector (FID) is commonly used for the analysis of waxes. It is mass-flow sensitive, and its response to hydrocarbons is linear with respect to the number of carbon atoms passing through the flame at a given time. Its response is in the form of a series of peaks that elute at discrete retention times. The area under each peak may be related to the amount of the specific component that is present in the sample. Calibration of the system is performed using a series of n-alkane standards, whose experimental retention times are related to their carbon numbers. GLC analysis can separate straight chain alkanes, or n-paraffins, from branched and cycloalkanes (iso-paraffins) of the same molecular mass up to C_{80}. [17] The result of this quantified separation is the carbon number distribution of the sample. GLC can quantify carbon chain lengths up to C_{120} if the system is operated to the maximum operating temperature of 440°C. For this reason, the technique is also referred to as high temperature gas chromatography (HTGC). [17, 18]

3.5.2 WAX ANALYSIS BY HTGC

The method used here for the HTGC analyses of waxes was based on that used in other Sasol laboratories. The carrier gas flow was optimised for the specific HTGC system used here by constructing its Van Deemter plot.

Experience showed that, contrary to supplier recommendations, it was not advisable to use helium as carrier gas when analysing the higher molecular mass waxes. Hydrogen, however, due to its reducing nature, prevents the build-up of the small quantities of decomposition products likely to form on the column. The lifetime of a column using hydrogen and helium as carrier gas

was ca. 3 months and ca. 2 weeks respectively! Considering the cost of a column, it is therefore worthwhile to ensure that adequate safety precautions are in place in order to make use of hydrogen as the carrier gas.

It was possible to use xylene as solvent medium to introduce a wax sample onto the column, rather than the appreciably more hazardous carbon disulfide, as the retention times of the first components of the waxes analysed did not coincide with that of the xylene solvent peak. The wax solution was heated in order to ensure solubilisation of the wax.

A reproducible injection technique using a thoroughly cleaned and warmed syringe is absolutely crucial to result integrity.

3.5.3 EXPERIMENTAL

HTGC analyses were performed on a Varian 3410. The system had a temperature programmable inlet, electronic pressure control and FID detector. A 10m, non-polar (100% dimethyl polysiloxane) megabore column of 0.53 mm internal diameter and 2.65 μm film thickness was used. A 10 μl injection volume of sonicated 0.05 % w/w wax in o-xylene solution was introduced directly onto the column. Analyses were performed from 50 °C to 440 °C, at a heating rate of 15 °C/min, with a 10 min isothermal at 440°C. The initial detector temperature was 60 °C and was programmed to 440 °C at maximum heating rate. Carrier gas was hydrogen at 7 ml/min. The system was controlled by HP 3365 software. Calibration was performed using n-alkane standards in the range C_{12} to C_{50} and a Polywax 655 standard.

3.6 INFRA-RED SPECTROSCOPY (IR)

3.6.1 THEORY

Atoms, molecules or other chemical species undergo characteristic changes in their energy states on absorption of electromagnetic radiation. Portions of the incident radiation are absorbed at specific wavelengths and result in twisting, bending, rotating and vibrational motions of atoms in the molecule. IR spectroscopy is the measurement of these interactions with radiation at wave

numbers between 14 000 and 20 cm^{-1}. The mid-infra-red region, which covers frequencies from 4000 to 200 cm^{-1}, is the spectral range of most interest. The resulting spectrum is a fingerprint of the functional groups that make up the molecule, as well as their relative configurations. Qualitative analysis of a sample is therefore possible, as the presence of specific functional groups in a sample is apparent from vibrational interactions at the corresponding characteristic wavelengths.

The basis of Fourier transform infra-red (FT-IR) spectroscopy, a variant of IR spectroscopy, is the two-beam interferometer designed by Michelson in 1891. A thermal source emits broadband infra-red radiation, which falls onto a beam splitter. Half of the radiation is reflected and travels a distance L onto a fixed mirror, which reflects it back along this distance and to the beam splitter. The other half of the radiation is transmitted, and follows a similar path of distance L, falling onto a moving mirror of the interferometer. This mirror can be moved precisely along the optical axis by an additional distance x, giving a total path length of the transmitted radiation of $2(L+x)$. An optical path difference of $2x$ occurs on recombination at the beam splitter. The beam leaves the interferometer, passes through the sample cell and is focussed on the detector. The radiation intensity $I(x)$, measured as a function of the displacement of the moving mirror, is the signal registered by the detector. This interferogram is mathematically transformed using a Fourier transform, to provide a single-beam spectrum. The resolution of the interferometer depends on the distance, x, the moving mirror travels, or the maximum optical path difference, $2x$. The advantages of FT-IR are shorter analysis time, improved signal-to-noise ratio and precise wave number calibration. [19]

3.6.2 WAX ANALYSIS BY IR

The IR analysis method used was that developed in other Sasol laboratories for wax analysis.

When preparing a KBr pellet, it is important to pay attention to sample homogeneity and concentration. The correct amount of sample gives a good analysis, with a full-scale paraffinic stretching vibration at ca. 2900 cm^{-1}. Too much sample results in this vibration being off-scale. The consequence is that the paraffinic overtone vibrations between ca 1800 and 2500 cm^{-1}, which are insignificant when interpreting an analysis, are now also amplified. As these vibrations

coincide with certain bands used to characterise other functionalities, such as an ester, this will lead to incorrect interpretation of the spectrum.

Failure to adequately purge the system with dry air or nitrogen manifests as an excessively noisy spectrum. The noise may be misinterpreted as specific functionalities. Furthermore, bands become apparent at > 3000 cm^{-1} and ca. 1620 cm^{-1}, due to moisture, and at ca. 2200 cm^{-1}, due to carbon dioxide.

3.6.3 EXPERIMENTAL

The IR analyses were performed on a Nicolet Magna 560 FT-IR, controlled using Omnic software. An analysis comprised 32 scans performed between wavenumbers 4000 and 400 cm^{-1}, using resolution and gain settings of 4. Approximately 0.2g of sample was compounded into a KBr pellet of standard dimensions.

3.7 OTHER ANALYSES

Other analytical techniques, viz. determinations of congealing point, drop melting point, viscosity, penetration, density, acid value and saponification value, were employed to further characterise the waxes.

3.7.1 CONGEALING POINT

Congealing point is a measure of the temperature at which a wax solidifies. It is the temperature at which a droplet of molten wax adhering to the bulb of a thermometer ceases to flow. [20]

3.7.2 DROP MELTING POINT

Drop melting point is the temperature at which a wax becomes sufficiently fluid to flow under gravity. A thermometer bulb is coated with wax and then placed in a test tube in a heated

glycerine bath. The temperature at which the first drop of wax falls from the thermometer is its drop melting point. The viscosity of the wax has a large influence on this characteristic. [21]

3.7.3 VISCOSITY

The viscosity of a wax is its resistance to flow under a shear stress in the molten state. It is a measure of the fluidity of the wax. The torque necessary to overcome the resistance from the molten wax to the rotation of a spindle of specific dimensions is a measure of its viscosity. [22]

3.7.4 DENSITY

Density is defined as mass per unit volume. It is an indication of how optimally the wax molecular chains pack in the solidified crystal, given a specific molecular mass and structure.

3.7.5 PENETRATION

Penetration is a measure of the hardness of the wax. The depth, in tenths of a millimetre, to which a standard needle penetrates into the wax at a specific temperature and under a specified load, is its penetration. [23]

3.7.6 ACID VALUE

The acid value of an oxidised wax is a measure of the amount of organic (carboxylic) acid functional groups present in the wax. It is the number of milligrams of potassium hydroxide necessary to neutralise these acids present in one gram of wax. [24]

3.7.7 SAPONIFICATION VALUE

The saponification value of an oxidised wax is a measure of the amount of carboxylic acid and ester functionalities present in the wax. It is the number of milligrams of potassium hydroxide necessary to neutralise these groups present in one gram of wax. This test is similar to that for

the acid value, but is performed at an elevated temperature to ensure saponification of the ester groups. [24]

3.7.8 MEK/ MIBK SOLUBLES

The amount of material present in a wax sample that will dissolve in methyl ethyl ketone (MEK), or methyl iso-butyl ketone (MIBK), at –32 °C, is referred to as the oil content of a wax. Its composition includes very low molecular mass and branched material. The higher this value, the more unsuitable the wax is for use in certain applications such as food, due to the adverse bioactivity of these materials. MEK and MIBK are used as solvents for lower and higher molecular mass waxes, respectively. [25]

3.8 REFERENCES

(1) M. E. Brown, Getting Started in Thermal Analysis, 1985, 3rd Ed., Rhodes University, Grahamstown.

(2) C. A. Sperati et al, J. Am. Chem. Soc., December 1953, 75, 6127-6133.

(3) ASTM D4419, American Society for Testing and Materials Standard, 1990, WorldWide Standards Service Plus, Issue 00-06 v4.0, Electronic Version.

(4) ASTM D341, American Society for Testing and Materials Standard, 1993, WorldWide Standards Service Plus, Issue 00-06 v4.0, Electronic Version.

(5) ASTM D3418, American Society for Testing and Materials Standard, 1999, WorldWide Standards Service Plus, Issue 00-06 v4.0, Electronic Version.

(6) R. J. Young and P. A. Lovell, Introduction to Polymers, 1991, 2nd Ed., Chapman and Hall, London.

(7) D. W. Bamborough and P. M. Dunkley, Adhesives Age, November 1990, 20-26.

(8) A. Renfrew and P. Morgan, Ed., Polythene. The Technology and Uses of Ethylene Polymers, 1957, 2nd Ed, Illiff, London.

(9) F. W. Billmeyer, Textbook of Polymer Science, 1984, 3rd Ed., John Wiley and Sons, New York.

(10) I. M. Ward, Mechanical Properties of Solid Polymers, 1983, 2nd Ed., John Wiley and Sons, Chichester.

(11) K. H. Illers, Rheol. Acta, 1964.

(12) H. Sha et al, Thermochim. Acta, 1991, 192, 233-242.

(13) G. V. Webber, Schümann Sasol Internal Memorandum SW1891, 1997.

(14) W. W. Jau et al, Modern Size-Exclusion Liquid Chromatography, 1979, John Wiley and Sons, New York.

(15) RAPRA Technology Ltd., RAPRA review report 83, Molecular Wight Characterisation of Synthetic Polymers, 1995, 7 (11).

(16) N. Naidoo, Schümann Sasol Internal Memorandum SW2702, 1998.

(16) E. R. Adlard (Ed.), Chromatography in the Petroleum Industry, Journal of Chromatography Library Series, 1995, Volume 56, Chapter 3, Elsevier Science.

(17) Medunsa Capillary Chromatography course notes, 1999.

(19) H. H. Willard et al, Instrumental Methods of Analysis, 1988, 7th Ed., Wadsworth Publishing Company, Belmont California.

(20) ASTM D938, American Society for Testing and Materials Standard, 1992, WorldWide Standards Service Plus, Issue 00-06 v4.0, Electronic Version.

(21) ASTM D127, American Society for Testing and Materials Standard, 1987, WorldWide Standards Service Plus, Issue 00-06 v4.0, Electronic Version.

(22) Sasol Analytical Method No. 1.121/78, 1978.

(23) ASTM D1321, American Society for Testing and Materials Standard, 1997, WorldWide Standards Service Plus, Issue 00-06 v4.0, Electronic Version.

(24) Sasol Analytical Method No. 2.72/84, 1984.

(25) ASTM D721, American Society for Testing and Materials Standard, 1997, WorldWide Standards Service Plus, Issue 00-06 v4.0, Electronic Version.

CHAPTER 4

THE FISCHER TROPSCH WAXES

4.1 SCHÜMANN SASOL FISCHER TROPSCH WAXES

4.1.1 INDUSTRIAL SYNTHESIS AND ECONOMIC SIGNIFICANCE

Sasol pioneered the use of the Fischer Tropsch process to synthesise hydrocarbon waxes and other products from a mixture of carbon monoxide and hydrogen (syngas), by passing steam over hot coal. [1] The synthesis is carried out using metallic catalysts, such as cobalt, iron or nickel. The selectivity of the synthesis process, in terms of the type of product formed, is influenced by the temperature and pressure employed. At normal pressures, a range of petroleum-like hydrocarbons is formed, from which waxes are derived by fractionation. Until recently, Sasol was the only plant in the world using this process. The hydrocarbon stream consists mainly of a mixture of n-alkanes in the range of approximately C_5 to C_{120}. Low levels of unsaturation and branching are present. Unsaturation is removed by hydrogenation.

One source claims that the consumption of Fischer Tropsch waxes is 100 000 t/a. [1] Fischer Tropsch waxes are used in many diverse applications, which include hot melt adhesives (HMAs), inks, paints, coatings, polishes, plastics, fruit coating emulsions, mould release agents, candles and many other speciality applications.

Paraflint H1 is a residue cut from the primary wax stream produced at Schümann Sasol SA (Pty) Ltd. It is further fractionated into lower and higher molecular mass fractions, viz. Paraflint C80 and Paraflint C105, respectively. Paraflint A1, and Paraflint A975 and Paraflint A28, are oxidised products based on Paraflint H1 and Paraflint C105, respectively.

The structure of a Fischer Tropsch wax is illustrated in Figure 4.1. [2] Zone A is an amorphous phase containing chain ends, and its extent is determined by the chain end concentration. This is about 4% for a Fischer Tropsch hard wax. Zone B is a rigid amorphous phase resulting from branching. Less than 5 methyl branches per 1000 carbon atoms occur in hard wax fractions. The mobile amorphous zone C consists of the lowest melting iso-paraffins that end up between crystallites during crystallisation. Zone D represents about 90% of the

volume of the wax and resembles a pure n-alkane. It normally has an orthorhombic structure below the melting point. [2]

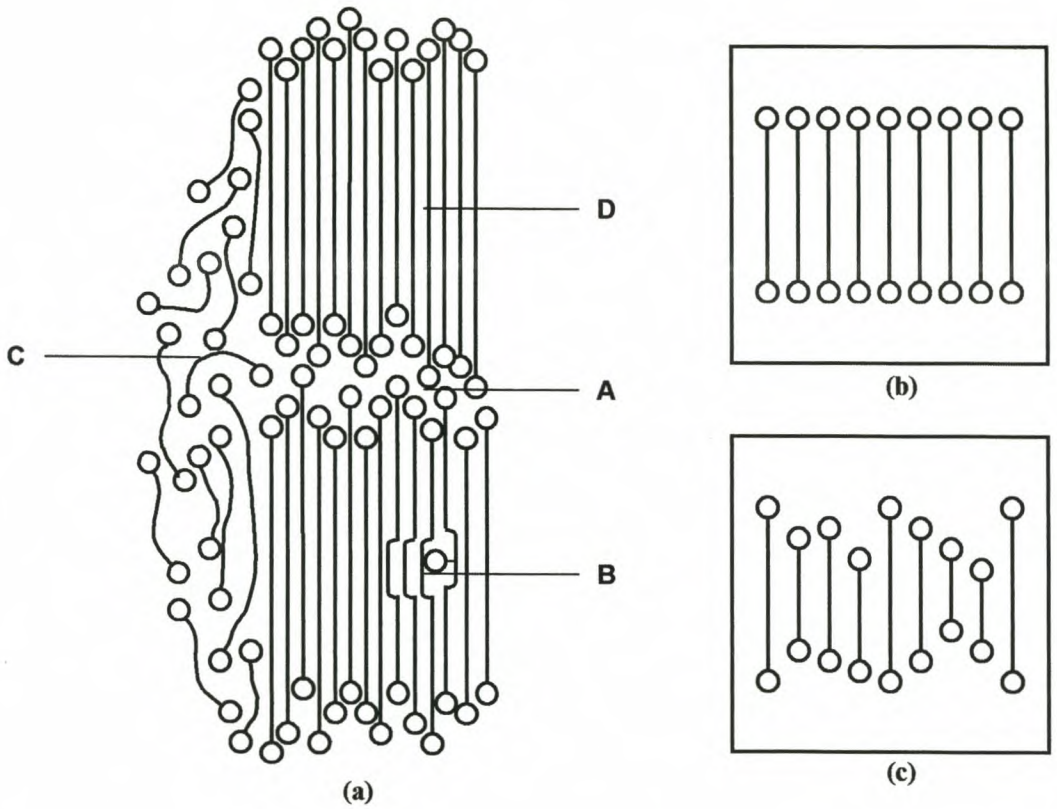

Figure 4.1: (a) Graphic representation of the structure of a paraffinic or Fischer Tropsch wax. A: Chain-end defect zone; B: branch defect zone; C: mobile amorphous zone; D: crystalline zone. (b) Regular arrangement of chains in a pure n-alkane. (c) Irregular arrangement of chains in a wax. [2]

Oxidation imparts desirable properties to the Fischer Tropsch waxes. These include ease of emulsifiability and tack. Oxidation of wax molecules proceeds according to a free radical mechanism. Chain scission therefore occurs. Functionalisation will preferentially occur at a secondary carbon atom site. The functionalities formed include hydroxyls, carbonyls, acids and esters. [3] The steric hindrance caused by the oxygenate groups causes a disruption of the crystal packing, in much the same way that branching does. It may therefore be expected that the functionalised product will have a lower crystallinity, and consequently fusion enthalpy, than its feed material. Furthermore, the chain scission that occurs during the reaction will produce lower molecular mass material. [3]

4.1.2 ANALYSIS PROFILE

Tables 4.1 and 4.2 summarise the results obtained from the instrumental analyses of the Schümann Sasol Fischer Tropsch waxes.

Table 4.1: Analysis results of the unfunctionalised Schümann Sasol Fischer Tropsch hard waxes

Analysis	Paraflint H1	Paraflint C80	Paraflint C105
DSC			
Melt range, °C	33-113	22-102	39-118
Maxima, °C	77/101	76	99/108
Fusion enthalpy, J/g	232	218	228
TG			
Onset temp., °C	332	310	417
Temp. @0.5% weight loss, °C	245	210	295
DTG max, °C	434	360	480
Rheometry			
T_{α}, °C	23	-11	28
T_{β}, °C	-	-	-
GPC			
M_n, Daltons	650	552	861
M_w, Daltons	813	579	1038
M_z, Daltons	1134	607	1311
P_d	1.25	1.04	1.21
HTGC			
Carbon no. spread	C_{14}->C_{95}	C_{14}-C_{86}	C_{14}->C_{95}
% n-paraffins	97.54	93.93	98.79
% iso-paraffins	2.46	3.07	1.21

Table 4.2: Analysis results of the functionalised Schümann Sasol Fischer Tropsch hard waxes

Analysis	Paraflint A1 (acid value = 27)	Paraflint A975 (acid value = 15)	Paraflint A28 (acid value = 29)
DSC			
Melt range, °C	12-102	21-110	19-108
Maxima, °C	71/93	92/103	90/102
Fusion enthalpy, J/g	165	191	166
TG			
Onset temp., °C	295	296	377
Temp. at 0.5% weight loss, °C	150	145	142
DTG maxima, °C	378/473/565	376/445/566	443/565
Rheometry			
T_α, °C	60	74	70
T_β, °C	-25	1	-11
GPC			
M_n, Daltons	540	869	723
M_w, Daltons	669	974	895
M_z, Daltons	867	1118	1120
P_d	1.24	1.12	1.24

4.1.2.1 DSC

The DSC analyses of the Fischer Tropsch hard waxes, with the exception of Paraflint C80, display very interesting bimodal melting behaviour (Figure 4.2). An examination of the literature has excluded all the most obvious reasons for bimodality, such as re-crystallisation, [4] polymorphism, [5] bimodal MMD and chain folding. [6]

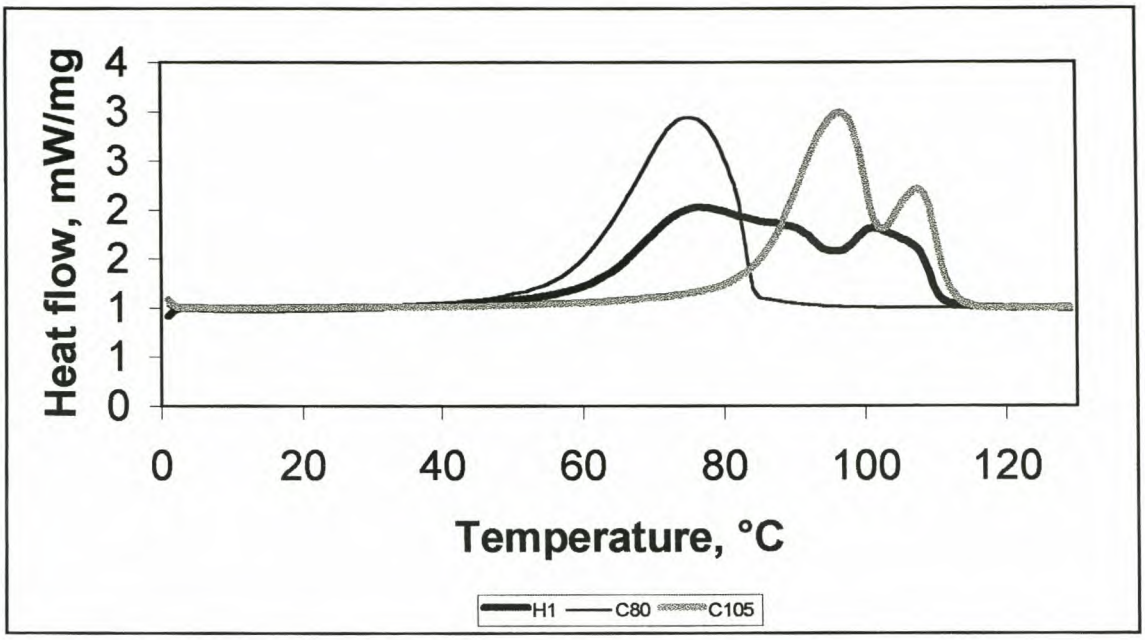

Figure 4.2: Comparison of the DSC analyses of the unfunctionalised Schümann Sasol Fischer Tropsch hard waxes

It is known that the presence of impurities in a sample results in the depression of its melting point. [7] These solubility effects are illustrated by comparing the DSC analyses of Paraflint waxes H1, C80 and C105 (Figure 4.2 and Table 4.1). The DSC melting curve of Paraflint C105, the high molecular mass fraction from Paraflint H1, shows from the DSC end of melt temperatures that the former contains higher melting material than the latter. This is impossible, considering the derivation of the samples. The DSC maxima of Paraflint C105 also occur at higher temperatures than those of the latter. Likewise, a comparison of the beginning of melt temperatures of Paraflint C80 and Paraflint H1 shows that the former (the lower molecular mass fraction from H1) contains lower melting material than the latter, which is again impossible. The DSC maximum of the former also appears at a slightly lower temperature than the latter. This illustrates the limitations of using DSC to compare molecular mass distributions of samples without obtaining more information regarding the nature of the samples. It is shown in the following sections of this chapter that the use of DSC in conjunction with other techniques will prevent the analyst from falling into this trap. It is, however, possible to draw tentative comparisons between different batches of the same type of wax in order to ascertain the consistency of a product with regard to its melting characteristics.

The fusion enthalpies of Paraflint H1 and Paraflint C105 are similar. This illustrates that there is a complex dependence of the fusion enthalpy on a number of factors, as discussed above.

The analyst should therefore be careful to read too much into the fusion enthalpies measured. It is, however, possible to directly compare the fusion enthalpies of different batches of the same product, or of samples with similar melting ranges.

Figures 4.3 and 4.4 and Table 4.2 illustrate the effect of functionalisation on the melting characteristics of wax samples. Paraflint A1 is Paraflint H1 oxidised to an acid value of 27 mg KOH/g. Paraflint A975 and Paraflint A28 are Paraflint C105 oxidised to acid values of 15 mg KOH/g and 29 mg KOH/g, respectively. In both cases, the oxidised waxes display a shift in their end of melt temperatures and DSC maxima to lower temperatures, as well as a decrease in their fusion enthalpies. As discussed in section 4.1.1, chain scission occurs during wax oxidation and functionalisation will preferentially occur at a secondary carbon atom site. This short chain material causes a solubility effect and is the reason for the shift in the DSC maxima to lower temperatures. The steric hindrance of the oxygenate groups disrupts the crystal packing. It may therefore be expected that the fuctionalised product will have a lower crystallinity, and consequently fusion enthalpy, than the original, unfunctionalised (feed) material. It is sensible to directly compare the DSC analyses of a sample and its chemically modified counterparts, as useful information may be obtained concerning the way in which functionalisation influences the melting properties of a wax.

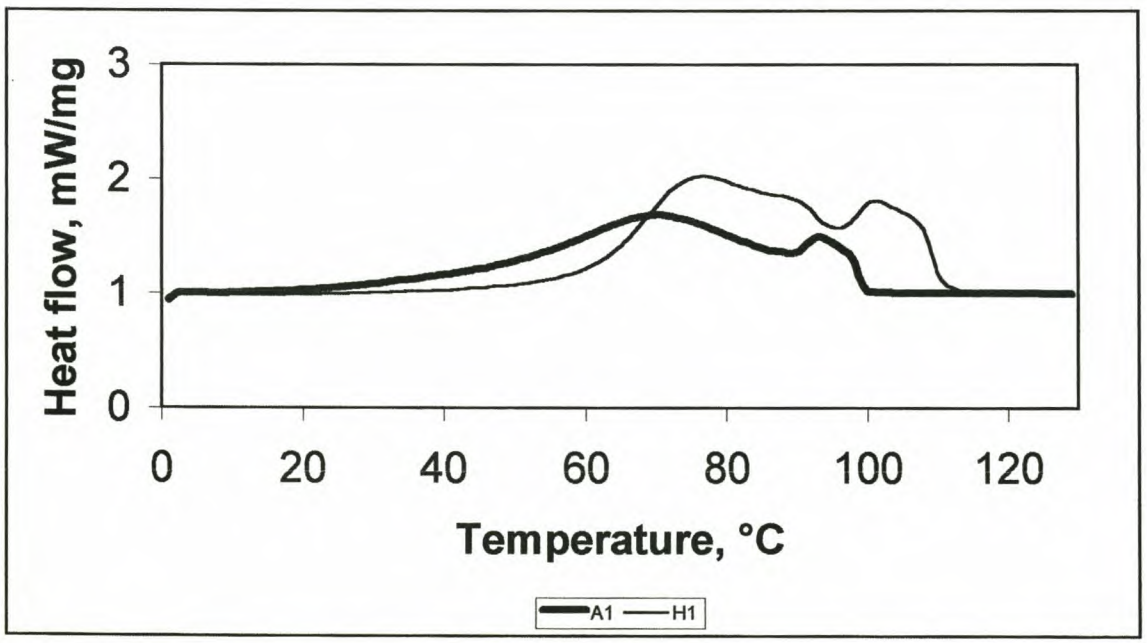

Figure 4.3: Comparison of the DSC analyses of Paraflint H1 and its functionalised counterpart

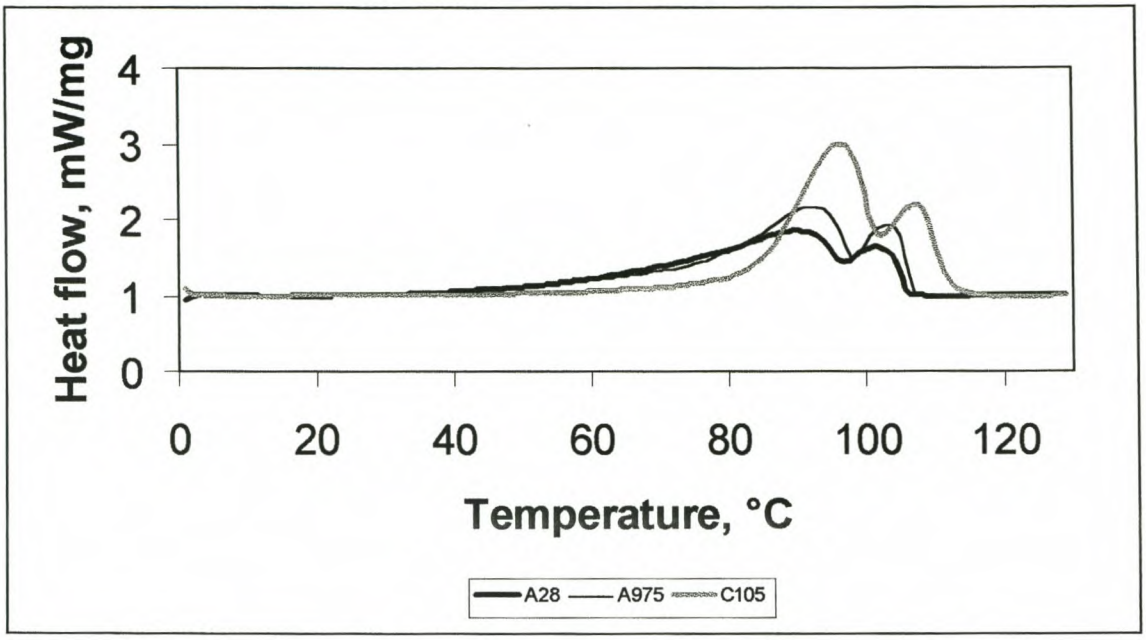

Figure 4.4: Comparison of the DSC analyses of Paraflint C105 and its functionalised counterparts

4.1.2.2 TG

The TG analyses of the Paraflint waxes H1, C80 and C105 are compared in Figure 4.5. Table 4.1 has shown that the TG onset temperatures of Paraflint H1 and Paraflint C80 are similar. The onset temperature of Paraflint C105 is much higher than those of the two aforementioned samples. This is to be expected, as Paraflint C80 and Paraflint C105 are the lower and higher molecular mass fractions, respectively, from Paraflint H1. Both Paraflint H1 and Paraflint C80 therefore contain material of the same molecular mass on the lower end of their carbon distributions. The DTG maxima increase, as expected, with increasing molecular mass along the series Paraflint C80< Paraflint H1< Paraflint C105. The waxes Paraflint C80 and Paraflint C105 also have narrower DTG peaks than Paraflint H1. This, again, is to be expected considering that they are cuts from Paraflint H1.

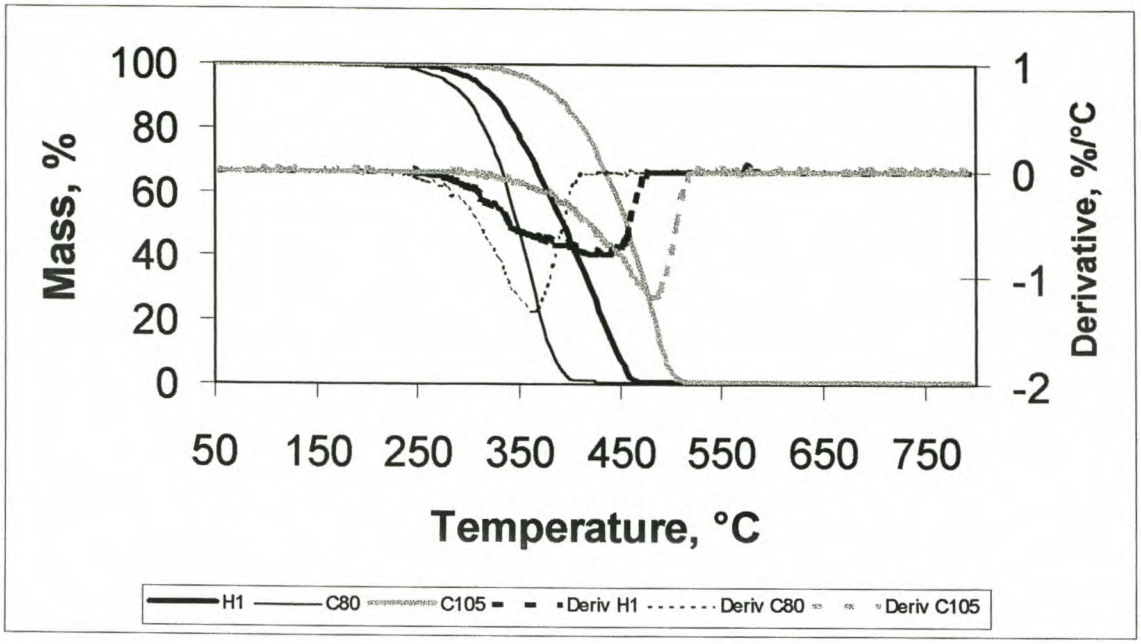

Figure 4.5: Comparison of the TG analyses of the unfunctionalised Schümann Sasol Fischer Tropsch hard waxes

The TG analyses of the functionalised wax Paraflint A1, is compared with that of its feed material Paraflint H1, in Figure 4.6. Figure 4.7 compares the TG analyses of the functionalised waxes Paraflint A975 and Paraflint A28 with that of their feed material, Paraflint C105. The TG onset temperatures of the functionalised Paraflint waxes A1, A975 and A28, (Table 4.2), are lower than those of their unfunctionalised counterparts. These findings substantiate the results of the DSC analyses. There it was noted that the melting peaks of the oxidised waxes shifted to lower temperatures, as a result of the formation of low molecular mass material during oxidation. The DTG plots of the functionalised waxes display a small characteristic peak at ca. 570°C. The reason for this is that the analysis atmosphere is switched from nitrogen to oxygen at 500°C, and its effect on the sample is noted at ca. 570°C, where any remaining carbonaceous residue is combusted to CO_2. This peak is not apparent in the analyses of the unfunctionalised waxes. Oxidation raises the boiling point of a hydrocarbon molecule. [8] The decomposition of the oxidised waxes is therefore not yet complete at ca. 570°C. Introduction of oxygen results in rapid burn-off of any remaining residue.

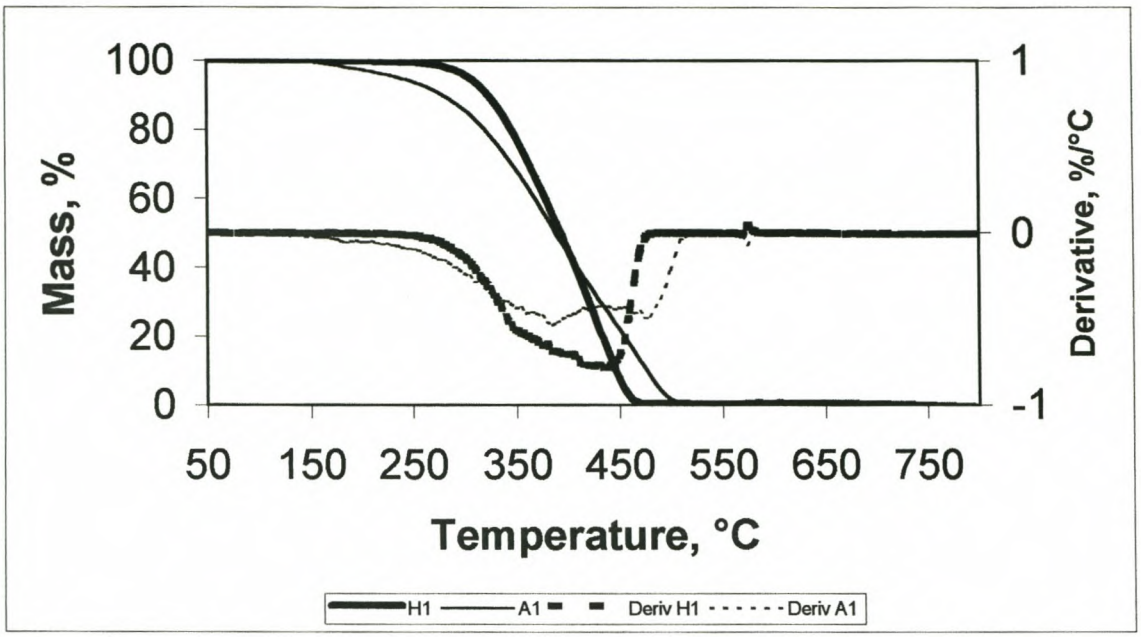

Figure 4.6: Comparison of the TG analyses of Paraflint H1 and its functionalised counterpart

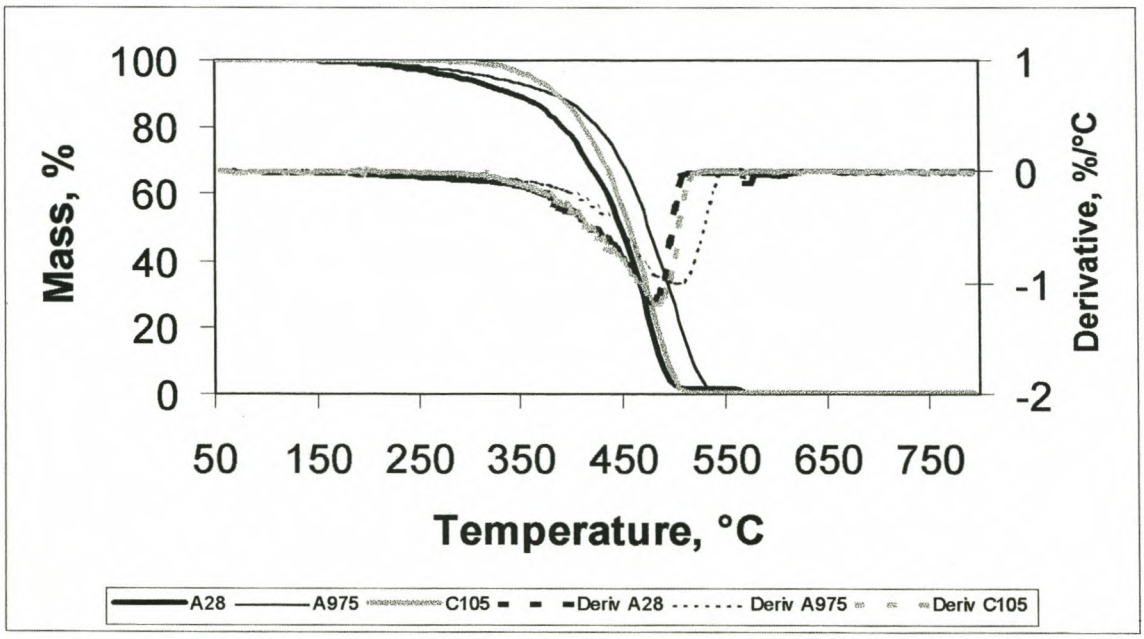

Figure 4.7: Comparison of the TG analyses of Paraflint C105 and its functionalised counterparts

4.1.2.3 RHEOLOGY

A comparison of the storage moduli (G') trends of the Paraflint waxes H1, C80 and C105 are shown in Figure 4.8. The wax hardness, and therefore crystallinity, decreases along the series Paraflint C105/ Paraflint H1> Paraflint C80. The G' results for Paraflint H1 and Paraflint C105 are indistinguishable. This implies that sample stiffness, brittleness, strength and toughness will also decrease along this series, while flexibility will increase (see section 3.3.1.1). At subambient temperatures, tan δ decreases along the series Paraflint C80> Paraflint H1> Paraflint C105, as seen in Figure 4.9. This implies that Paraflint C105 has the greatest cohesive strength, and therefore the lowest flexibility in the series (see section 3.3.1.2). Paraflint C105 has the highest molecular mass of these three waxes and therefore the lowest free volume, due to low branch content and a smaller contribution of end groups to crystal-packing disruption. Only one relaxation transition is observed on the tan δ curves of these three unfunctionalised waxes. T_γ is not apparent as it occurs below the initial temperature of the experiment. T_β is absent due to negligible levels of branching in these waxes. The value of T_α increases along the series Paraflint C80< Paraflint H1< Paraflint C105, in line with the increase in molecular mass (see section 3.3.1.4).

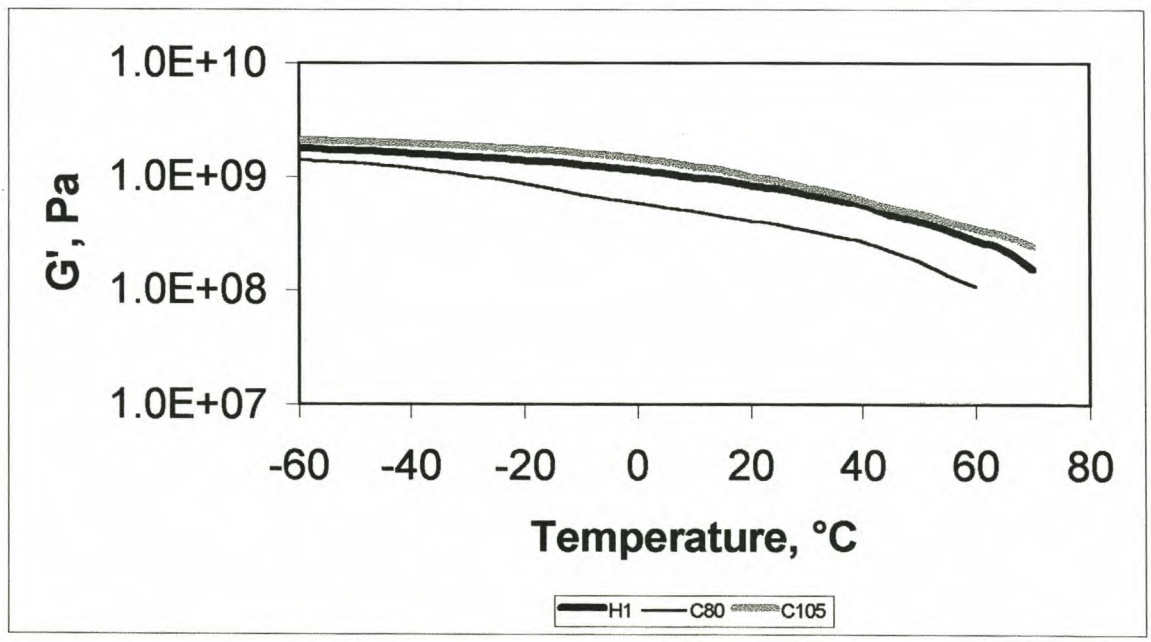

Figure 4.8: Comparison of the storage moduli of the unfunctionalised Schümann Sasol Fischer Tropsch hard waxes

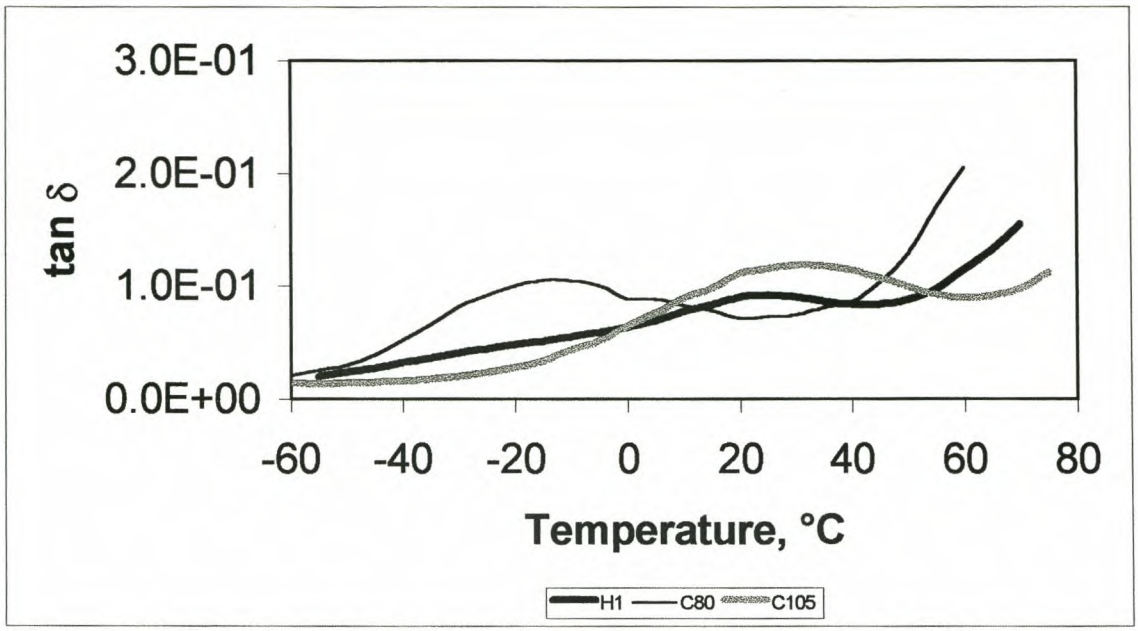

Figure 4.9: Comparison of the tan δ curves of the unfunctionalised Schümann Sasol Fischer Tropsch hard waxes

The storage moduli of the functionalised Fischer Tropsch hard waxes are lower than those of their unfunctionalised counterparts (Figure 4.10), implying decreased hardness, stiffness and brittleness (see section 3.3.1.1). This is due to disruption in the crystallinity upon the introduction of oxygenate functionalities. The functionalised Fischer Tropsch hard waxes display higher tan δ values than their respective unfunctionalised counterparts (Figure 4.11), which is indicative of their lower cohesivity. This implies greater flexibility, which is to be expected, as the introduction of polar groups will increase the free volume because of disruption of the crystal packing (see section 3.3.1.2). The functionalised waxes display both T_α and T_β relaxation transitions. The T_α transitions occur at higher temperatures than observed for the unfunctionalised counterparts. The polar interactions restrict rotation, thereby delaying the occurrence of the relaxation transition until a higher temperature. The T_β transition is ascribed to the presence of the functional groups, which are effectively short chain branches (see section 3.3.1.4).

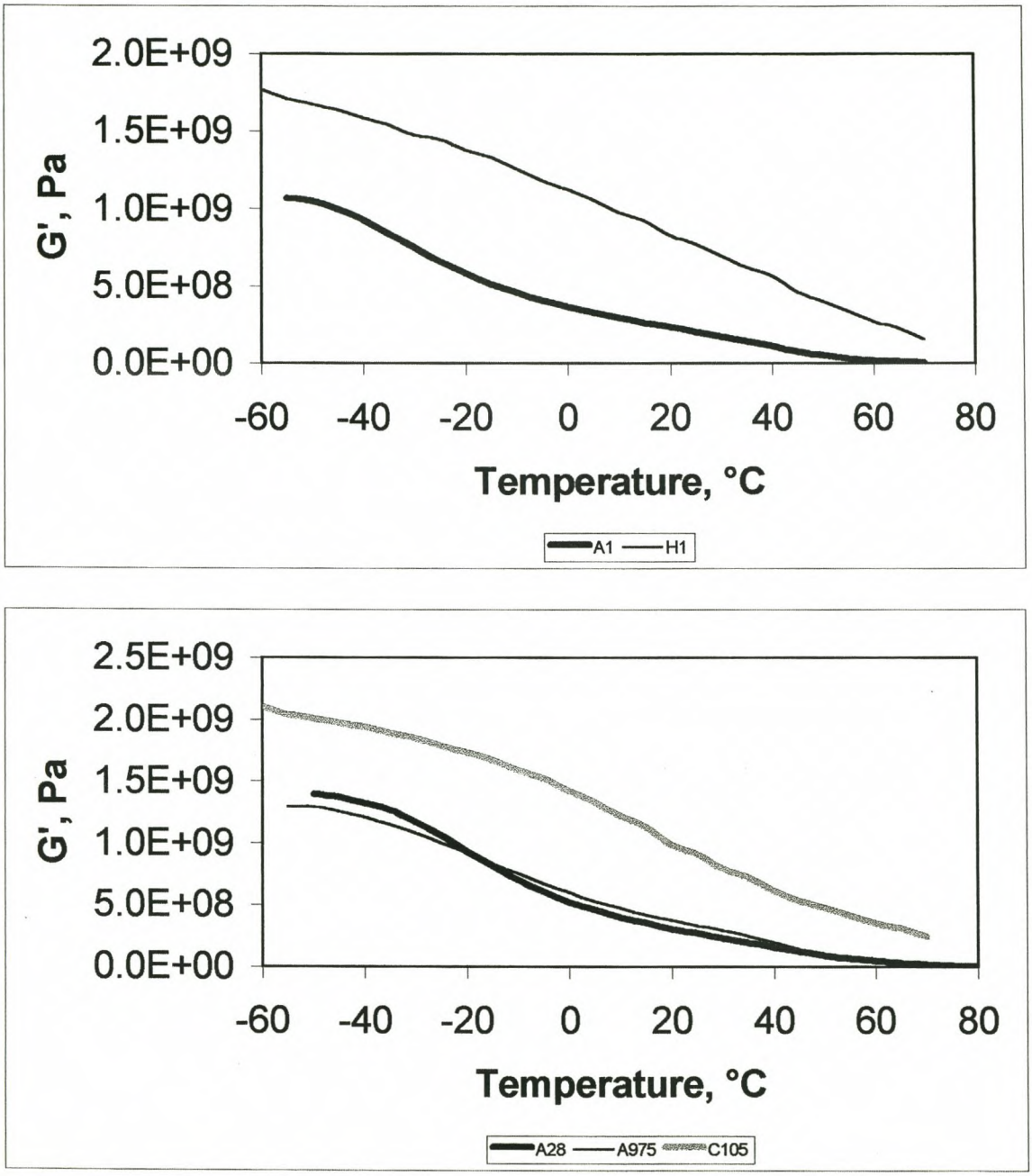

Figure 4.10: Comparison of the storage moduli of the functionalised Schümann Sasol Fischer Tropsch hard waxes

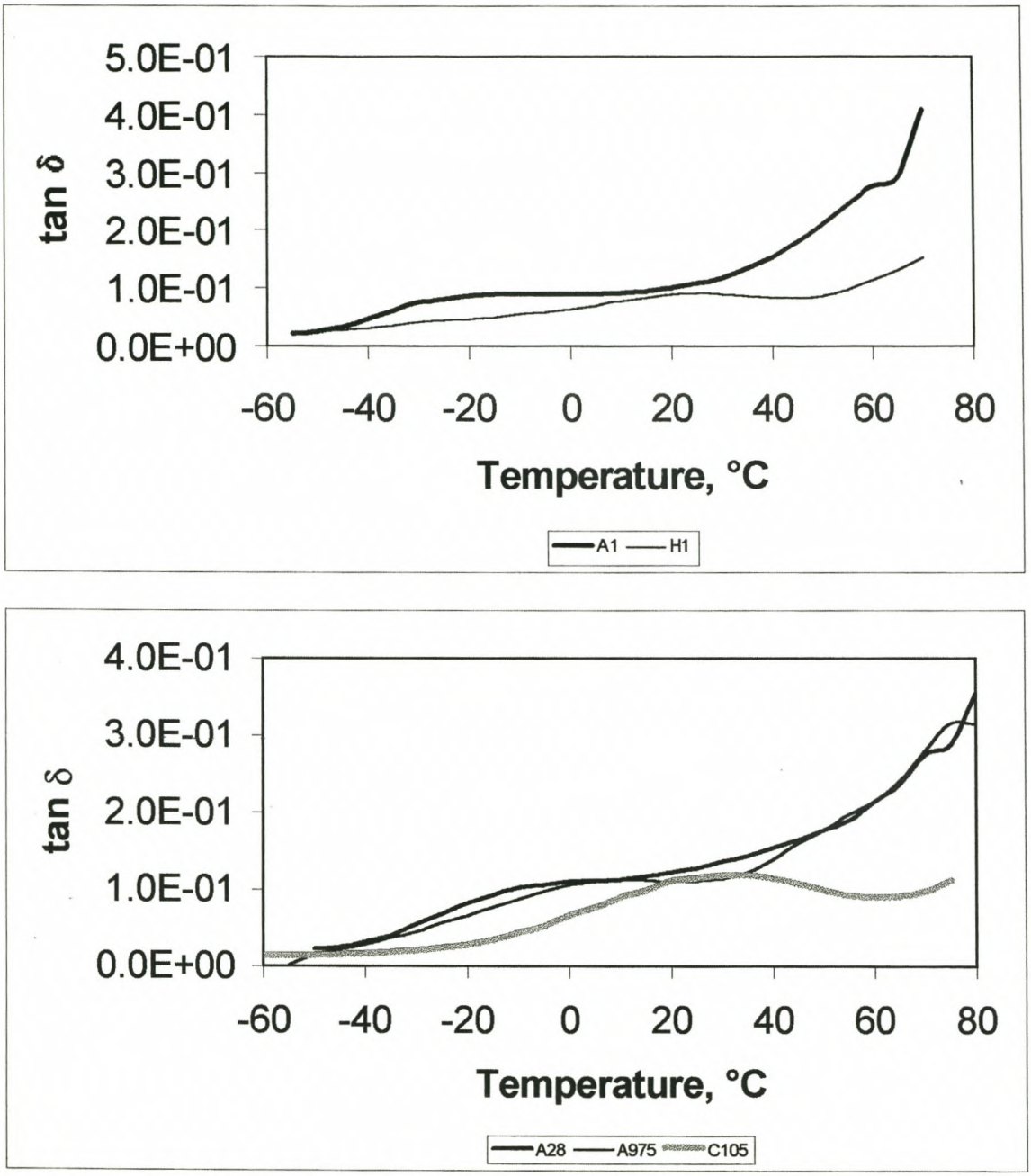

Figure 4.11: Comparison of the tan δ curves of the functionalised Fischer Tropsch hard waxes

4.1.2.4 GPC

The GPC analyses of the unfunctionalised Schümann Sasol Fischer Tropsch waxes (Figure 4.12 and Table 4.1) show that all three molecular mass averages, viz. M_n, M_w, M_z, increase along the series Paraflint C80< Paraflint H1< Paraflint C105. This is in agreement with the DSC and TG data, and with the manner in which the waxes are derived, viz. Paraflint C80 and Paraflint C105 are low and high molecular mass fractions from Paraflint H1, respectively. The waxes do not display bimodal MMDs, ruling this out as the reason for the melting bimodality observed in the DSC analyses of Paraflint H1 and Paraflint C105 (see section 4.1.2.1).

The functionalised Fischer Tropsch waxes (Figures 4.13 and 4.14 and Table 4.2) have lower molecular mass parameters than their unfunctionalised counterparts. This confirms that the shift in the DSC melting peaks of the former to lower temperatures, when compared to the latter, is the result of scission of the longer chain molecules during oxidation (see section 4.1.2.1).

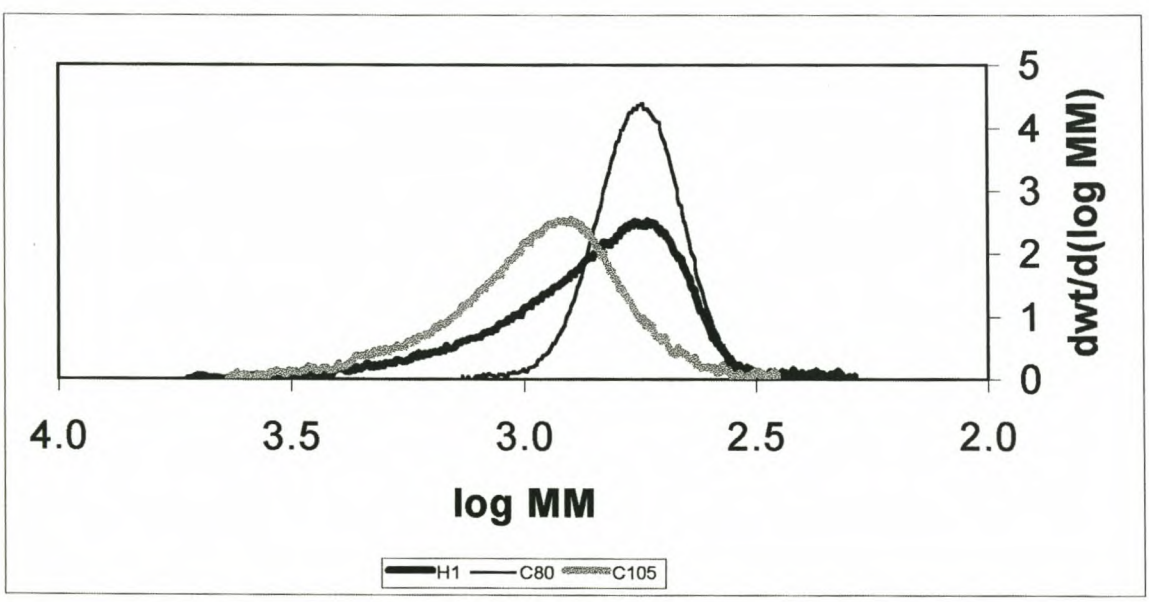

Figure 4.12: Comparison of the GPC analyses of the unfunctionalised Schümann Sasol Fischer Tropsch hard waxes

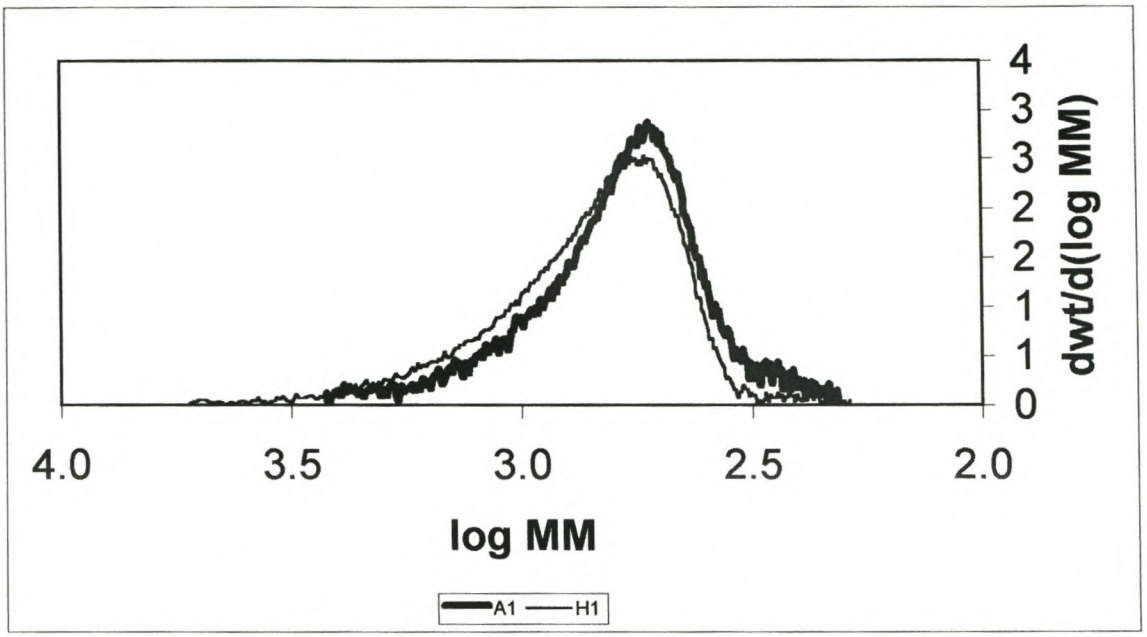

Figure 4.13: Comparison of the GPC analyses of Paraflint H1 and its functionalised counterpart

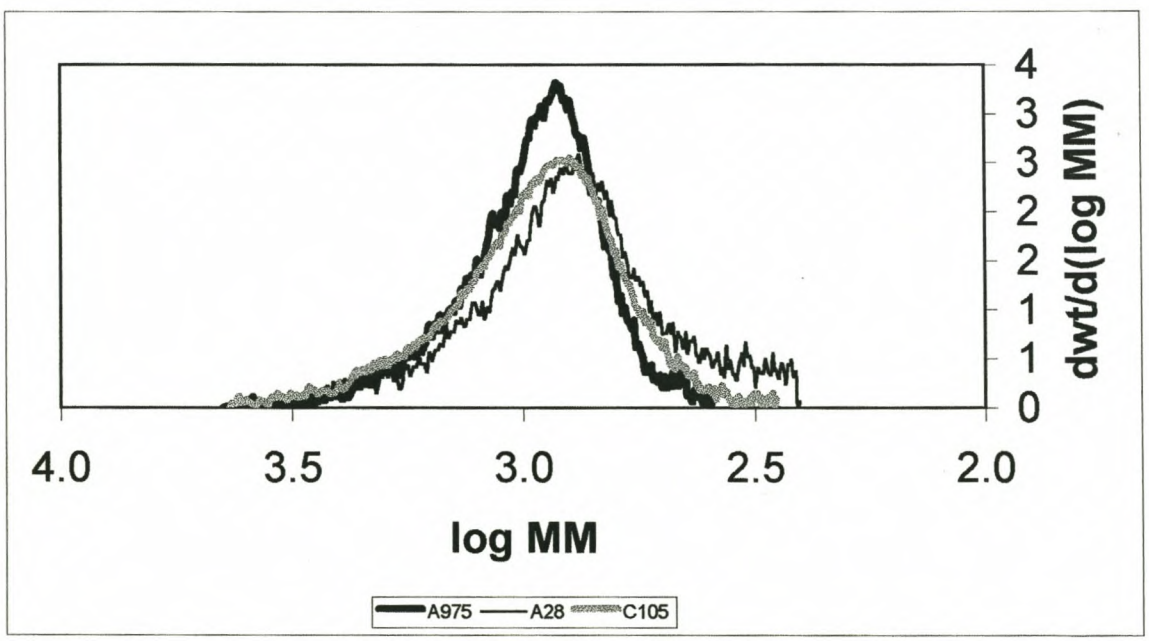

Figure 4.14: Comparison of the GPC analyses of Paraflint C105 and its functionalised counterparts

4.1.2.5 HTGC

HTGC analyses of the unfunctionalised Fischer Tropsch hard waxes appear in Figure 4.15 and Table 4.1. Wax carbon distribution increases along the series Paraflint C80< Paraflint H1< Paraflint C105, as observed from the GPC analyses (see section 4.1.2.4). The carbon distributions of Paraflint H1 and Paraflint C105 are incomplete, due to the inability of the technique to analyse the very high molecular mass components present. The low iso-paraffin content of these waxes is indicative of a low level of branching (Table 4.1). It decreases along the series Paraflint C80> Paraflint H1> Paraflint C105. Considering the manner in which Paraflint C80 and Paraflint C105 are derived, this shows that the branched material is more concentrated in the lower molecular mass portion of Paraflint H1. HTGC analyses were not performed on the functionalised Fischer Tropsch hard waxes, as it was suspected that they will adsorb to and damage the column stationary phase.

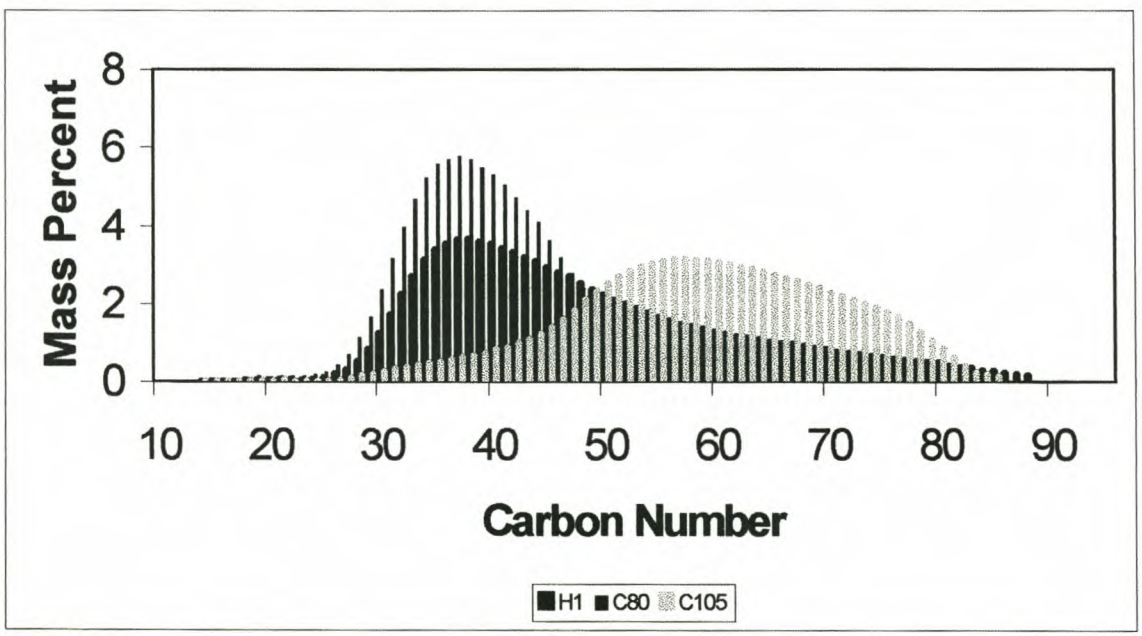

Figure 4.15: Comparison of the HTGC analyses of the unfunctionalised Schümann Sasol Fischer Tropsch hard waxes

4.1.2.6 IR

The IR analyses of Paraflint waxes H1, C80 and C105 (Figure 4.16) show the characteristic paraffinic stretching, bending and rocking vibrations at ca. 2900, 1400 and 720 cm^{-1}. The IR analyses of Paraflint waxes A1, A975 and A28 (Figure 4.17) display, in addition to the above

characteristic paraffinic vibrations, hydroxyl (3500-3600 cm^{-1}), carboxylic (ca. 1720 cm^{-1}) and ester (ca. 1740 cm^{-1}) functionalities. These are due to the carboxylic acids, ketones, aldehydes, alcohols and esters, which are known to form during wax oxidation.

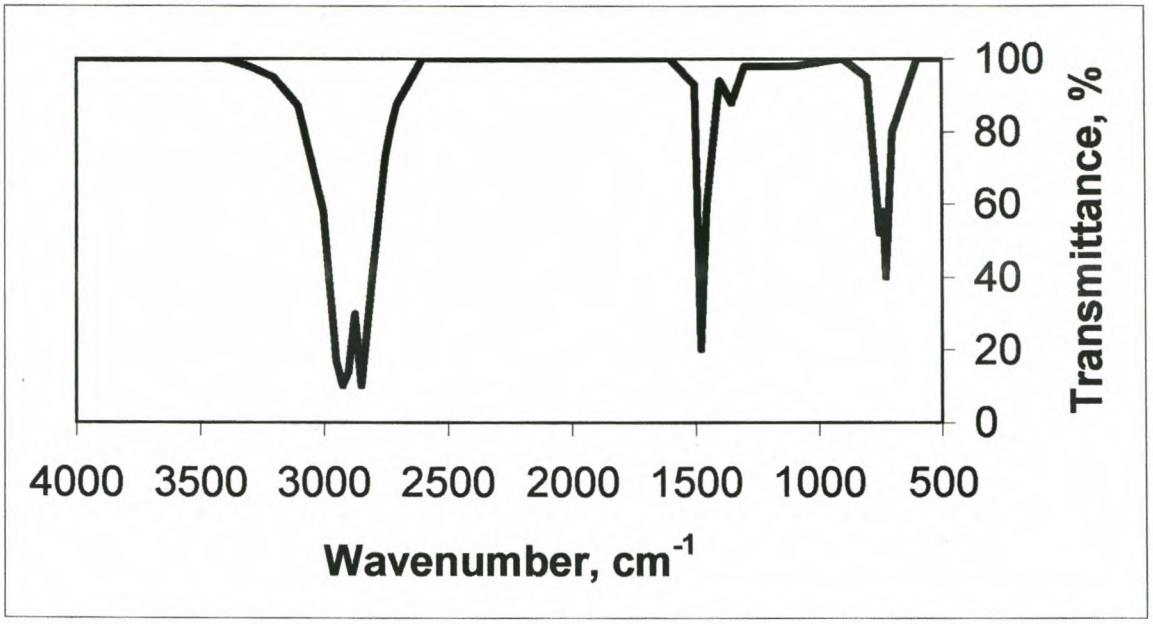

Figure 4.16: Typical IR analysis of an unfunctionalised Schümann Sasol Fischer Tropsch hard wax

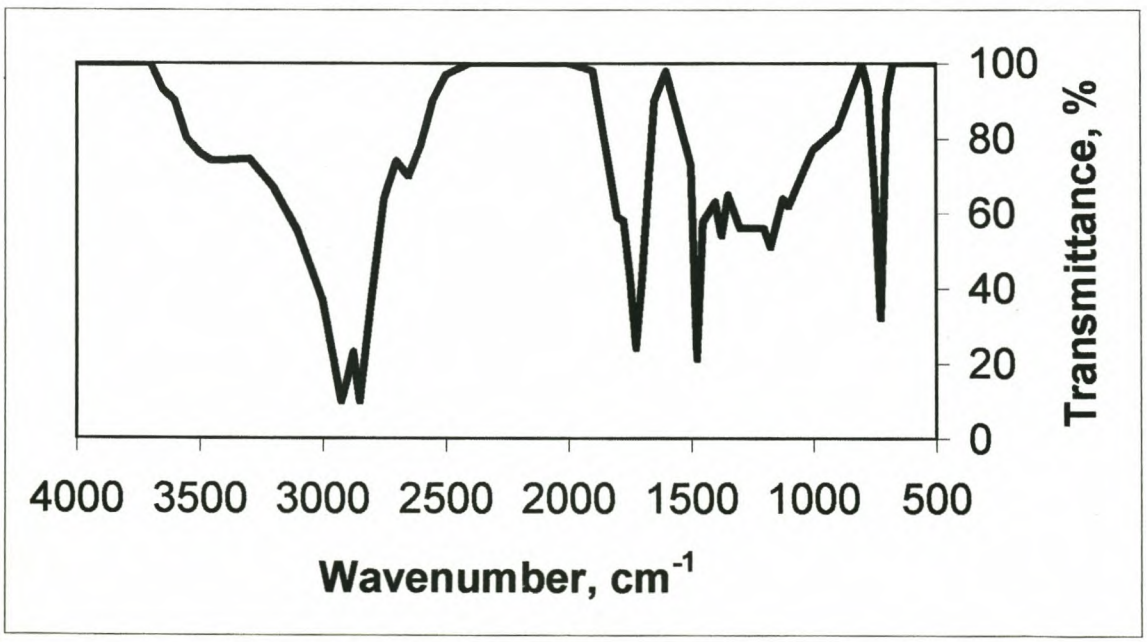

Figure 4.17: Typical IR analysis of a functionalised Schümann Sasol Fischer Tropsch hard wax

4.1.2.7 WET CHEMICAL ANALYSES

The wet chemical analysis data of the Schümann Sasol Fischer Tropsch waxes is tabulated in Table 4.3.

Table 4.3: Physical properties of the Schümann Sasol Fischer Tropsch waxes

Analysis	Paraflint H1	Paraflint C80	Paraflint C105	Paraflint A1	Paraflint A975	Paraflint A28
Congealing point (°C)	97	80	102	86	97	95
Drop melting point (°C)	106	85	117	102	110	105
Viscosity @135°C (cP)	7.9	3.9	15.0	11.0	15.0	19.0
Penetration @25°C (dmm)	1	6	1	8	2	4
Penetration @65°C (dmm)	23	66	6	113	33	69
Density @25°C (g/cm^3)	0.94	0.92	0.95	0.95	0.94	0.94
Acid number (mgKOH/g)	-	-	-	27	15	29
Saponification number (mgKOH/g)	-	-	-	55	30	56
MEK solubles (%)	-	0.3	-	-	-	-
MIBK solubles (%)	0.8	-	0.1	-	-	-

The congealing and drop melting points, viscosities and penetration values at 65°C of the unfunctionalised waxes increase along the series Paraflint C80< Paraflint H1< Paraflint C105. This correlates with the increase in molecular mass and DSC end of melt temperature observed in this series (see Table 4.1). Wax oxidation results in a decrease in the congealing and drop melting points, and penetration values at both 25°C and 65°C, of the functionalised waxes in relation to those of their unfunctionalised feed materials. A comparison of the viscosity values shows an increase in the values after functionalisation of the waxes. This is to be expected due to the effect of molecular structure and hydrogen bonding. It is interesting

to note the direct correlation between the penetration at 65°C, a temperature at which the differences in hardness of wax samples are magnified, and the acid and saponification numbers, which quantify the concentration of oxygenate functionalities. As discussed previously (see section 4.1.1), oxidation results in the disruption of the crystal lattice, with a consequent decrease in crystallinity and therefore hardness. This is in agreement with the storage modulus data (see section 4.1.2.3).

4.2 SHELL FISCHER TROPSCH WAXES

4.2.1 INDUSTRIAL SYNTHESIS AND ECONOMIC SIGNIFICANCE

The Shell Middle Distillate Process (SMDS) technology is a modern version of the Fischer Tropsch process. The process is three stage. Syngas (carbon monoxide and hydrogen) is produced in the first stage by partially oxidising natural gas with pure oxygen. The second stage involves passing the syngas through synthesis reactors, where the Fischer Tropsch reactions take place over a highly active and selective proprietary Shell catalyst. The reaction conditions favour the formation of long chain paraffinic wax molecules. In the third stage, the wax molecules are converted into middle distillates by mild hydrocracking. The middle distillate stream is fractionated to produce a wide variety of products, including kerosene, gas oil, naphtha, waxes, solvents, lubricants and detergent feedstocks. [1] The waxes are similar in composition and structure to the unfunctionalised Schümann Sasol Fischer Tropsch waxes. SX 30, SX 50, SX 70 and SX 100 are wax fractions of increasing molecular mass, with their approximate melting points indicated by the numbers in the name of the grade.

4.2.2 ANALYSIS PROFILE

The analysis properties of the Shell Fischer Tropsch waxes are tabulated in Table 4.4.

Table 4.4: Analysis results of the Shell Fischer Tropsch waxes

Analysis	Shell SX 30	Shell SX 50	Shell SX 70	Shell SX 100
DSC				
Melt range, °C	0-39	3-61	13-91	38-114
Maxima, °C	6/34	39/57	71	91/104
Fusion enthalpy, J/g	173	197	220	231
TG				
Onset temp., °C	187	236	283	353
Temp. at 0.5% weight loss, °C	132	165	205	275
DTG maxima, °C	215	275	322	410
Rheometry				
T_α, °C	-*	-45	-38	1
T_β, °C	-*	-	-	-
GPC				
M_n, Daltons	267	350	456	722
M_w, Daltons	270	359	471	795
M_z, Daltons	274	368	488	889
P_d	1.01	1.03	1.03	1.10
HTGC				
Carbon no. spread	C_{16}-C_{21}	C_{20}-C_{21}	C_{22}-C_{49}	C_{14}->C_{88}
% n-paraffins	94.53	90.25	94.08	98.77
% iso-paraffins	5.47	9.75	5.92	1.23

* Analysis not performed due to sample properties

4.2.2.1 DSC

The DSC analyses of the four Shell wax samples shown in Figure 4.18, illustrate how the shapes of the curves vary as the DSC melting maximum increases in a family of synthetic hydrocarbon waxes.

The DSC analyses of both SX 30 and SX 50 display bimodality. It is known that n-alkanes which melt between 60°C and 75°C display polymorphic behaviour due to the occurrence of a crystal lattice or solid-solid transition. [9] Pure n-alkanes may assume hexagonal, orthorhombic, monoclinic or triclinic crystal structures, depending on the specific n-alkane. [5] Figure 4.19 illustrates the differences between these forms. Once impurities are introduced into an n-alkane with carbon chain length $<C_{39}$, such as in a wax sample which contains a

mixture of a series of n-alkanes, the components are able to exist in an orthorhombic form only, which converts to a hexagonal form a few degrees below the melt temperature. [10] Wax samples having an average carbon number $>C_{39}$, such as SX 70, cannot undergo the orthorhombic-hexagonal transition due to a decrease in the mobility of the longer chains. [11] SX 100 also displays melting bimodality. From the temperatures at which the DSC maxima occur (see Table 4.4), it may be speculated that the cause of this is similar to the phenomenon noticed on the DSC analyses of the Paraflint waxes H1 and C105 (see section 4.1.2.1).

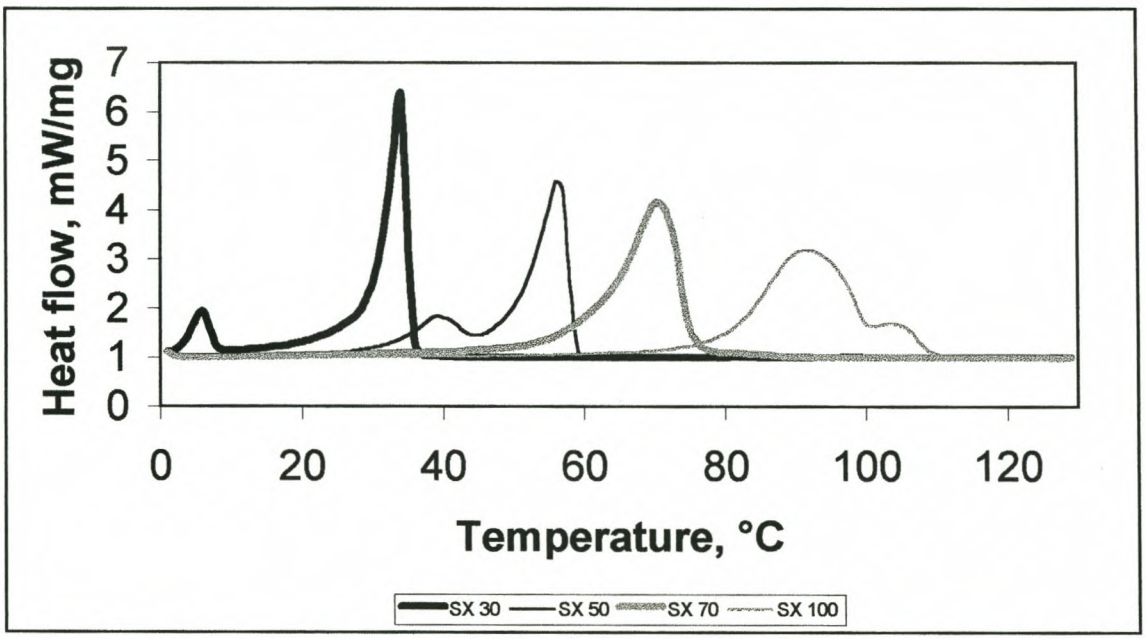

Figure 4.18: Comparison of the DSC analyses of the Shell Fischer Tropsch waxes

Figure 4.19: The seven crystal systems or forms. [12] Waxes can assume either the hexagonal or orthorhombic form.

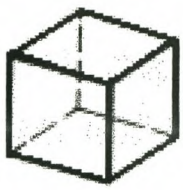

Cubic
x=y=z
α=β=γ=90°

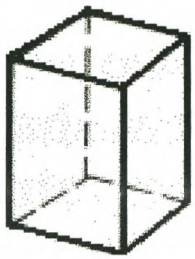

Tetragonal
x=y≠z
α=β=γ=90°

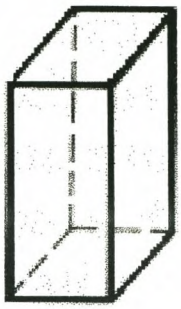

Orthorhombic
x ≠y ≠z
α=β=χ=90°

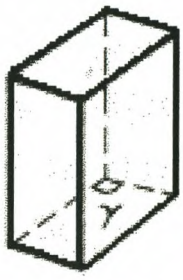

Monoclinic
x ≠y ≠z
α=β=90° ≠γ

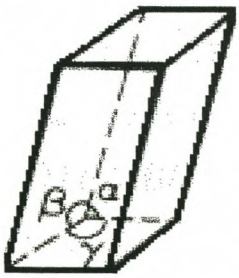

Triclinic
x ≠y ≠z
α ≠ β ≠ γ ≠ 90°

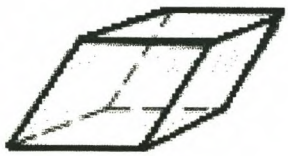

Trigonal
x=y=z
α=β=γ ≠ 90°

Hexagonal
x=y=u ≠ z
z ⊥ to x, y, u, which are inclined at 60°

4.2.2.2 TG

The TG analyses of the Shell Fischer Tropsch waxes are compared in Figure 4.20. Table 4.4 shows that both the TG onset and DTG maximum temperatures increase as the molecular mass of the samples increase along the series SX 30<SX 50<SX 70<SX 100. The DTG plots indicate that SX 100 has the broadest decomposition range, and therefore the broadest molecular mass distribution.

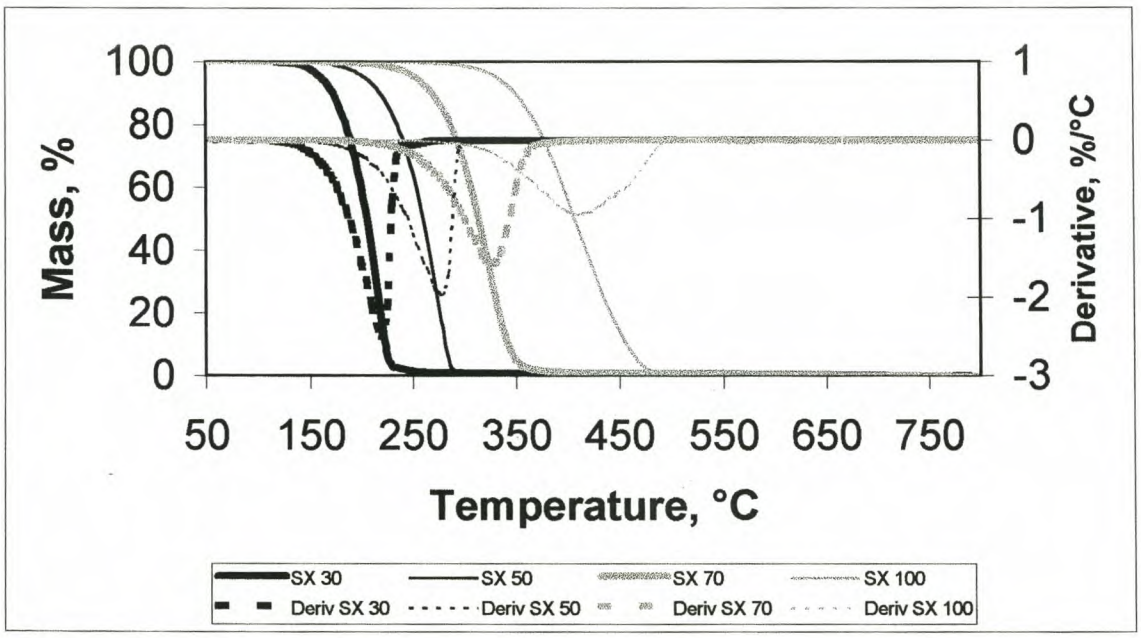

Figure 4.20: Comparison of the TG analyses of the Shell Fischer Tropsch waxes

4.2.2.3 RHEOLOGY

The Shell wax rheology data shown in Figure 4.21 indicates the expected trend of decreasing storage modulus with decreasing molecular mass. This implies decreasing hardness, crystallinity, stiffness, brittleness, strength and toughness, but increasing flexibility, for the same series (see section 3.3.1.1). Below –20 °C, tan δ data decreases with increasing molecular mass (Figure 4.22). This means that the higher molecular mass waxes display greater cohesive strength and lower flexibility due to a smaller free volume (see section 3.3.1.2). This is in agreement with the G' data, which shows that the higher molecular mass waxes are more crystalline. Once again, it is observed that the temperature of the α–transition increases as the molecular mass of the samples increase and flexibilities

decrease (see sections 3.3.1.4 and 4.1.2.3). The T_β transitions are not apparent, due to low levels of branching.

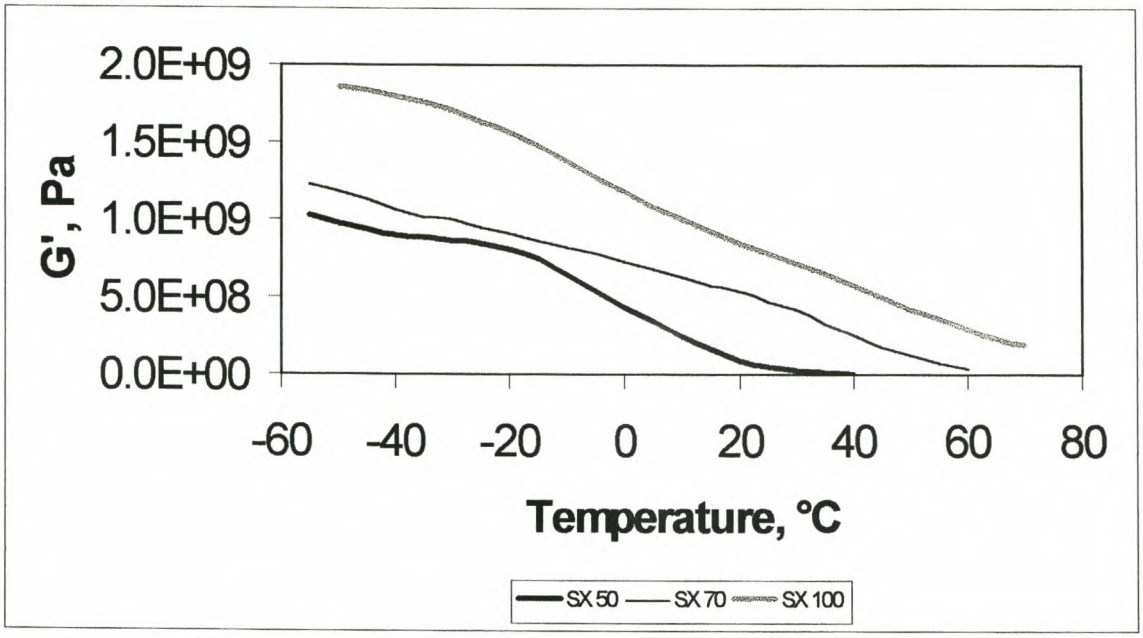

Figure 4.21: Comparison of the storage moduli of the Shell Fischer Tropsch waxes

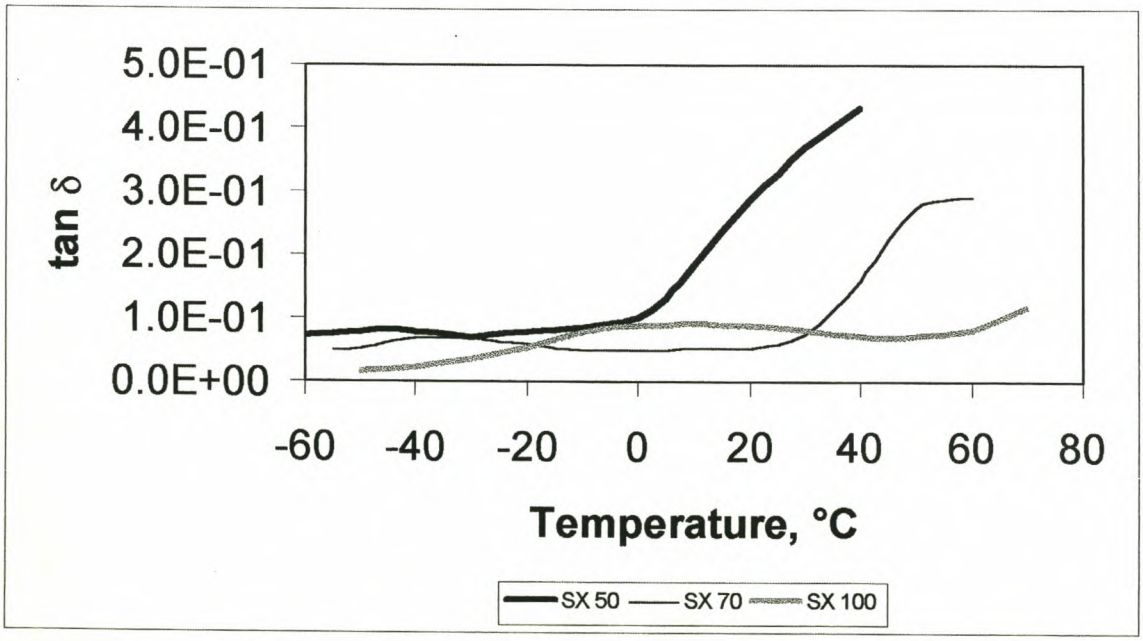

Figure 4.22: Comparison of the tan δ curves of the Shell Fischer Tropsch waxes

4.2.2.4 GPC

Figure 4.23 compares the GPC analyses of the Shell waxes. The molecular mass parameters (Table 4.3) of these waxes increase along the series SX 30<SX 50<SX 70<SX 100, in agreement with the DSC and TG trends observed. SX 100, which displays bimodal DSC melting behaviour, does not have a bimodal molecular mass distribution, and therefore behaves similarly to the higher melting Schümann Sasol products. SX 100 has a narrower MMD than Paraflint H1, as seen by its higher M_n and lower M_z parameters (see section 4.1.2.4). Its polydispersity value confirms that it has the broadest MMD of the four Shell waxes.

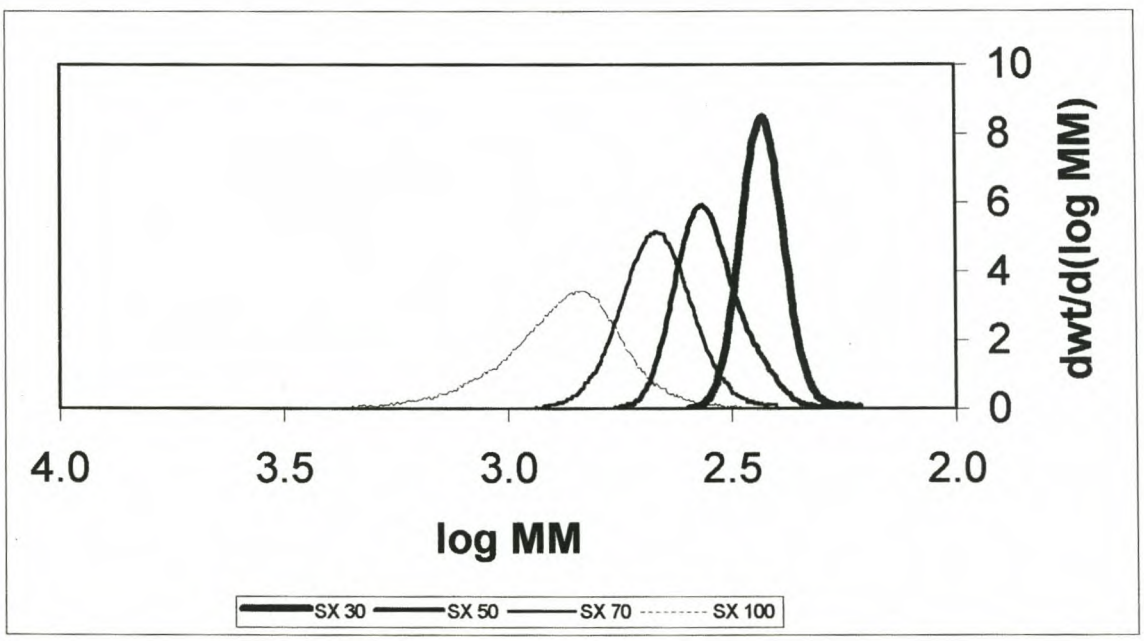

Figure 4.23: Comparison of the GPC analyses of the Shell Fischer Tropsch waxes

4.2.2.5 HTGC

The HTGC analyses of the Shell waxes (Figure 4.24 and Table 4.4) follow the same trend as their GPC analyses. The carbon distribution and the spreads become heavier along the series SX 30<SX 50<SX 70<SX 100. The content of iso-paraffinic material decreases along the series SX 50>SX 70>SX 100 (Table 4.4), indicating that, as for the Schümann Sasol Fischer Trospch waxes (see section 4.1.2.5), there is a predominance of unbranched material in the heavier wax fractions.

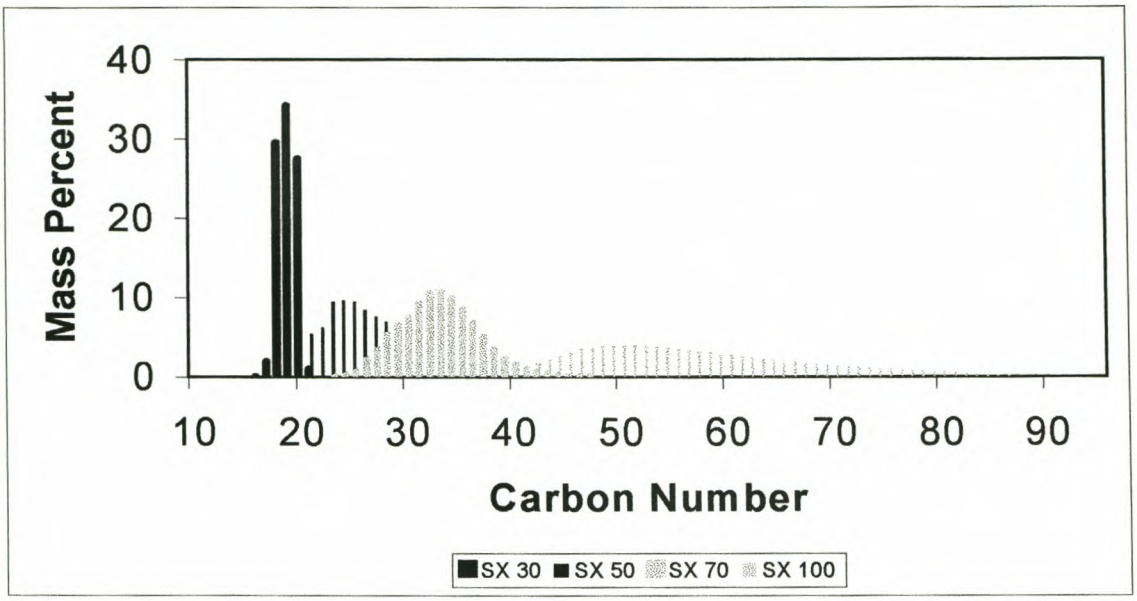

Figure 4.24: Comparison of the HTGC analyses of the Shell Fischer Tropsch waxes

4.2.2.6 IR

The IR analyses of the Shell Fischer Tropsch waxes display only the paraffinic stretching, bending and rocking vibrations, and are therefore similar to those of the unfunctionalised Schümann Sasol Fischer Tropsch waxes (Figure 4.25 and section 4.1.2.6).

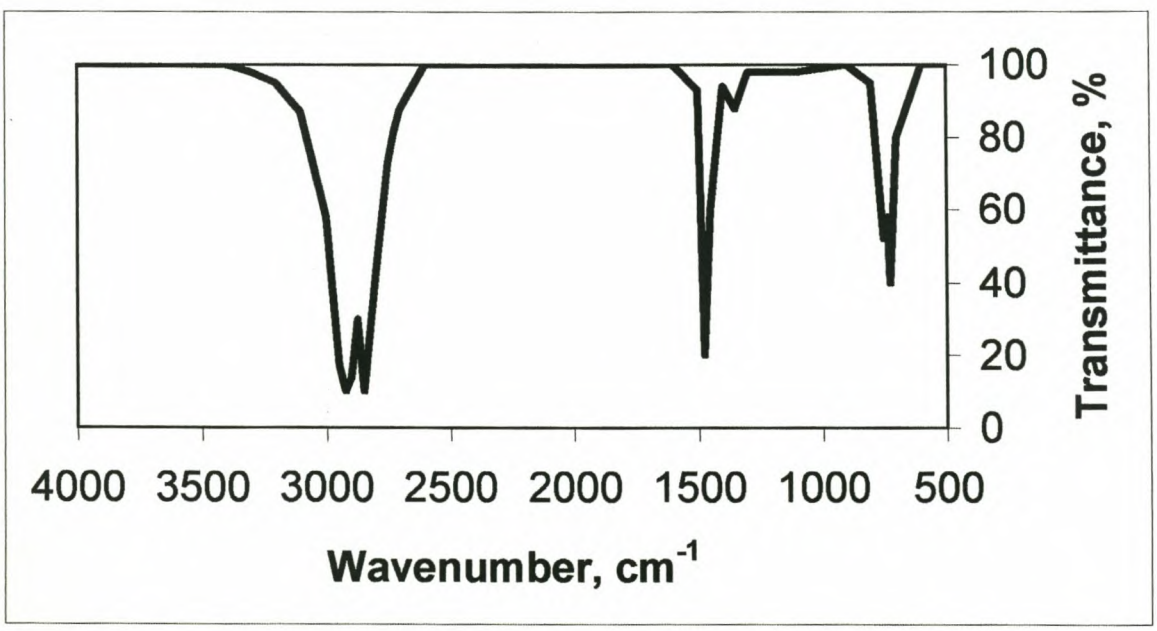

Figure 4.25: Typical IR analysis of a Shell Fischer Tropsch wax

4.2.2.7 WET CHEMICAL ANALYSES

Table 4.5 compares the physical properties of the Shell Fischer Tropsch waxes. The observed trends are similar to those previously discussed for the Schümann Sasol Fischer Tropsch waxes (see section 4.1.2.7). The congealing and drop melting points increase with increasing DSC maxima and end of melt temperatures (see Table 4.4). Similarly, viscosity values increase with increasing wax molecular mass. Penetration at 25°C and 65°C decreases with increasing molecular mass, indicating an increase in the wax hardness, as was predicted from a comparison of the storage modulus data (see section 4.2.2.3). It is interesting to observe that the densities increase along the series SX 30<SX 50<SX 70<SX 100, confirming that the wax structures become more linear with increasing molecular mass. This shows that the branched material formed during synthesis is predominantly of shorter chain length.

Table 4.5: Physical properties of the Shell Fischer Tropsch waxes

Analysis	Shell SX 30	Shell SX 50	Shell SX 70	Shell SX 100
Congealing point (°C)	32	54	73	96
Drop melting point (°C)	*	52	90	109
Viscosity @135°C (cP)	0.7	1.2	3.0	7.4
Penetration @25°C (dmm)	*	42	12	<1
Penetration @65°C (dmm)	*	*	148	23
Density @25°C (g/cm^3)	0.73	0.83	0.84	0.88
MEK solubles (%)	5.31	2.15	0.16	-
MIBK solubles (%)	-	-	-	0.14

* Not possible to perform analysis due to wax properties

4.3 RELEVANCE OF FISCHER TROPSCH WAX PROPERTIES TO THEIR APPLICATIONS

The Fischer Tropsch medium melting and hard waxes are particularly suitable as components in HMAs. The low viscosities (Tables 4.3 and 4.5) of waxes such as Paraflint H1, Paraflint

C80, Paraflint C105 and SX 100 will result in a significant reduction in viscosity, and improvement in surface wetting, of the HMA. This will improve HMA processability, and will ultimately decrease the end user's cost. A typical HMA processing temperature is 170°C. Waxes having a temperature @0.5% decomposed parameter that is greater than 170°C are regarded as having sufficient thermal stability for this application. Obviously, the higher this temperature, the better, as the HMA is kept in its molten state for several hours. The thermal stabilites of the above mentioned four waxes are all acceptable (see Tables 4.1 and 4.4). The combination of high congealing point, or DSC end of melt temperature, and narrow melting range of these four Fischer Tropsch waxes will impart good set time properties to the HMA. Examination of the tan δ data indicates that good HMA flexibility will be obtained when using Paraflint C80 or SX 70 in low-temperature packaging applications (see sections 4.1.2.3 and 4.2.2.3).

The higher molecular mass Fischer Trospch waxes are only suitable for use in paste polish applications at low addition levels, where they promote gloss and durability of the polish formulation. Higher levels of addition of these waxes will reduce the ease of application of the polish. Paraflint C80, with its intermediate DSC melting range and molecular mass, imparts a good balance of buffability and paste hardness to polishes (see sections 4.1.2.1 and 4.1.2.4). Oxidation of the high molecular mass Fischer Trospch waxes results in a slight reduction in the DSC end of melt temperature, fusion enthalpy, and storage modulus, and therefore crystallinity, and molecular mass (Tables 4.1 and 4.2). Besides allowing the wax to then be saponified, in order to induce gelling of the polish, the wax will not have such a profound effect on the ease of application, gloss and durability of the polish. Oxidised waxes are usually characterised by the occurrence of a DTG peak at ca. 560°C, on the introduction of an oxygen atmosphere (see Table 4.2).

Fischer Tropsch hard waxes are most suited to ink applications. The hardness and high molecular masses of Paraflint H1, Paraflint C105 and SX 100 impart good rub and scuff resistance to the ink film (see Tables 4.1 and 4.4). The low viscosities of Paraflint H1 and Paraflint C105 allow micronisation by way of spraying rather than grinding (see Tables 4.3 and 4.5). The more regular spherical particles detract less from the gloss of the ink film than the irregular particles of ground waxes do.

The Fischer Tropsch hard waxes Paraflint H1, Paraflint C105 and SX 100, due to their high molecular mass and thermal stabilities (temperature @0.5% decomposed parameter), are suitable for use as external lubricants in PVC processing (see Tables 4.1 and 4.4).

The DSC melt range, hardness (G'), tan δ (flexibility), molecular mass, congealing point, penetration and MEK properties of SX 50 and SX 70 indicate that they are suitable for use as candle base waxes (see Tables 4.4 and 4.5). The occurrence of a solid-solid transition during melting goes hand in hand with a volume change, due to different space group conformations that are assumed by the different crystal modifications. The harder, higher melting and higher molecular mass Fischer Tropsch waxes, such as Paraflint C80, and to an extent Paraflint H1 and SX 100, may be used as low level additives to improve candle gloss. Tan δ results show that Paraflint H1 and SX 100 are very brittle waxes, and will therefore cause the candles to crack if too much is added (see sections 4.1.2.3 and 4.2.2.3).

4.4 REFERENCES

(1) Ullmann's Encyclopedia of Industrial Chemistry, 2000, 6th Ed., Electronic Release.

(2) E. C. Reynhardt, J. Phys. D: Appl. Phys, 1985, 18, 1185-1197.

(3) N. M. Emanuel Ed., The Oxidation of Hydrocarbons in the Liquid Phase, 1967, Pergamon Press, Oxford.

(4) C. Wang et al, Polymer Bulletin, 1997, 39, 185-192.

(5) S. P. Srivastava et al, J. Phys. Chem. Solids, 1993, 54 (6), 639-670.

(6) G. Ungar et al, Science, July 1985, 229, 386-389.

(7) P. E. Slade and L. T. Jenkins Ed., Thermal Characterisation Techniques – Techniques and Methods of Polymer Evaluation, 1970, Volume 2, Marcel Dekker Inc., New York.

(8) R. C. Weast and M. J. Astle Ed., CRC Handbook of Chemistry and Physics, 1982, 62nd Ed., CRC Press Inc., Florida.

(9) D. S. Barmby et al, Proceedings 6th World Petroleum Congress, 1963, VI (21), 1-17.

(10) J. F. Johnson, Ind. Eng. Chem., 1954, 46, 1046-1048.

(11) W. R. Turner, Ind. Eng. Chem. Prod. Res. Develop., 1971, 10 (3), 238-258.

(12) J. W. Mullin, Crystallisation, 1972, 2nd Ed., Butterworths, London.

CHAPTER 5

THE POLYETHYLENE WAXES

5.1 INDUSTRIAL SYNTHESIS AND ECONOMIC SIGNIFICANCE

Polyethylene (PE) waxes may be classified as: (1) PE waxes produced by high-pressure polymerisation; (2) copolymeric PE waxes produced by high-pressure polymerisation; (3) polyolefin waxes produced by Ziegler-Natta polymerisation; and (4) degradation polyolefin waxes. [1]

These waxes are produced as either first-intention products, or are by-products from the manufacture of plastics. The quantity of polyethylene waxes currently consumed worldwide is ca. 200 000 t/a. [1] High-pressure PE waxes account for ca. 70% of this volume. The remainder consists essentially of low-pressure Ziegler products. Degradation products are less important in terms of quantity.

The transition from polyethylene plastic to polyethylene wax is approximately when the weight average molecular mass (M_w) drops below ca. 37 000 g/mol. [1] M_w and degree of branching are the two wax properties that dominate the characteristics of this type of wax. Melt viscosity rises exponentially with increasing molecular mass. Crystallinity, hardness, melting point and congealing point increase as the degree of branching decreases. Unbranched homopolymeric PE waxes have a high degree of crystallinity as a result of their undistorted linear molecular structure. [1]

PE waxes are used in HMAs, plastics processing, inks, paints and coatings.

5.1.1 LOW-PRESSURE POLYOLEFIN WAXES

PE waxes are produced by the Ziegler-Natta low-pressure process using organometallic catalysts. The Ziegler-Natta waxes have a mainly linear molecular structure, like their high-density polyethylene (HDPE) plastic homologues and contain short side chains. For the direct

synthesis of polymer waxes from propylene or higher α-olefins, only the Ziegler-Natta process is suitable. The Ziegler-Natta PE waxes currently on the market have average molecular masses between 800 and 8000 g/mol, and therefore bridge the gap between Fischer Tropsch and paraffin waxes, and HDPE thermoplastics. Besides controlling chain length, the polymerisation process allows the degree of crystallinity to be adjusted in order to produce both hard and brittle high melting point products, as well as softer, flexible products with lower melting points. [1] Examples of this type of wax are Petrolite's Polywax 1000, Polywax 2000 and Polywax C4040.

5.1.2 HIGH-PRESSURE POLYETHYLENE WAXES

These waxes are produced at high pressure and temperature in the presence of radical formers. Their molecular masses are considerably lower than those of plastics. The molecular mass range is adjusted during polymerisation by the addition of regulators. As radical polymerisation always leads to the formation of branched products, these waxes consist mainly of branched molecular chains, with long chain branching. They are therefore also often referred to as low-density polyethylene (LDPE) waxes. High-pressure PE waxes contain a small proportion of double bonds, whose distribution in the macromolecule depends on the production process. [1] Escomer H101, formerly produced by Exxon, is an example of a LDPE wax.

5.1.3 COPOLYMERIC POLYETHYLENE WAXES

Numerous other monomers, such as vinyl acetate or acrylic acid, may be added to ethylene during the high-pressure process to produce copolymeric PE waxes. This results in considerable changes in product properties, such as higher polarity and lower crystallinity. Ethylene vinyl acetate waxes are used as additives in metallic automotive paints, as dispersing agents in pigment concentrates and as a component of hot melt adhesives. Ethylene acrylic acid waxes are readily emulsified for use in floor polishes and mould release agents. [1] An example of this type of wax is Escomer H101, produced using carbon monoxide as comonomer. It was successfully promoted in HMAs due to its ease of adherence to difficult substrates. It is also an example of a LDPE wax. It is, however, no longer available commercially.

5.1.4 DEGRADATION POLYOLEFIN WAXES

The molecular chain of high molecular mass polyolefins can be cleaved into smaller molecules, having waxy character, by heating in the absence of air. The starting materials are usually high- and low-density polyethylene, isotactic polypropylene and polybutene. Despite the unfavourable energy balance of this process, it is used because of its technological simplicity. Degradation PE waxes contain significantly more double bonds than comparable waxes formed by high-pressure polymerisation. [1] The Epolene N range of waxes manufactured by Eastman are examples of degradation polyethylene waxes.

5.2 ANALYSIS PROFILE

The results from the instrumental analysis of the polyethylene waxes are given in Table 5.1.

5.2.1 DSC

The DSC analyses of various PE waxes are shown in Figures 5.1-5.3. Table 5.1 shows that the DSC beginning of melt temperatures are low, and that the actual melting peak is preceded by a low intensity shoulder that extends over a number of degrees Celsius. This is probably due to the presence of low molecular mass material, and shows that the PE waxes have broad melting ranges. The melting peaks of Polywax 1000, Polywax 2000 and Escomer H101 display bimodality. The first (lower temperature) and second (higher temperature) peaks can be attributed to the melting of extended chain (EC) crystals and folded chain (FC) crystals, respectively. [2] The onset of chain folding is at ca. C_{100}. [2] The absence of bimodality from the melting profile of Polywax C4040, and its relatively low DSC maximum, is therefore probably due to the presence of only EC crystals. This will be discussed again later under section 5.2.4. The DSC analysis of Polywax 2000 shows that the first peak is poorly resolved from the second. This indicates that the wax assumes a predominantly chain folded conformation on crystallisation. This will also be discussed further under section 5.2.4. The shape of the degradation polyethylene wax's DSC curve is similar to that of Polywax 2000, indicating that its crystalline morphology is predominantly chain folded crystals. The difference in the positions of the main peaks on the DSC analyses of these two waxes indicates differing fold lengths, and therefore lamellae thicknesses. [2]

Table 5.1: Analysis results of some PE waxes

	HDPE waxes			Copolymer LDPE wax	Degradation PE wax
Analysis	**Polywax 1000**	**Polywax 2000**	**Polywax C4040**	**Escomer H101**	**Epolene N-21**
DSC					
Melt range, °C	33-119	72-126	42-108	8-115	27-118
Maxima, °C	104/108	100/122	94	95/109	115
Fusion enthalpy, J/g	258	264	222	204	190
TG					
Onset temp., °C	436	458	363	417	448
Temp. @0.5% weight loss, °C	265	315	235	255	176
DTG maxima, °C	478	491	420	474	482/566
Rheometry					
T_α, °C	43	46	20	18	44
T_β, °C	-	-	-	-31	-2
GPC					
M_n, Daltons	1033	2229	724	895	2800 [3]
M_w, Daltons	1184	2593	788	1446	6500 [3]
M_z, Daltons	1371	3071	860	2656	-
P_d	1.15	1.16	1.09	1.62	2.32
HTGC					
Carbon no. spread	C_{16}->C_{98}*	C_{14}->C_{98}	C_{16}-C_{94}*	C_3->C_{79}#	C_{16}->C_{84}
% n-paraffins	96.08	96.34	99.49	74.86	63.55
% iso-paraffins	3.92	3.66	0.51	25.14	36.45

* Even carbon numbers only

Odd carbon numbers only

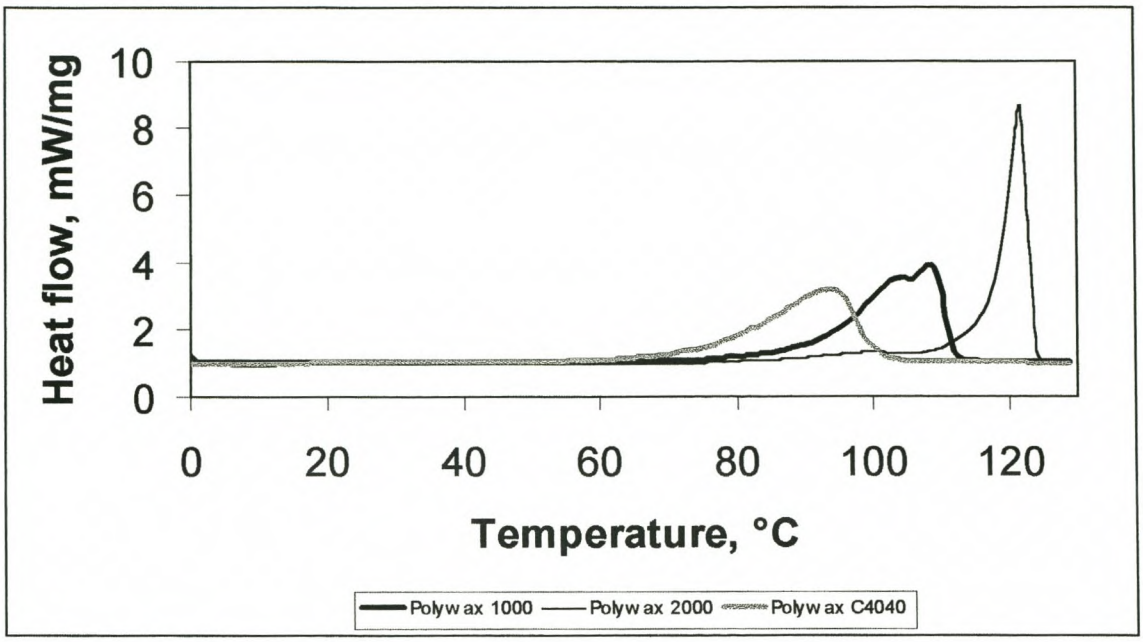

Figure 5.1: Comparison of the DSC analyses of some HDPE waxes

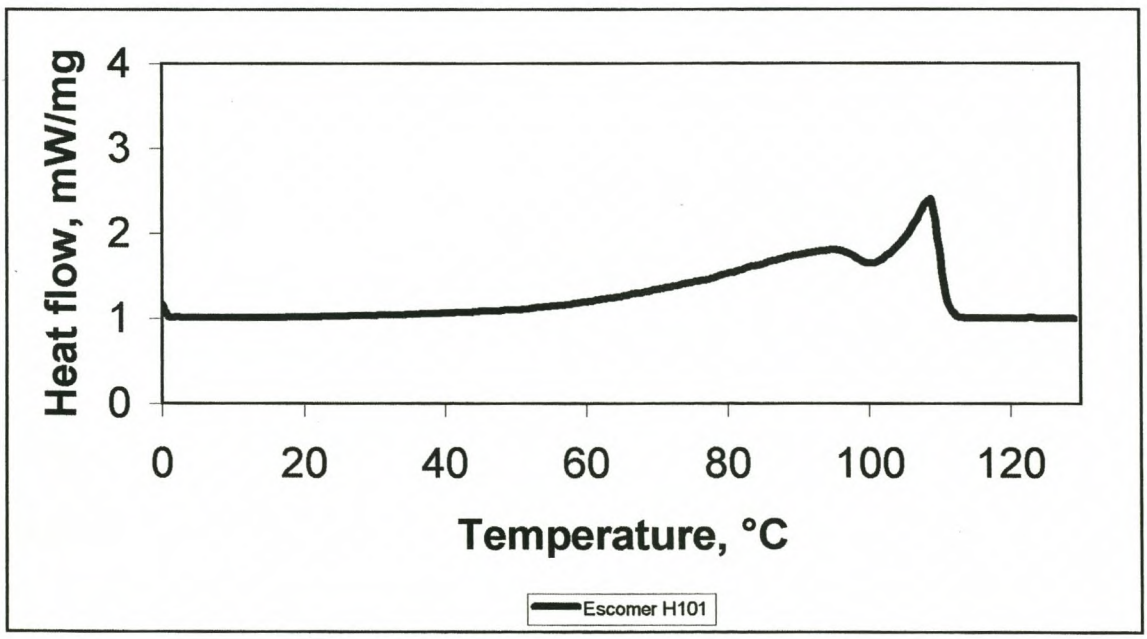

Figure 5.2: DSC analysis of a LDPE copolymer wax

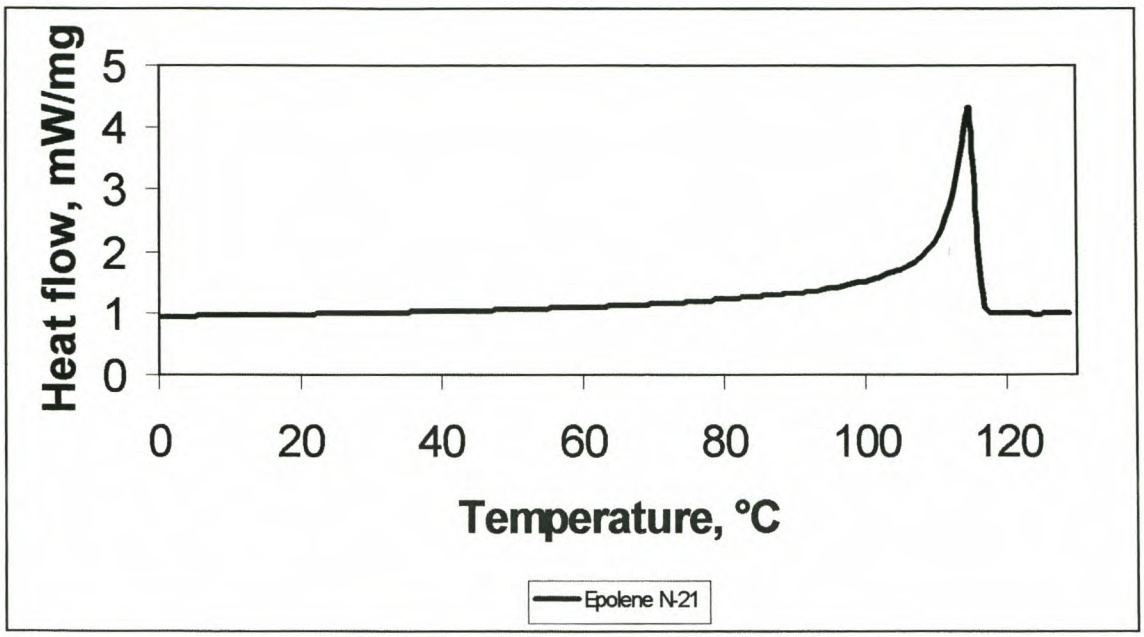

Figure 5.3: DSC analysis of a degradation PE wax

5.2.2 TG

The PE waxes, with the exception of Polywax C4040, display high TG onset and DTG maximum temperatures (Figures 5.4 and 5.5). This indicates that these waxes are relatively high molecular mass waxes.

A characteristic of the TG analyses of polyethylene waxes is a high TG onset temperature. This is often misleading, as visual inspection of the TG curves show relatively low start of decomposition temperatures, due to the presence of low molecular mass material. For this reason, it is more appropriate to evaluate wax thermal stability using the temperature at which 0.5% of the sample has decomposed, i.e. the higher this temperature, the greater the initial thermal stability of the wax. This light material is apparent in the DSC analysis of the waxes as a relatively low beginning of melt temperature. The DTG maximum of Polywax C4040 (Figure 5.4 and Table 5.1) is lower than those of the other PE waxes, in keeping with its lower DSC maximum.

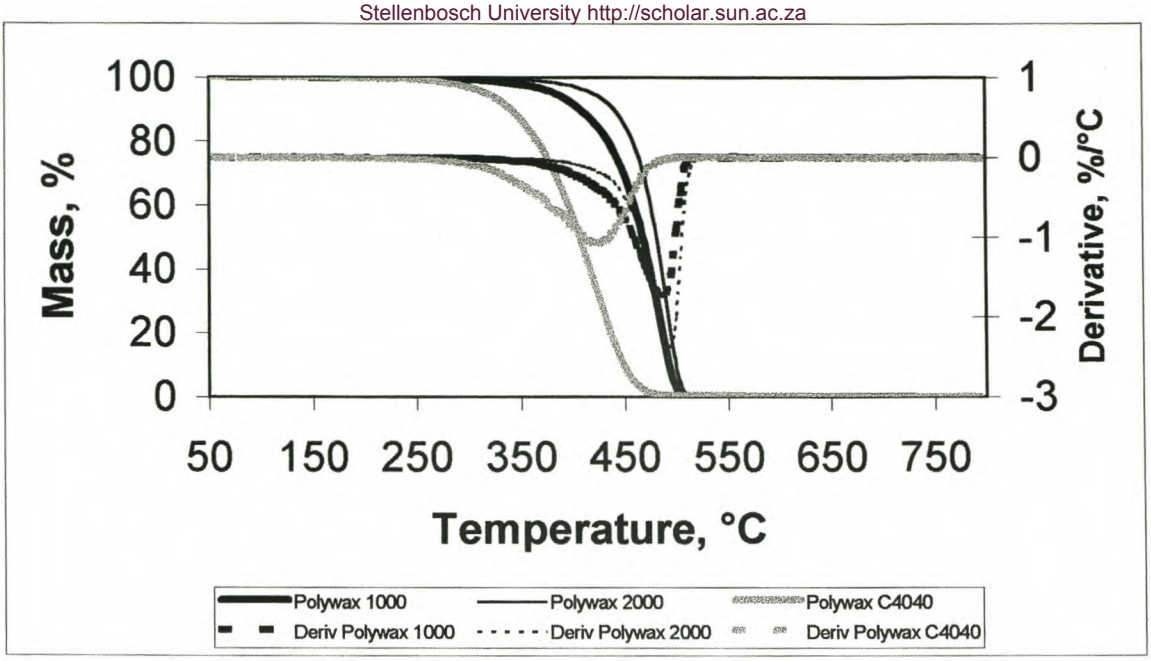

Figure 5.4: Comparison of the TG analyses of some HDPE waxes

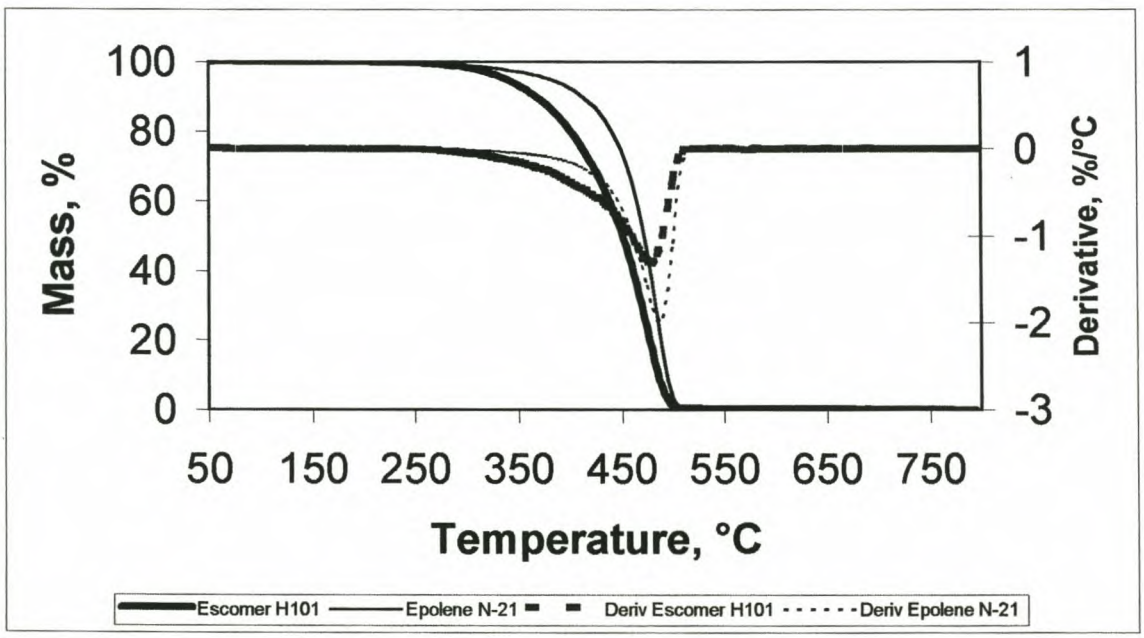

Figure 5.5: Comparison of the TG analyses of LDPE copolymer and degradation PE waxes

5.2.3 RHEOLOGY

Figure 5.6 shows a comparison of the storage modulus data of the polyethylene waxes examined in this study. G' decreases along the series Polywax 1000>Polywax C4040>Polywax 2000>Epolene N-21>Escomer H101 at 25°C. As a result, it is to be expected that the mechanical properties of hardness, stiffness and brittleness will also decrease along the same series, while the flexibilities increase. Furthermore, it may be deduced that a trend of decreasing crystallinities, and increasing free volumes will also be apparent (see section

3.3.1.1). As Polywax 2000 and Epolene N-21 have the highest molecular masses, this seems to be anomalous behaviour. However, considering the deductions made concerning the crystalline morphologies of these two waxes from their DSC analyses, they will contain more crystalline imperfections due to their tendency to chain fold. This will lower the crystallinities and increase the free volume components, with the greatest effect apparent with the Epolene wax. The reason for this is that Epolene N-21 has a higher molecular mass, but lower DSC maximum than Polywax 2000 which indicates that it has a smaller fold length.

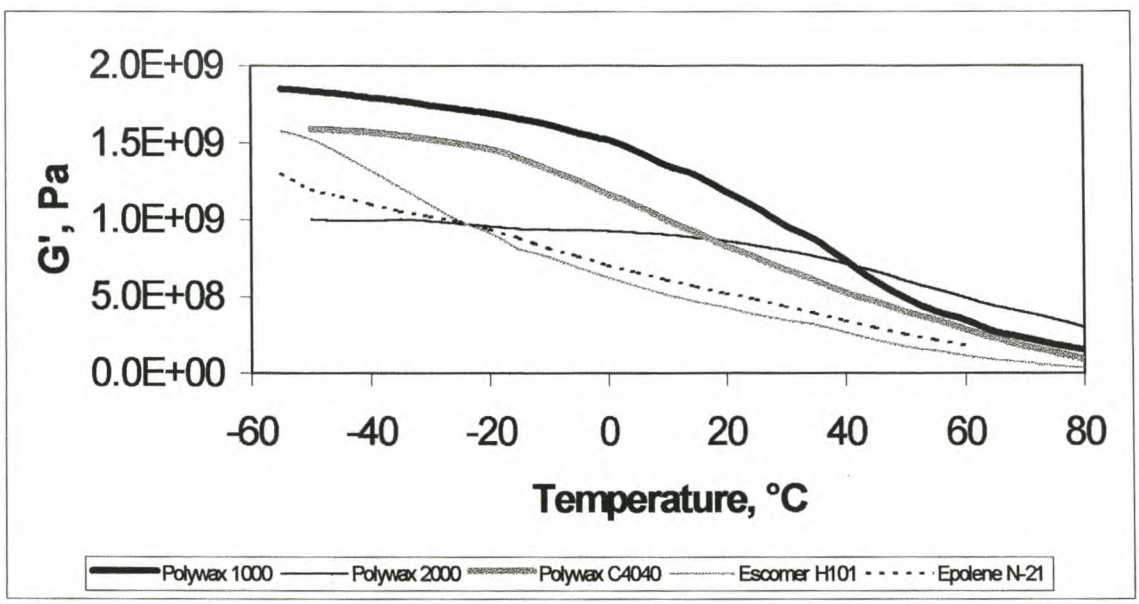

Figure 5.6: Comparison of the storage moduli of some PE waxes

The tan δ curves of some PE waxes are compared in Figure 5.7. The general trend observed at subambient temperatures is a decrease in the cohesive strengths along the series Polywax 2000/ Polywax 1000>Polywax C4040>Epolene N-21>Escomer H101, and an increase in the flexibilities and free volumes along the series Polywax 2000/ Polywax 1000<Polywax C4040<Epolene N-21<Escomer H101, as the tan δ values increase (see section 3.3.1.2). Only the T_α transition is observed in the analyses of the HDPE waxes, while both the T_α and T_β transitions are apparent in the analyses of Escomer H101 and Epolene N-21, due to their branched and/ or functionalised natures. This analysis shows that Epolene N-21 is also based on a LDPE wax. The temperature of the α-transition increases, as predicted, with increasing wax molecular mass (see section 3.3.1.4 and Table 5.1).

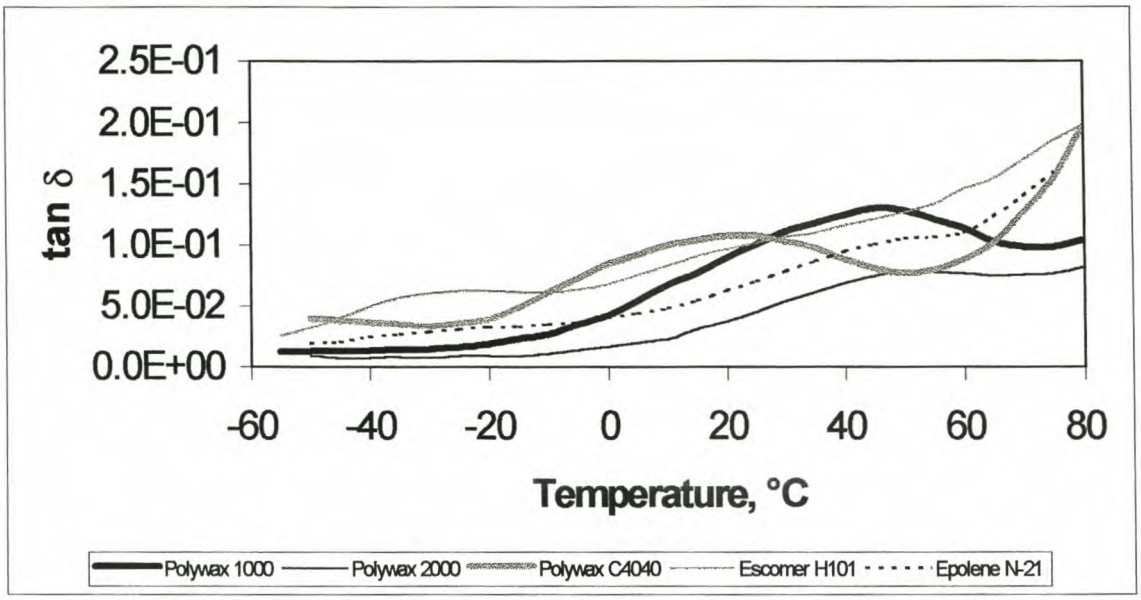

Figure 5.7: Comparison of the tan δ curves of some PE waxes

5.2.4 GPC

It was not possible to quantify the MMD of Epolene N-21 as a portion of its material elutes before the exclusion limit of the columns used. This indicates that the wax contains carbon chains with molecular masses that are greater than 10,000. Analysis results obtained from the literature indicate that the M_n and M_w parameters for this wax equate to carbon chain lengths of ~C_{200} and ~C_{400} respectively. [3] The carbon chain length is derived by dividing the molecular mass parameter by 14, which is the molecular mass of a CH_2 repeat unit. Its single DSC melting peak is therefore due to the wax molecules assuming a FC conformation on crystallisation (see section 5.2.1). The HDPE waxes Polywax 1000 and Polywax 2000 have the highest molecular masses of the waxes analysed here (see Figure 5.8 and Table 5.1). Their DSC analyses (see section 5.2.1) showed that their melting peaks have long, low shoulders on the low temperature side of the peaks. This is caused by their high polydispersities measured in the GPC data (Table 5.1). The DSC analyses showed that Polywax 1000 displayed well-defined DSC melting bimodality, while Polywax 2000 did not. Bimodality in PE waxes is due to the presence of extended chain (EC) and folded chain (FC) crystals, with the onset of chain folding being at ca. C_{100}. [2] The reason for Polywax 2000's poorly defined melting bimodality is now confirmed by its GPC analysis. Its M_n parameter translates to a carbon chain length of approximately C_{159}. The molecular morphology of Polywax 2000 must therefore be predominantly FC crystals. Polywax C4040 has a relatively low MMD. Its molecular mass parameters do not differ significantly from those of Shell SX-100. As the molecular mass parameters of Polywax C4040 all translate to carbon chain lengths of $<C_{100}$, all chains should assume the EC morphology. The absence of DSC melting bimodality is therefore to be expected. Shell SX-100 does, however, display bimodal melting

behaviour. The reason for this comparatively anomalous behaviour is unclear. Escomer H101 is characterised by a very broad MMD, with both very low and very high molecular mass material present (P_d = 1.6). The GPC parameters indicate that both EC and FC material is present, which is confirmed by its bimodal DSC analysis (see section 5.2.1).

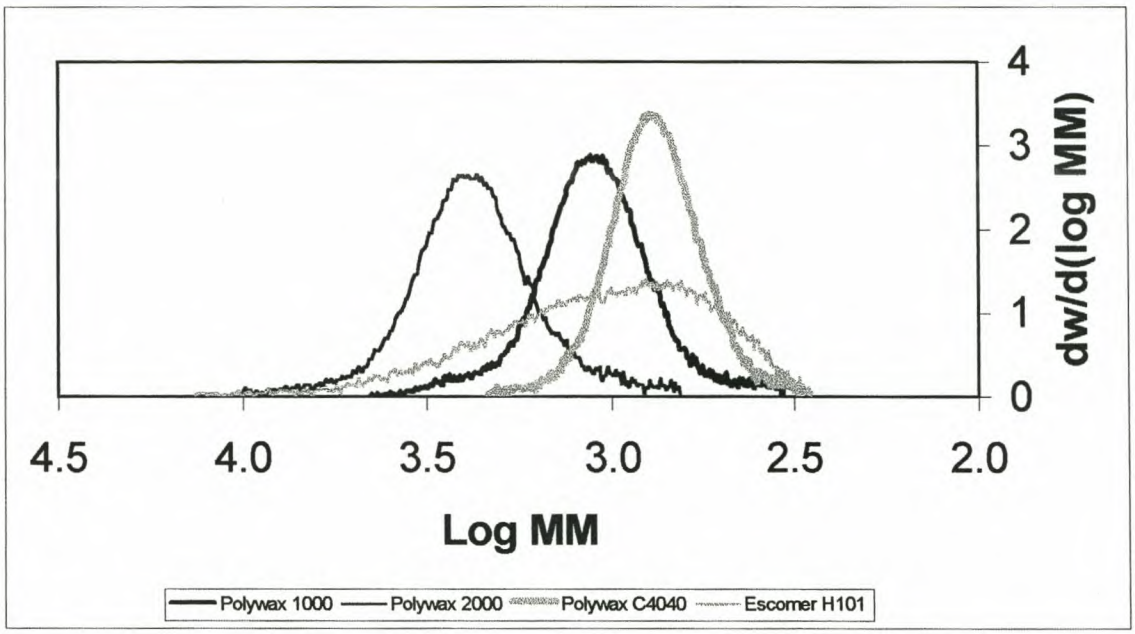

Figure 5.8: Comparison of the GPC analyses of some PE waxes

5.2.5 HTGC

The basis of the HTGC analytical technique is a boiling point separation, and its usefulness is therefore limited to analysing materials that evaporate over the range of operation. It is not advisable to perform HTGC analysis of samples containing predominantly very high molecular mass material, such as most PE waxes, as the non-volatile material will remain on the column and result in its deterioration. Figures 5.9 and 5.11 show that Polywax 1000 and Polywax C4040, formed by the polymerisation of ethylene, display carbon distributions containing only the expected even carbon numbers. Figure 5.10 shows that Polywax 2000 consists of both odd and even carbon chain lengths, with the amount of each odd lower than those of the neighbouring evens. This indicates that a degree of degradation has occurred in the wax. The distribution of Escomer H101, the copolymer wax, contains only odd carbon numbers (Figure 5.12). This is obviously a function of the polymerisation process, and the way in which it is terminated. The degradation PE wax is comprised of both odd and even carbon chain lengths, according to its HTGC analysis (Figure 5.13). The same phenomenon that was

observed with Polywax 2000, concerning the relative amounts of odd and even carbon chain lengths, is also apparent here, confirming that the latter wax had undergone degradation.

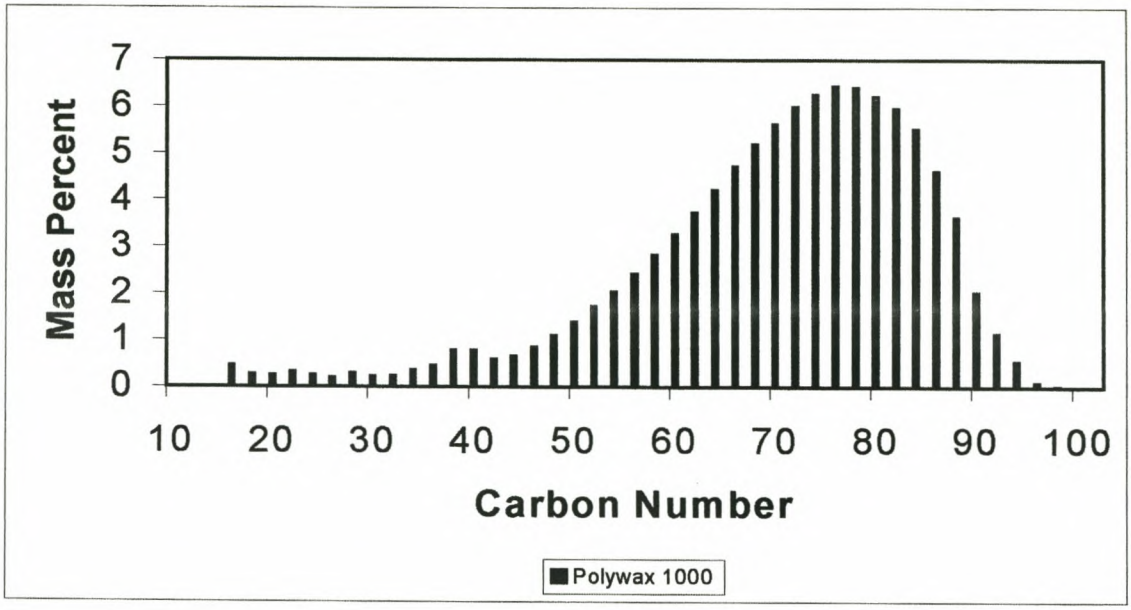

Figure 5.9: HTGC analysis of Polywax 1000

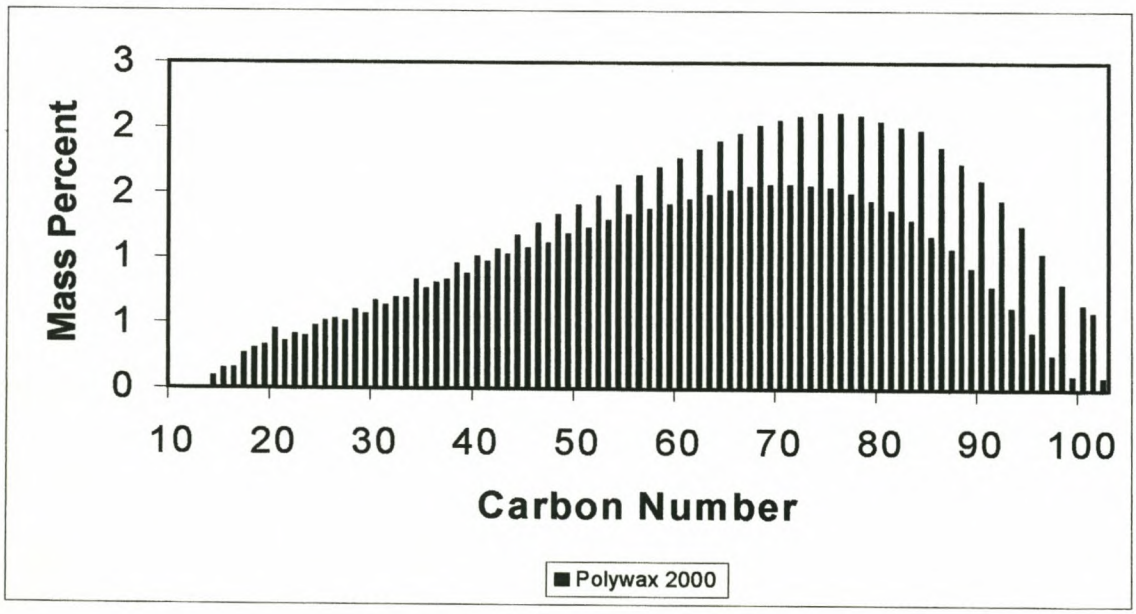

Figure 5.10: HTGC analysis of Polywax 2000

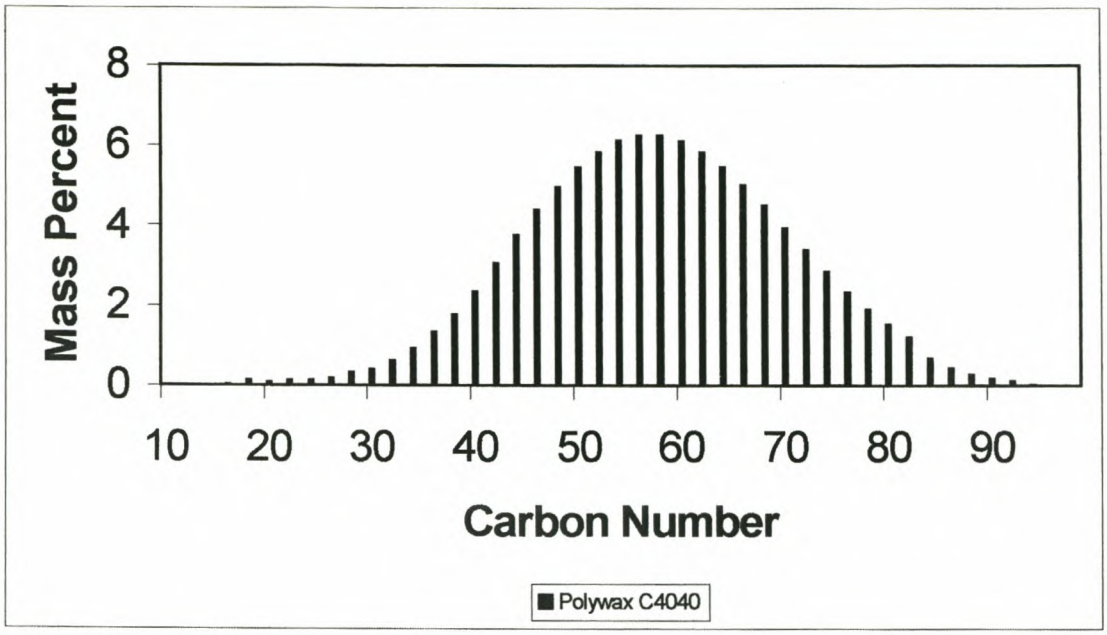

Figure 5.11: HTGC analysis of Polywax C4040

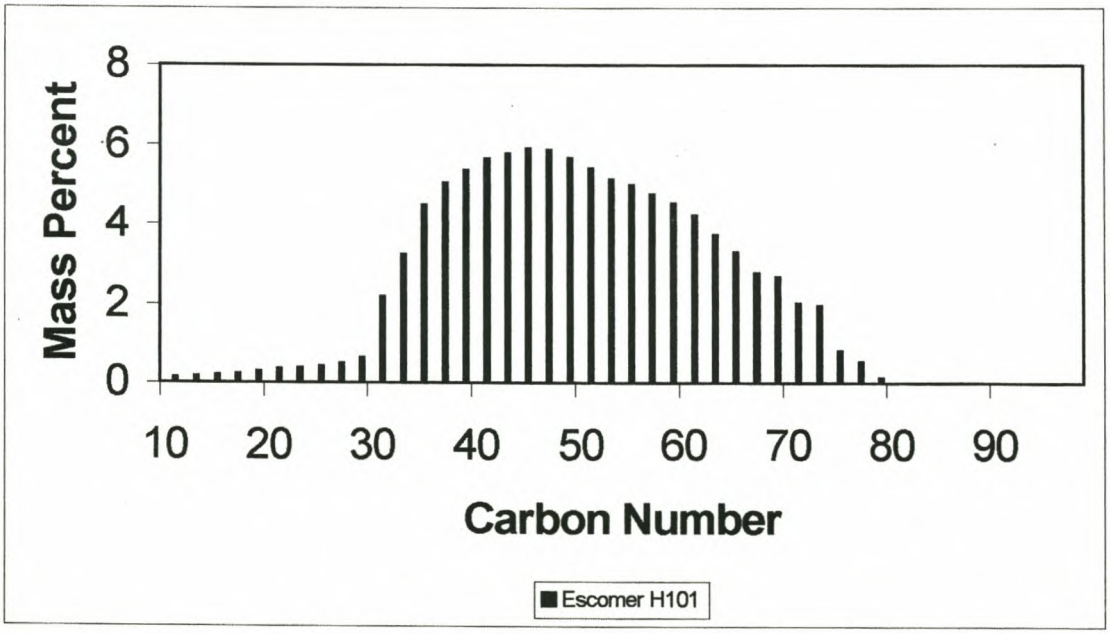

Figure 5.12: HTGC analysis of Escomer H101

5.2.6 IR

The IR analyses of Polywax 1000 and Polywax C4040 show the characteristic paraffinic stretching, bending and rocking vibrations at ca. 2900, 1400 and 720 cm^{-1}. For this reason, the IR analysis of only Polywax 1000 is included (Figure 5.14). IR analysis cannot distinguish between polymethylenic and polyethylenic material. [4] These analyses are therefore similar to those of the Fischer Tropsch waxes (see sections 4.1.2.6 and 4.1.2.7). Figure 5.15 shows an

IR analysis that is typical of Polywax 2000 and Epolene N-21. The broadened 2900 cm^{-1} paraffinic stretch vibration, the acidic carbonyl vibration at ca. 1722 cm^{-1} and the olefinic band at ca. 1650 cm^{-1} indicate the formation of acids and unsaturation during decomposition. The IR analysis of Escomer H101 (Figure 5.16) also displays the characteristic paraffinic vibrations, as well as that of the ketone functionality (ca. 1720 cm^{-1}). This is to be expected, as it is known that this wax is a copolymer of ethylene and carbon monoxide.

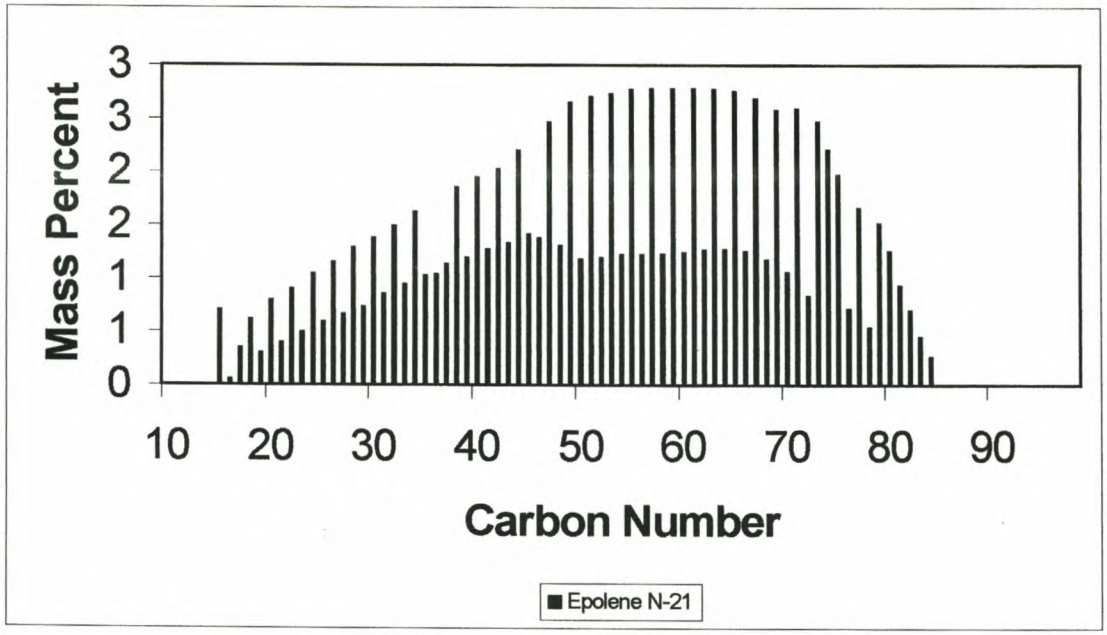

Figure 5.13: HTGC analysis of Epolene N-21

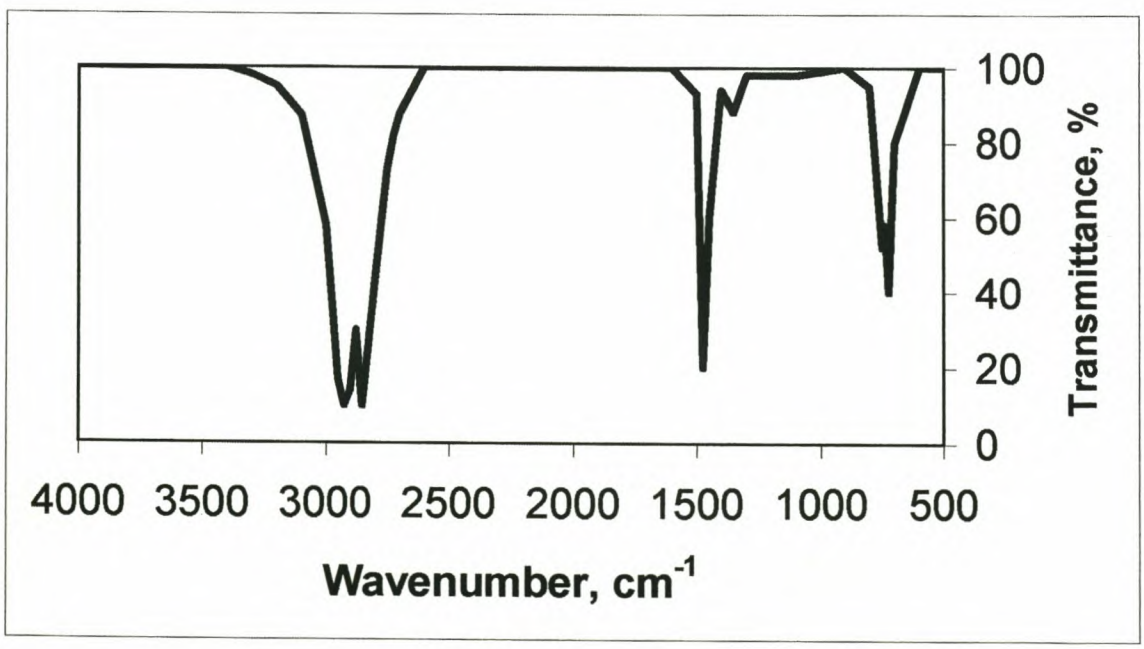

Figure 5.14: IR analysis of Polywax 1000

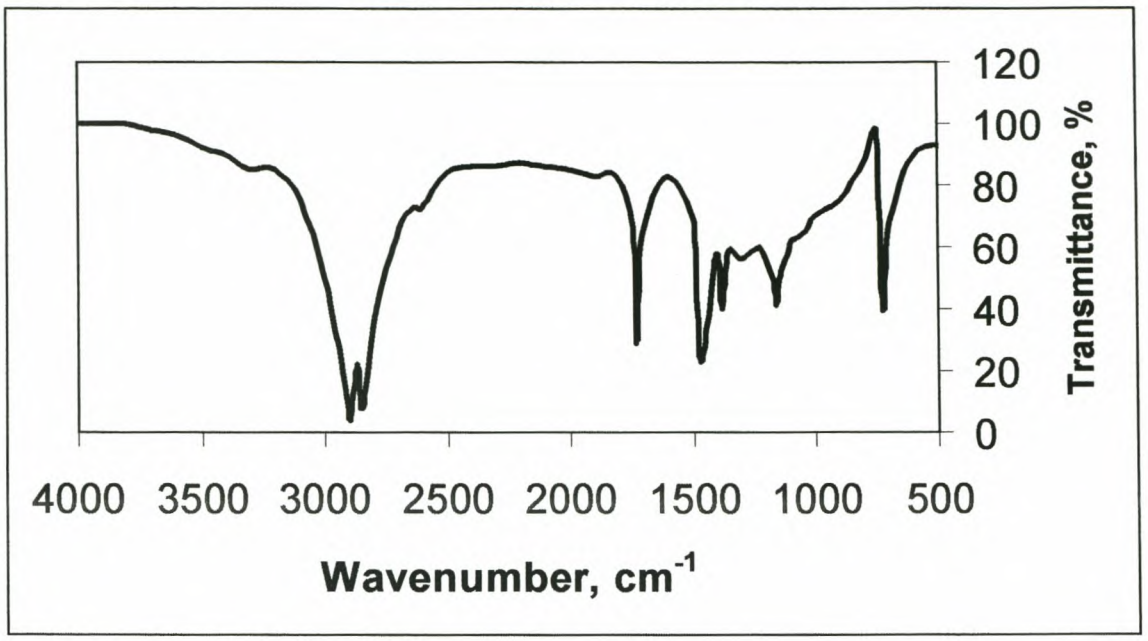

Figure 5.15: Typical IR analysis of Polywax 2000 and Epolene N-21

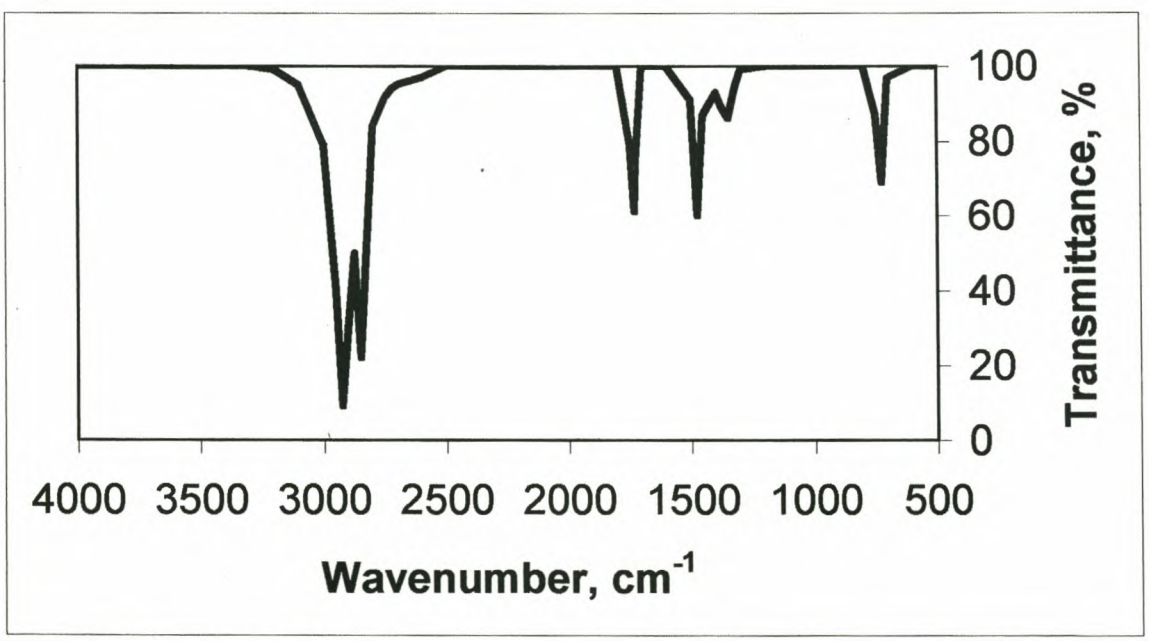

Figure 5.16: IR analysis of Escomer H101

5.2.7 WET CHEMICAL ANALYSES

The results of the wet chemical analyses of the polyethylene waxes studied here are given in Table 5.2. The congealing point and drop melting points decrease with decreasing DSC end of melt temperature (see Table 5.1). The exception is Epolene N-21, which has a higher drop melting point than predicted by DSC. This is due to its very high viscosity, which also

prevented determination of its congealing point. The wax viscosities increase with increasing M_w. A good correlation is noted between the G' data and penetration values at 25°C, which show that hardness increases along the series Escomer H101<Polywax C4040<Polywax 2000<Polywax 1000<Epolene N-21 (see section 5.2.3). At 65°C the hardness trend is slightly different: it increases along the series Escomer H101<Polywax C4040<Polywax 1000<Epolene N-21<Polywax 2000. The reason for this is apparent from the DSC beginning of melt temperatures, which indicate that there is some material in Polywax 1000 and Epolene N-21 that is already melting at this temperature (see Table 5.1). Density increases in accordance with the tan δ data, confirming that although Polywax 2000 has a high molecular mass, its predominantly chain folded conformation lowers its crystallinity, due to the difficulty in accommodating the folds into the crystal lattice. It would therefore be expected that the density of Epolene N-21 would also be low. An explanation for its anomalously high density is that the presence of both odd and even carbon numbers, as well as only folded chains, contribute to more optimal crystal packing.

Table 5.2: Physical properties of some polyethylene waxes

Analysis	HDPE waxes			Copolymer LDPE wax	Degradation PE wax
	Polywax 1000	Polywax 2000	Polywax C4040	Escomer H101	Epolene N-21
Congealing point (°C)	105	112	96	101	-*
Drop melting point (°C)	115	129	106	110	120
Viscosity @135°C (cP)	14.3	55.7	7.1	22.3	491
Penetration @25°C (dmm)	1.0	0.5	1.5	3.0	<0.1
Penetration @65°C (dmm)	5.0	2.0	9.5	33.0	4.0
Density @25°C (g/cm^3)	0.90	0.84	0.89	0.85	0.95
MIBK solubles (%)	0.04	0.03	0.60	0.16	0.70

* Wax too viscous for analysis

5.3 RELEVANCE OF THE PE WAX PROPERTIES TO THEIR APPLICATIONS

The PE waxes are competitors to the Fischer Trospch hard waxes in most applications. The final choice of which wax is used is usually a trade off for the end user between performance and price.

The viscosities of the PE waxes are higher than those of the Fischer Tropsch hard waxes (see Tables 4.3, 4.5 and 5.2), and therefore do not reduce the viscosity of a HMA system to the same extent as do the latter. First-intention PE waxes, or by-product PE waxes that have been cleaned up to remove excess monomer or solvent, usually impart better high-temperature properties to a HMA than the Fischer Tropsch waxes do. Some manufacturers, however, are prepared to use a by-product PE wax, accepting its slightly poorer thermal stability for the price advantage. Although the PE waxes have high DSC end of melt temperatures, their DSC melting ranges are broad in comparison to those of the Fischer Tropsch waxes, and this may have a negative effect on the HMA set time (see Tables 4.1, 4.4 and 5.1). The presence of high molecular mass material in a PE wax will have a detrimental effect on the desired flexibility of the HMA. It is necessary to consult the rheology and GPC data in order to determine the effect of wax structure and molecular mass on this property. Polywax C4040 is a PE wax having the most optimal balance of properties for HMAs. This is due to its narrow DSC melting range, suitable TG decomposition characteristics, relatively low molecular mass and good flexibility (tan δ) (see Table 5.1). An advantage of formulating with Escomer H101 is that the latter, due to its ketone functionality, provides good specific adhesion to aluminium and PVC substrates.

The PE waxes do not serve a function in paste polish applications unless they are oxidised. Even then, they will only be added in very small quantities to impart durability to the formulation.

Due to their high molecular masses, low penetration and high storage modulus values, the PE waxes will impart good mechanical properties, such as rub and scuff resistance, to an ink film (see Tables 5.1 and 5.2 and section 5.2.3). These waxes are micronised by grinding as their viscosities are too high to enable micronisation by spraying. The irregular particle form may detract even more from the gloss of the ink film than would the regular spherical Fischer Trospch particles, due to uneven reflection of light.

The PE waxes are suitable external lubricants in PVC processing, due to their high molecular masses and thermal stabilities (see Table 5.1). Evaluation of the temperature @0.5% decomposed parameter in conjunction with the PVC processing temperature will ensure optimal performance of the wax (see Table 5.1). Should this parameter be too low, as in the case of PE waxes containing too much low molecular mass material, problems such as the build-up of charred wax may result. Oxidised PE waxes possess both the chemical and physical properties required for use as internal lubricants in PVC processing.

Due to their high crystallinites, the PE waxes may be used in candle wax blends to improve the gloss of the finished candle. As with the Fischer Trospch waxes, low addition levels are recommended, as their high storage modulus values predict that they will impart brittle properties to the candle (see section 5.2.3).

5.4 REFERENCES

(1) Ullmann's Encyclopedia of Industrial Chemistry, 2000, 6th Ed., Electronic Release.

(2) M. Sawodny et al, Makromol. Chem. Macromol. Symp., 1990, 39, 229-247.

(3) Eastman product brochure, Epolene Waxes, Eastman Chemical Company, 1994.

(4) H. H. Willard et al, Instrumental Methods of Analysis, 1988, 7th Ed., Wadsworth Publishing Company, Belmont California.

CHAPTER 6

THE PETROLEUM WAXES

6.1 PARAFFIN WAX AND MICROWAX

6.1.1 INDUSTRIAL SYNTHESIS AND ECONOMIC SIGNIFICANCE

Petroleum wax may be classified as either paraffin wax (macrocrystalline wax) or microwax (microcrystalline wax), depending on its natural occurrence and crystallinity. Petroleum waxes are contained in crude petroleum and are obtained during the refining of oil. Depending on the source of the petroleum, the wax content can vary between 2% (Rumanian crude) and 30% (Indonesian crude). It is, however, generally between 3 and 15% in crude petroleum from the main production areas. Because of their higher molecular masses, and therefore higher boiling ranges, waxes become concentrated in atmospheric distillation residues during the refining of crude petroleum. The residues are then processed to lubricating oils, and waxes are obtained in each fraction of the vacuum distillation. The presence of wax increases the pour point of the oil due to poor solubility, and must therefore be removed. Paraffin waxes are obtained from light and middle lubricating oil cuts by vacuum distillation. Paraffin waxes also include so-called intermediate waxes, which are derived from heavy lubricating oil distillates, and are intermediates between macrocrystalline and microcrystalline waxes with regard to structure and composition. Microcrystalline waxes originate from vacuum residues and from the sediments of paraffinic crude oil. [1]

In 1992, 9.5×10^5 t of paraffin and microcrystalline waxes were produced in the USA, 8×10^5 t in Asia, 6.5×10^5 t in Western Europe, 2.6×10^5 t in Germany alone, 2×10^5 t in Eastern Europe and 4×10^5 t in the rest of the world. The worldwide consumption of petroleum waxes was ca. 2.8×10^6 t in 1992, of which 5×10^5 t was in Western Europe, 2×10^5 t in Eastern Europe, 8.5×10^5 t in the USA and 9×10^5 t in Asia. [1]

The average molecular mass of a petroleum-based wax is dependent on the boiling range of the particular lubricating oil distillate from which it is derived. The composition of paraffin waxes is

predominantly a mixture of straight chain alkanes. A low level of methylene branching is present, as well as a very small fraction of monocyclic alkanes. The molecular mass, amount of iso- and cycloalkanes present, and strength of branching usually increase along the series paraffin wax<intermediate wax<microwax. Paraffin and intermediate waxes contain n-alkanes in the range C_{18} to C_{45}, and C_{22} to C_{60}, respectively, and have a total content of cyclo- and iso-alkanes of 0-40%, and 30-60%, respectively. [1]

Depending on the degree of refinement, paraffin waxes may be classified as follows: [1]

(1) Crude waxes, also known as slack waxes;

(2) Slack wax raffinates (scale waxes);

(3) Deoiled slack waxes;

(4) Soft waxes;

(5) Semi-refined waxes;

(6) Filtered (decolourised) waxes;

(7) Fully-refined waxes.

Refining slack waxes starts with deoiling, by either solvent or sweating methods, to obtain harder, higher value products. [1] They fulfil purity criteria for the production of packaging materials for foods and for the formulating of cosmetics and pharmaceuticals. Microwaxes are used in coatings for food packaging, lubrication of plastics, cheese waxes, chewing gum bases, decorative candles, polishes, ozone protective agents in the rubber industry and additives for explosives.

6.1.2 ANALYSIS PROFILE

The analytical results of the fully-refined paraffin waxes and microwaxes examined here are given in Table 6.1.

Table 6.1: Analysis results of some fully-refined paraffin waxes and microwaxes

	Fully-refined paraffin waxes		Microwaxes	
Analysis	**Ter Hell 6039**	**Chinese wax grade 58/60°C**	**Mobil 2360**	**Be Square 195**
DSC				
Melt range, °C	23-63	23-60	9-83	21-92
Maxima, °C	43/59	40/57	43	62/85
Fusion enthalpy, J/g	185	196	126	181
TG				
Onset temp., °C	291	252	322	422
Temp. at 0.5% weight loss, °C	212	185	215	236
DTG maxima, °C	338	288	379	483
Rheometry				
T_α, °C	37	35	19	50
T_β, °C	-	-	-37	-20
GPC				
M_n, Daltons	411	383	557	710
M_w, Daltons	422	390	610	805
M_z, Daltons	433	398	670	926
P_d	1.03	1.02	1.10	1.13
HTGC				
Carbon no. spread	C_{14}-C_{67}	C_{14}-C_{68}	C_{18}-C_{24}	C_{24}-C_{70}
% n-paraffins	75.13	90.15	82.52	92.61
% iso-paraffin	24.87	9.85	17.48	7.39

6.1.2.1 DSC

The refining of slack waxes, the precursor to paraffin waxes, starts with deoiling, by either solvent or sweating methods, to obtain harder and higher-value products. [1] The oily fraction of these waxes is defined as the amount of material soluble in methyl ethyl ketone (MEK) at -32°C. [2] Fully and semi-refined paraffin waxes contain <0.5% and >0.5% MEK soluble material, respectively. The paraffin waxes studied here are fully-refined paraffin waxes grade 58/60°C, of German (Ter Hell 6039) and Chinese origins, respectively. The DSC plots of these two waxes are compared in Figure 6.1. A transition is apparent at a temperature below the melting transition. As previously discussed (see section 4.2.2.1), this is indicative of a solid-solid transition. [3,4] Although both

waxes are of the same grade, the DSC melting maximum of the Ter Hell wax is slightly higher than that of the Chinese wax.

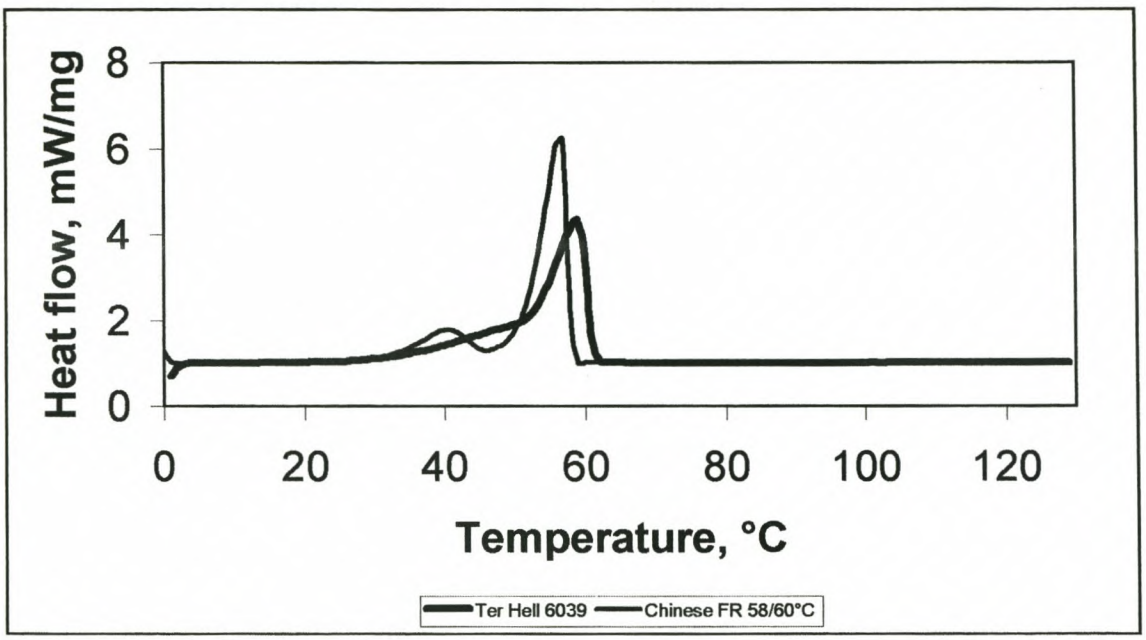

Figure 6.1: Comparison of the DSC analyses of some fully-refined paraffin waxes

Figure 6.2 shows a DSC comparison of the two microwaxes studied here, viz. Mobil 2360 and Be Square 195, which are medium and high melting respectively. Their broad DSC melt ranges are indicative of broad molecular mass distributions and their relatively low fusion enthalpies are to be expected, considering their branched structures. The reason for the melting bimodality of Be Square 195 is uncertain. From the position of the DSC melting peak, it is probably not due to polymorphism.

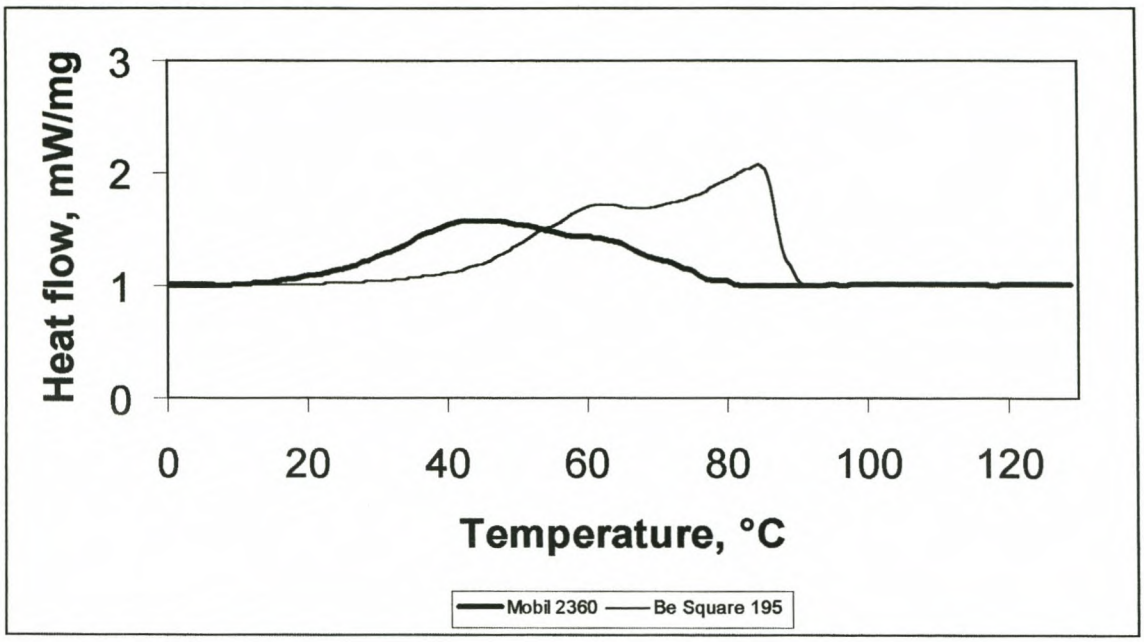

Figure 6.2: Comparison of the DSC analyses of some microwaxes

6.1.2.2 TG

The TG analyses of the two fully-refined paraffin waxes, Ter Hell 6039 and Chinese 58/60°C, (Figure 6.3) show that the German wax decomposes at a higher temperature range than the Chinese wax. This correlates with the melting behaviour described in section 6.1.2.1. The TG data indicates that the microwaxes, Be Square 195 and Mobil 2360, display greater thermal stabilities than the paraffin waxes (Figure 6.4). This is due to the higher molecular mass material and large cyclic side branches which are present in the microwaxes, both of which result in decomposition at higher temperatures.

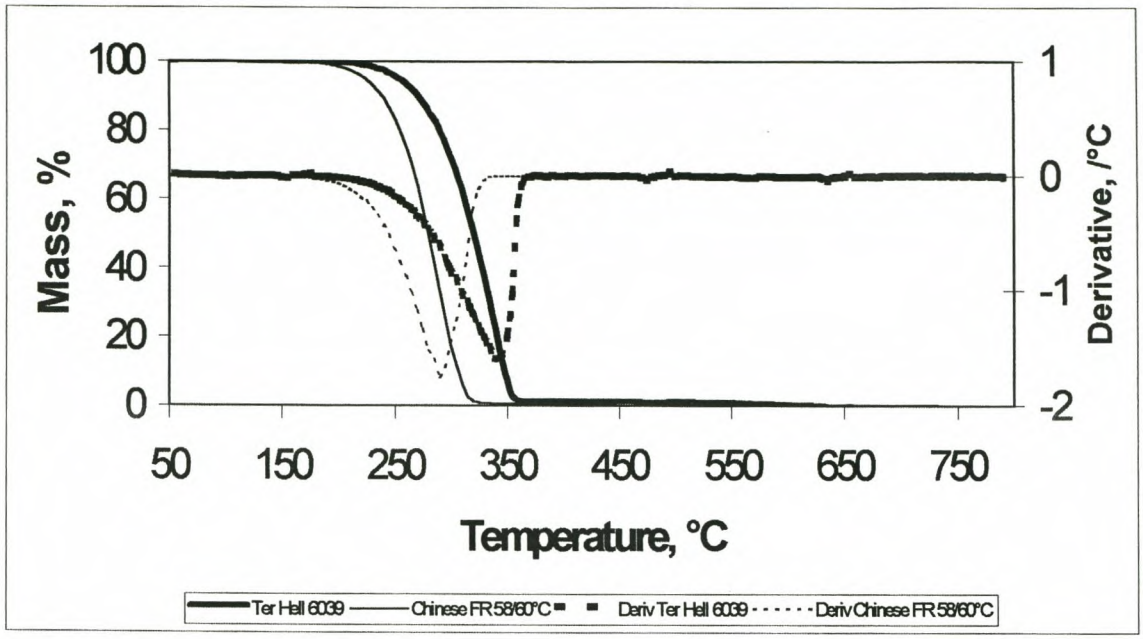

Figure 6.3: Comparison of the TG analyses of some fully-refined paraffin waxes

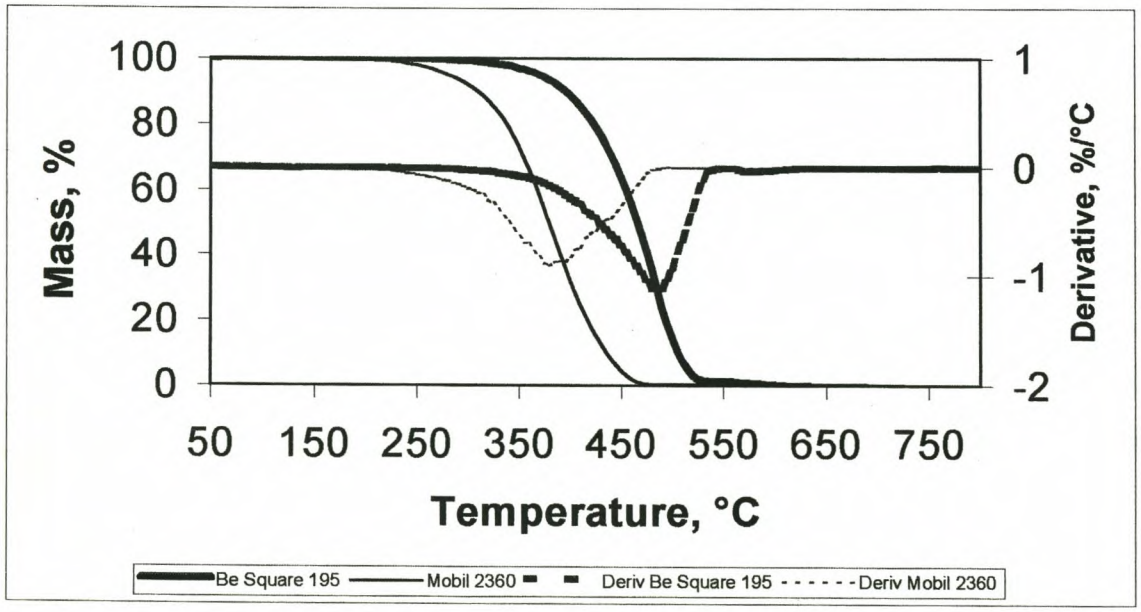

Figure 6.4: Comparison of the TG analyses of some microwaxes

6.1.2.3 RHEOLOGY

The storage modulus values measured for this set of waxes are much lower than those of the Fischer Tropsch and polyethylene waxes (see Figures 4.8, 4.21 and 5.6) . Empirically, the former waxes are also much softer than the latter. The storage moduli of the paraffin waxes and Be Square 195 are similar, but are higher than those of Mobil 2360 (Figure 6.5). This indicates that the former waxes are harder and less flexible than Mobil 2360. The microwaxes display higher tan δ values than the paraffin waxes up until the onset of melting at ca. 15°C (Figure 6.6). This correlates with the fact that microwaxes contain large side chain branches, which will contribute to their greater free volume, greater flexibility and lower cohesive strength (see section 3.3.1.2). The data confirms that Mobil 2360 is the more flexible microwax. Both the T_α and T_β transitions may be seen on the tan δ curves obtained for the microwaxes, due to large scale branching, whereas only the former transition is apparent for the paraffin waxes (see section 3.3.1.4).

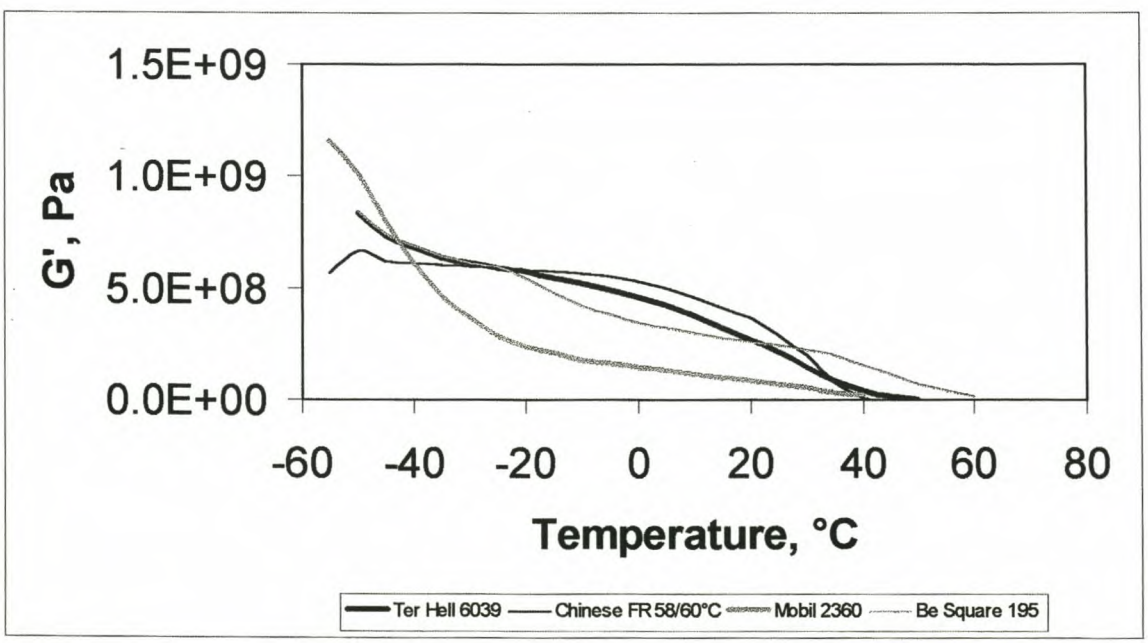

Figure 6.5: Comparison of the storage moduli of some fully-refined paraffin waxes and microwaxes

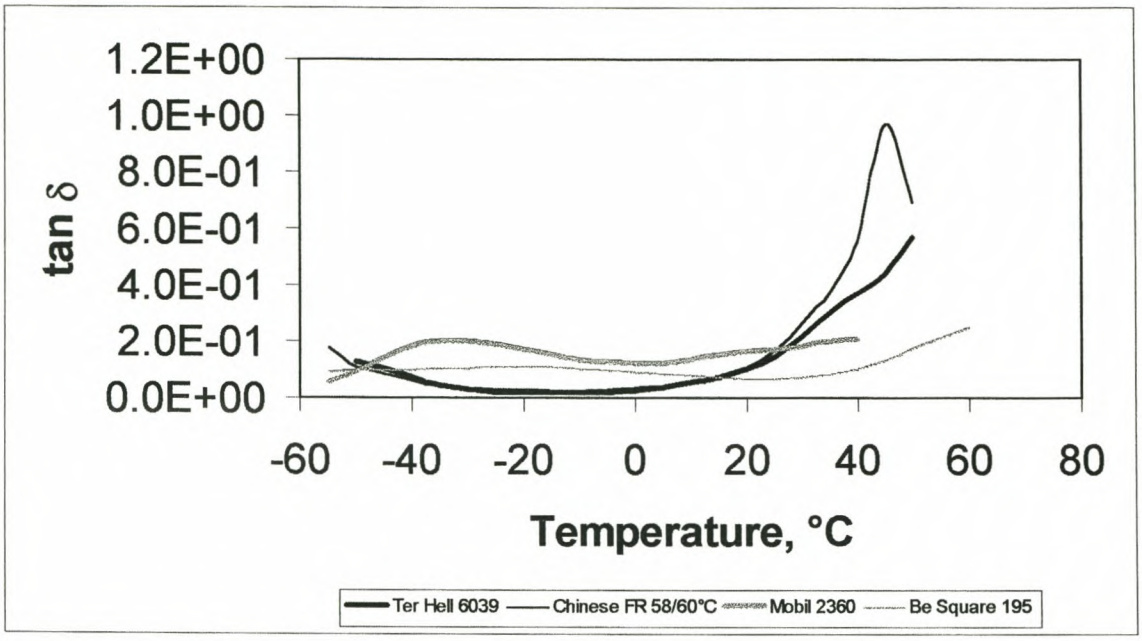

Figure 6.6: Comparison of the tan δ curves of some fully-refined paraffin waxes and microwaxes

6.1.2.4 GPC

The GPC analysis parameters for the two low-melting paraffin waxes analysed here do not differ significantly (Figure 6.7). Visual inspection of the analyses, however, shows that the German wax does have a slightly wider MMD than the Chinese wax. Be Square 195, the higher melting microwax of the two analysed, also has a much higher MMD than Mobil 2360 (Figure 6.8). There is no evidence of molecular mass bimodality, therefore ruling this out as the cause of melting bimodality (see section 6.1.2.1). These results are complementary to the DSC and TG results.

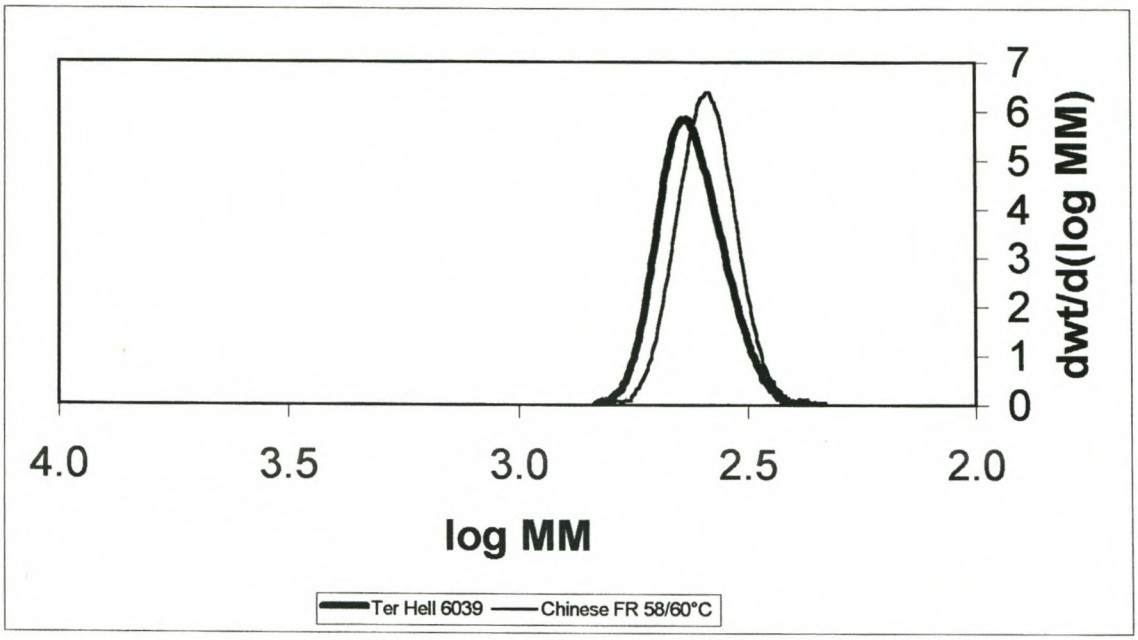

Figure 6.7: Comparison of the GPC analyses of some fully-refined paraffin waxes

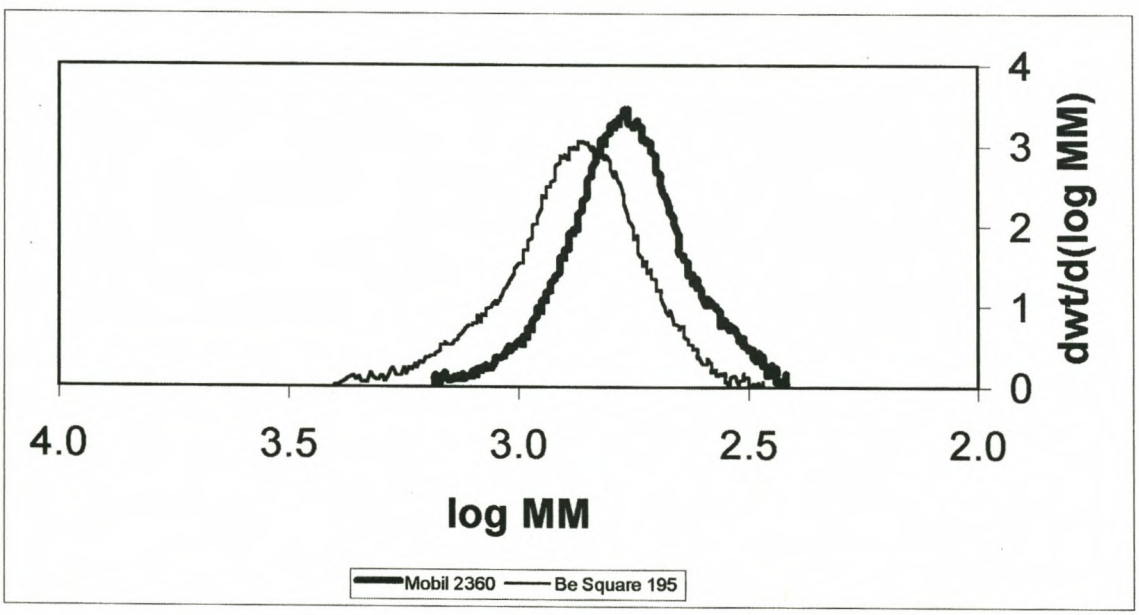

Figure 6.8: Comparison of the GPC analyses of some microwaxes

6.1.2.5 HTGC

HTGC analyses display the same trends observed from the GPC data for both the paraffin waxes (Figure 6.9) and the microwaxes (Figure 6.10).

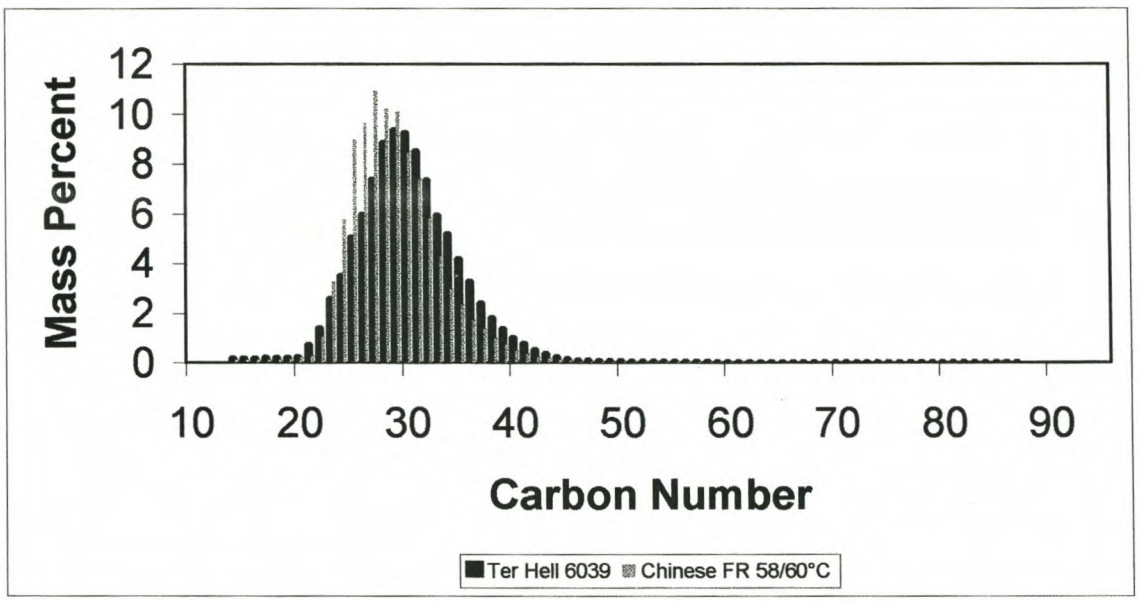

Figure 6.9: Comparison of the HTGC of some fully refined paraffin waxes

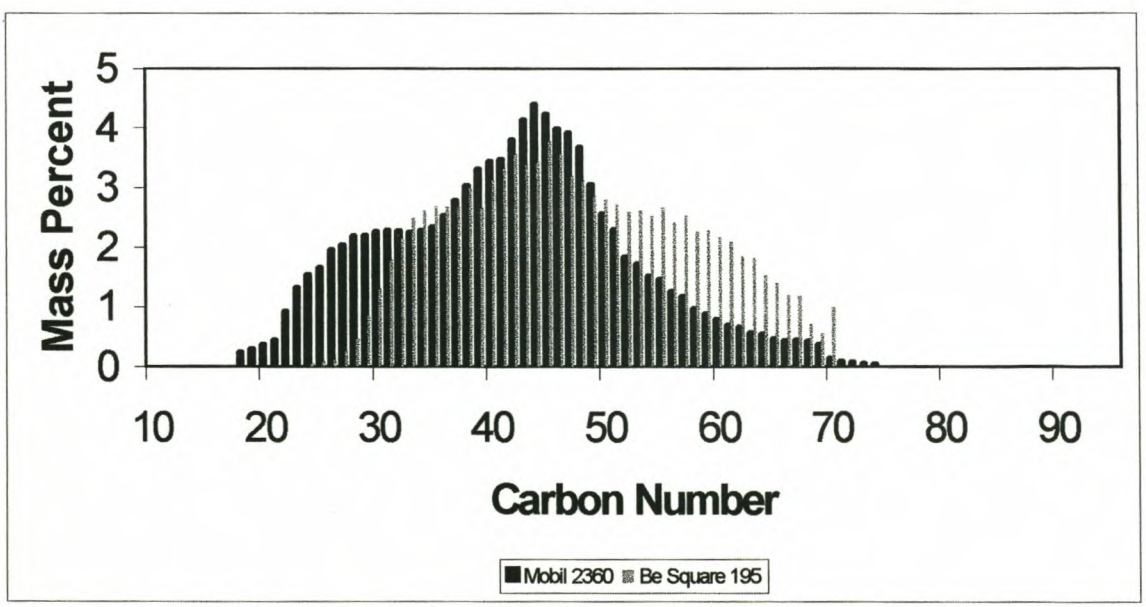

Figure 6.10: Comparison of the HTGC analyses of some microwaxes

6.1.2.6 IR

IR analyses of the paraffin waxes and microwaxes (Figure 6.11) show the characteristic paraffinic stretching, bending and rocking vibrations at ca. 2900, 1400 and 720 cm^{-1}. IR analysis cannot discriminate between these two waxes, as the vibrations of the large cyclic side groups present in the microwaxes occur at the same frequencies as those of straight chain paraffinic functionalities. [5] They are therefore also indistinguishable from the IR analyses of the Fischer Tropsch and polyethylene waxes discussed previously in sections 4.1.2.6, 4.2.2.6 and 5.2.6.

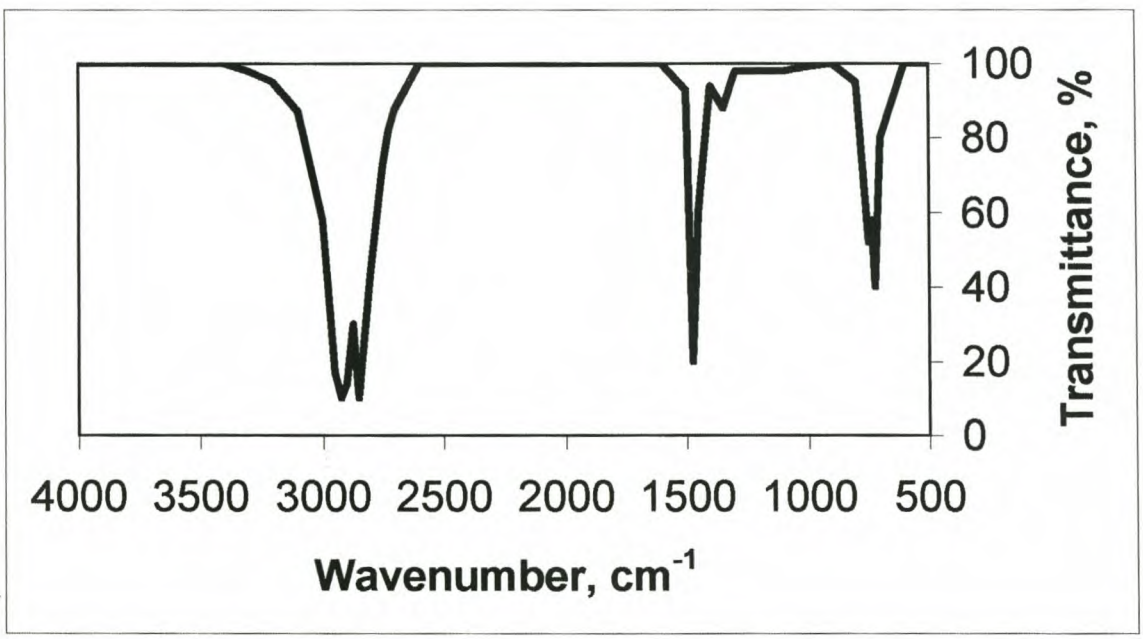

Figure 6.11: Typical IR analysis of a fully-refined paraffin wax and microwax

6.1.2.7 WET CHEMICAL ANALYSES

Table 6.2 shows the results of the wet chemical analyses of the paraffin waxes and microwaxes examined in this study. The DSC, TG, GPC and HTGC analyses of the two paraffin waxes showed that, although the waxes are of the same grade, the German wax has slightly higher melting, decomposition and molecular mass ranges than the Chinese wax (see Table 6.1). The congealing and drop melting points are similar, the former being the analysis used to determine wax grade. Experience has shown that the reason for this phenomenon can be explained as net result of the balance of the plasticiser effect of the MEK solubles content and wax molecular weight. This may in fact indicate that wax grade is a misleading concept. It is interesting to note that experience has shown that the MEK solubles content of

the German paraffin waxes are usually higher than the Chinese waxes of similar grade. The congealing and drop melting points, and viscosities of the microwaxes are higher than those of the paraffin waxes, as indicated by the DSC end of melt temperatures and free volume effects (branching), respectively (see Table 6.1 and section 6.1.2.3). This is confirmed by the density analyses. The penetration values at 25 °C do not correlate to the G' data, due to a larger analysis error when analysing softer materials (see section 6.1.2.3).

Table 6.2: Physical properties of some fully-refined paraffin waxes and microwaxes

Analysis	Paraffin waxes		Microwaxes	
	Ter Hell 6039	Fully-refined Chinese wax grade 58/60°C	Mobil 2360	Be Square 195
Congealing point (°C)	60	59	76	85
Drop melting point (°C)	60	60	80	89
Viscosity @135°C (cP)	3.6	3.5	5.0	8.3
Penetration @25°C (dmm)	22	12	26	6
Penetration @65°C (dmm)	*	*	*	185
Density @25°C (g/cm^3)	0.89	0.87	0.70	0.93
MEK solubles (%)	0.43	0.14	2.50	0.42

* Not possible to perform analysis due to wax properties

6.2 MEDIUM MELTING, NARROW MMD, PETROLEUM-BASED WAXES

6.2.1 INDUSTRIAL SYNTHESIS AND ECONOMIC SIGNIFICANCE

The waxes examined here are petroleum-based waxes with a high n-paraffin content and a narrow molecular mass distribution and melting range. They are a series of low-yield fractions, prepared by repetitive distillation from other suitable petroleum based waxes, and therefore sell at a premium. Their melting points increase along the series HNP 3<HNP 10<HNP 9. Their main application is in thermal transfer or solid inks, where their function is to effect transfer of the pigment onto a printable substrate by melting.

6.2.2 ANALYSIS PROFILE

Table 6.3 summarises the results obtained from the instrumental analyses of the medium melting, narrow MMD, petroleum-based waxes.

Table 6.3: Analysis results of some medium melting, narrow MMD, petroleum-based waxes

Analysis	HNP 3	HNP 10	HNP 9
DSC			
Melt range, °C	40-69	31-78	55-79
Maxima, °C	53/66	70/75	76
Fusion enthalpy, J/g	208	225	220
TG			
Onset temp., °C	297	340	342
Temp. at 0.5% weight loss, °C	222	209	212
DTG maxima, °C	331	379	382
Rheometry			
T_{α}, °C	-45	-30	-31
T_{β}, °C	-	-	-
GPC			
M_n, Daltons	421	501	501
M_w, Daltons	429	510	511
M_z, Daltons	436	519	521
P_d	1.02	1.02	1.02
HTGC			
Carbon no. spread	C_{20}-C_{65}	C_{20}-C_{49}	C_{20}-C_{47}
% n-paraffins	97.42	95.70	91.0
% iso-paraffins	2.58	4.30	9.0

6.2.2.1 DSC

The DSC analyses (Figure 6.12) again illustrate the effect of the increase in melting point on the DSC curve along a homologous series of waxes. HNP 3 and HNP 10 display bimodality, which can again be attributed to a solid-solid transition. HNP 9, which has a DSC maximum at 75°C, which is only 1°C higher than that of HNP 10, does not undergo this transition (Table 6.3). [3,4]

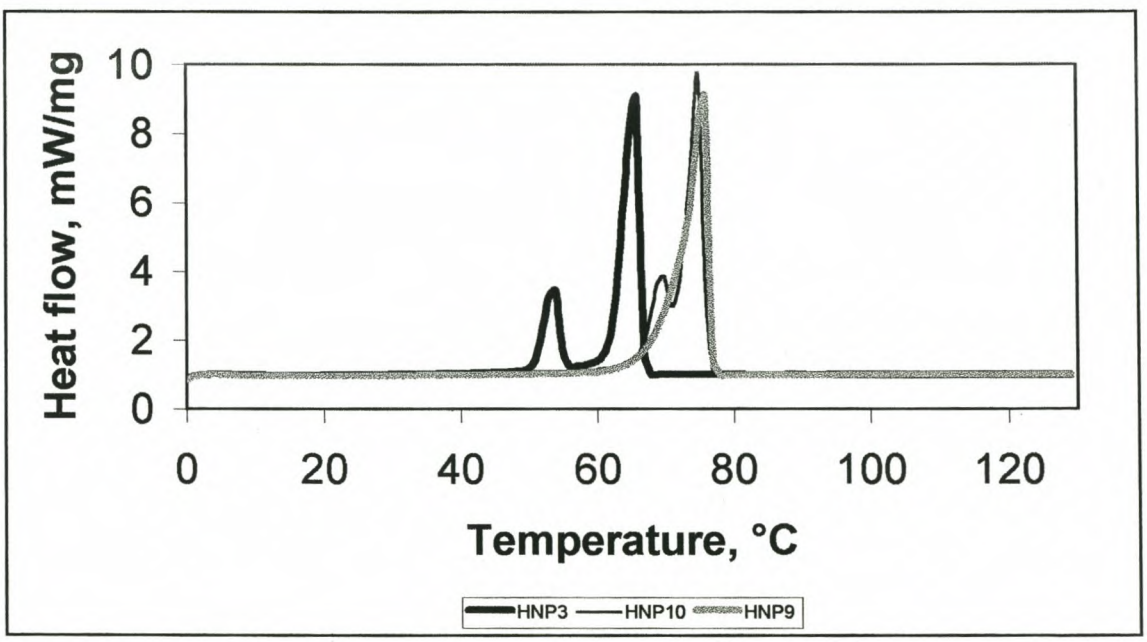

Figure 6.12: Comparison of the DSC analyses of some medium melting, narrow MMD, petroleum-based waxes

6.2.2.2 TG

The TG onset temperatures and DTG maxima of HNP 3 are significantly lower than those of HNP 10 and HNP 9 (Figure 6.13). The decomposition profiles of HNP 10 and HNP 9 are very similar. This is in agreement with the observation made concerning the DSC maxima.

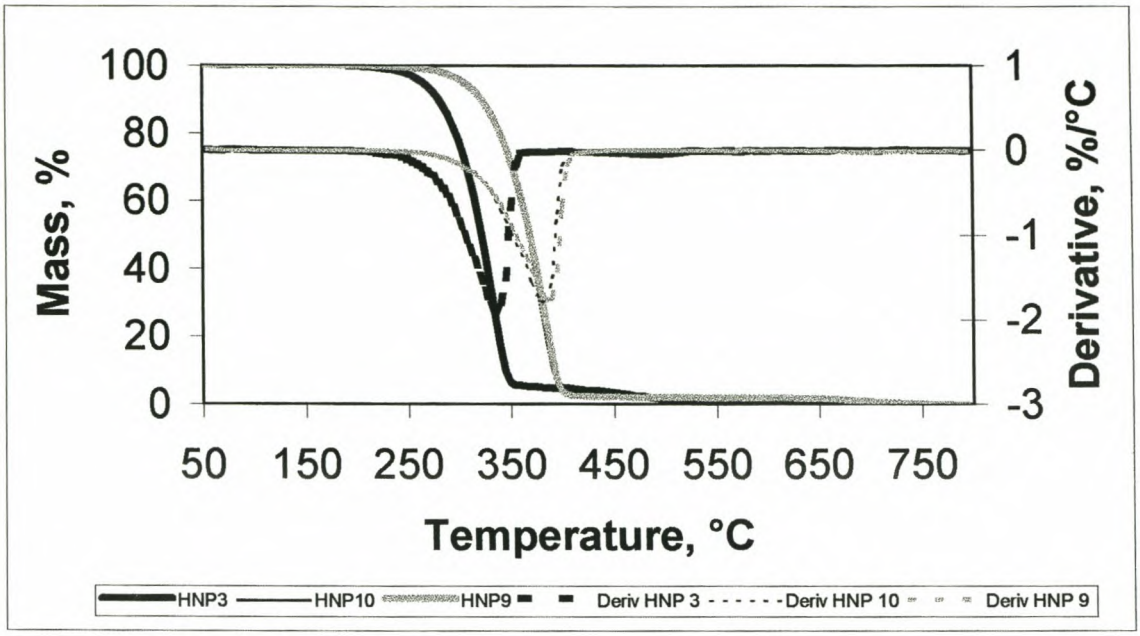

Figure 6.13: Comparison of the TG analyses of some medium melting, narrow MMD, petroleum-based waxes

6.2.2.3 RHEOLOGY

Figure 6.14 shows that the G' data of HNP 10 and HNP 9 are identical, while that of HNP 3 is slightly lower than these. Consequently, HNP 3 should be comparatively a softer, more flexible wax than the former waxes. However, the tan δ results in Figure 6.15 do not confirm this observation. An explanation is that the mechanical properties of these soft waxes are actually indistinguishable, due to the similarities in their other properties. The temperatures of the α-transitions increase with increasing molecular mass, as expected (see section 3.3.1.4).

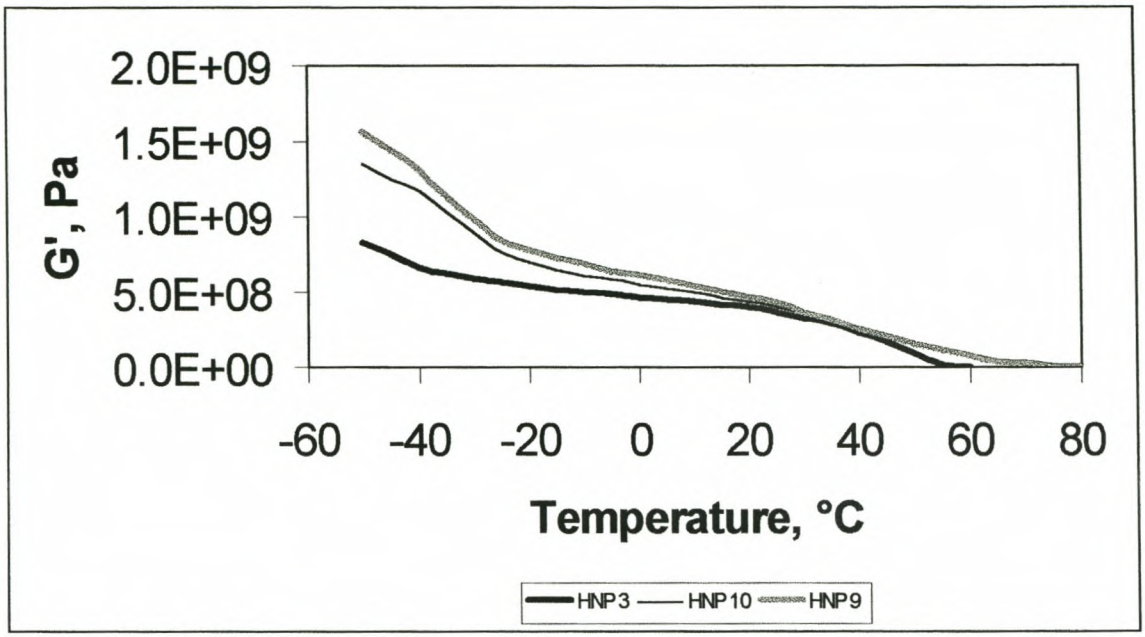

Figure 6.14: Comparison of the storage moduli of some medium melting, narrow MMD, petroleum-based waxes

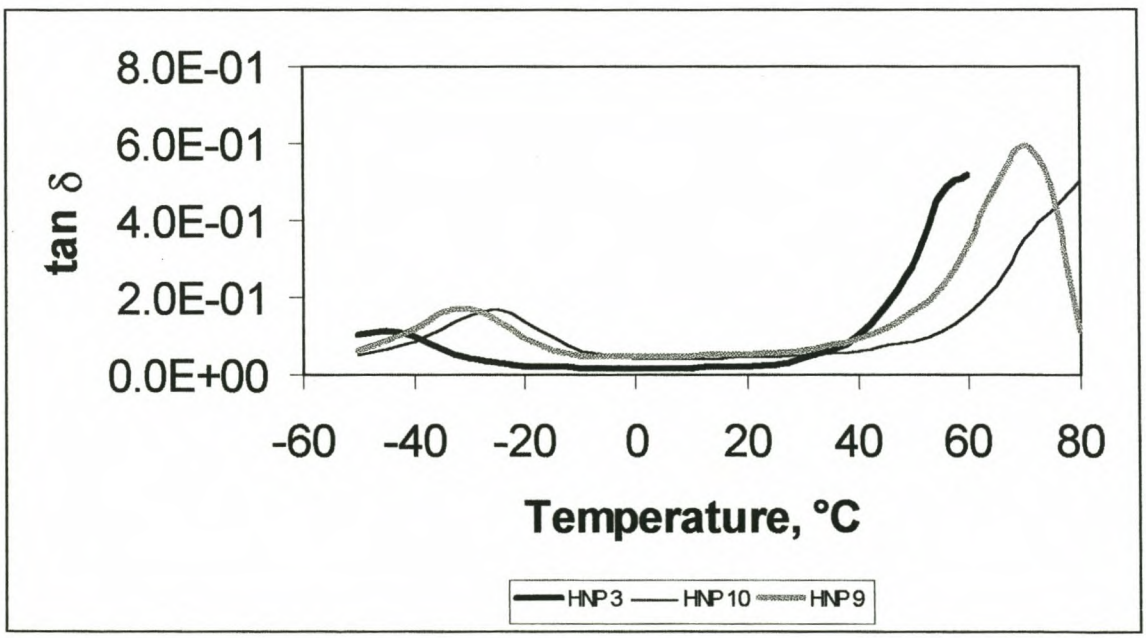

Figure 6.15: Comparison of the tan δ curves of some medium melting, narrow MMD, petroleum-based waxes

6.2.2.4 GPC

The GPC analysis parameters of HNP 3 differ significantly from those of HNP 10 and HNP 9. Those of the latter two waxes cannot be distinguished from each other. Past experience with these analyses has shown that the DSC sensitivity to small variations in different batches of a wax is far superior to that of GPC. [6] The reason for this is due to the higher repeatability of DSC analyses.

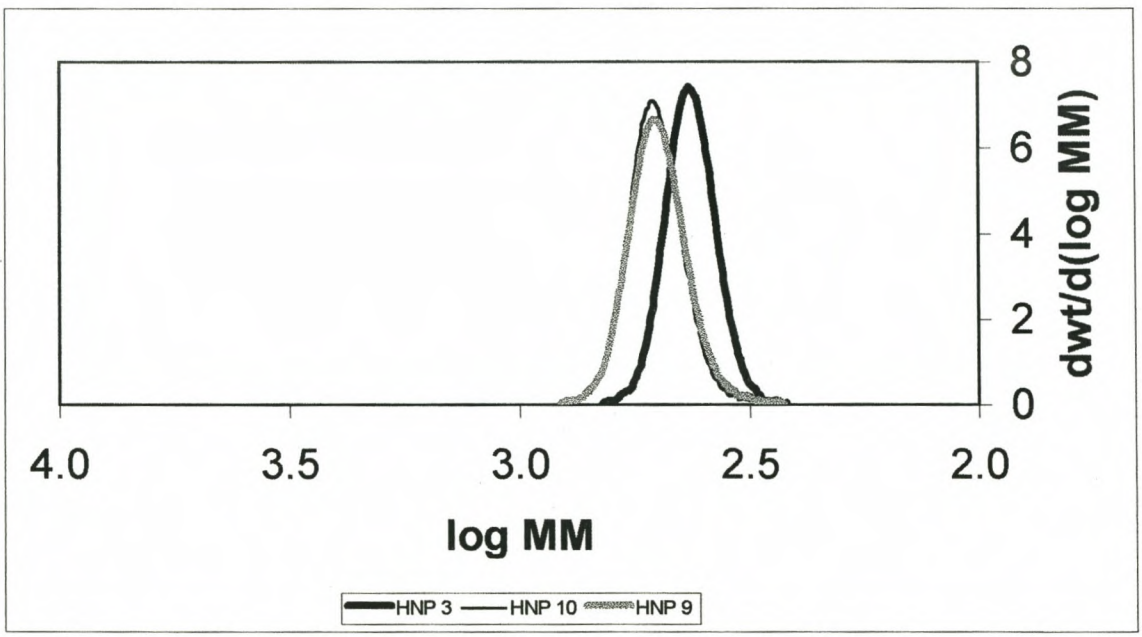

Figure 6.16: Comparison of the GPC analyses of some medium melting, narrow MMD, petroleum-based waxes

6.2.2.5 HTGC

The HTGC analyses of the HNP waxes indicate the same trends in terms of relative carbon number distribution as was seen from the GPC analyses (Figure 6.17).

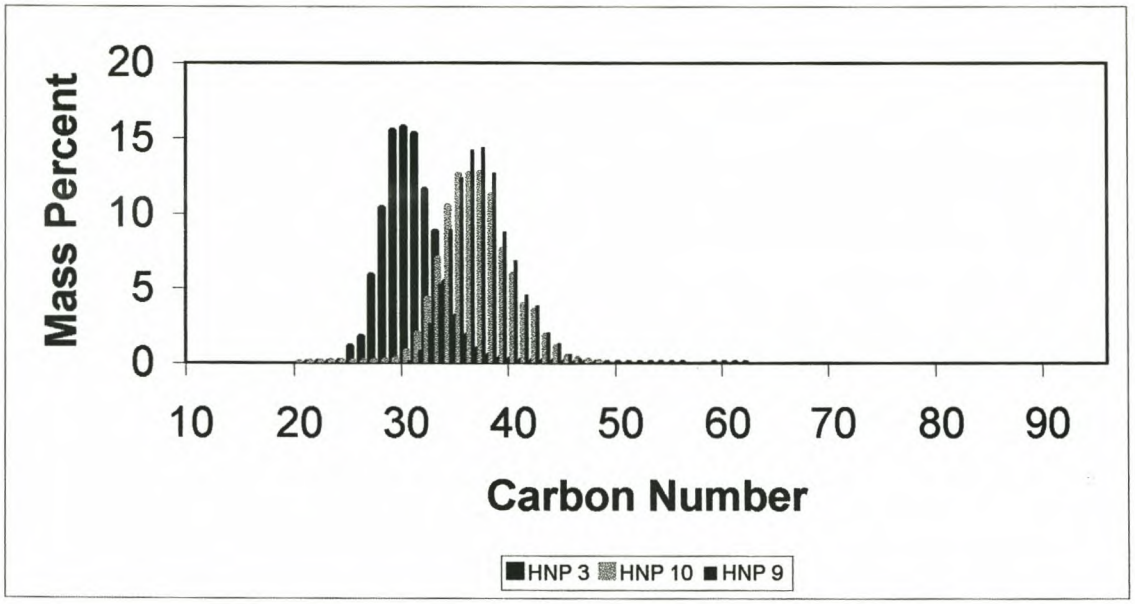

Figure 6.17: Comparison of the HTGC analyses of some medium melting, narrow MMD, petroleum-based waxes

6.2.2.6 IR

IR analysis confirms that the only functionalities present in these waxes are paraffinic. The analysis is therefore identical to that shown in Figure 6.11.

6.2.2.7 WET CHEMICAL ANALYSES

Table 6.4 shows that the congealing and drop melting points, viscosity and density analyses of HNP 10 and HNP 9 are identical. The congealing and drop melting points of HNP 3 are lower than those of the former waxes, in accordance with the DSC end of melt property (see Table 6.3). HNP 10 is softer at 25°C than the other HNP waxes. This is due to its lower DSC beginning of melt temperature. The MEK solubles content of HNP 3 is significantly higher than those of HNP 10 and HNP 9. This is in contradiction to the HTGC data, which showed that the iso-paraffin content of the former wax is by comparison lower. This, however,

indicates that the branched material present in HNP 10 and HNP 9 is not soluble in MEK at –32°C, and is therefore of a higher molecular mass.

Table 6.4: Physical properties of some medium melting, narrow MMD petroleum-based waxes

Analysis	HNP 3	HNP 10	HNP 9
Congealing point (°C)	65	74	75
Drop melting point (°C)	64	77	76
Viscosity @135°C (cP)	3.3	3.3	3.6
Penetration @25°C (dmm)	7.0	4.5	7.0
Penetration @65°C (dmm)	-*	-*	-*
Density @25°C (g/cm^3)	0.76	0.77	0.77
MEK solubles (%)	2.7	<0.1	<0.1

* Not possible to perform analysis due to wax properties

6.3 RELEVANCE OF THE PETROLEUM WAX PROPERTIES TO THEIR APPLICATIONS

Paraffin and microwaxes are used in HMA formulations. Paraffin waxes are relatively inexpensive, they have very low viscosities and are therefore good diluents (see Table 6.2). However, their low temperature at 0.5% decomposed parameters (see Table 6.1) indicate that formulations containing these waxes will deposit undesirable decomposition product residue in the area around the HMA melt pot. TG and rheology analyses also indicate that they will impart poor high temperature performance and mechanical strength, respectively, to the HMA (see Table 6.1 and section 6.1.2.3). The low congealing points of these waxes will result in long HMA set times (see Table 6.2). The only advantage of using a paraffin wax in a HMA formulation is therefore cost. Microwaxes are also often used, mainly because their branched structures impart flexibility to the HMA formulation. This was observed from the tan δ analyses of these waxes (see section 6.2.2.3). The relatively low storage modulus values of the microwaxes indicate that they will reduce the tensile strength of the HMA (section 6.2.2.3). It can also be predicted from the DSC end of melt temperatures and congealing points, which are significantly lower than those of the Fischer Tropsch hard and PE waxes, that they will impart poor setting properties to the HMA (see Tables 4.1, 5.1 and 6.1). Depending on the

type of microwax used, incorporation of a microwax should not have a detrimental effect on the high temperature performance of the HMA.

The ease of application and buffability of a paste polish is promoted by the inclusion of low melting, low molecular mass and low congealing point waxes, such as the paraffin waxes, in the formulation. The paraffin wax, due to its softness and compatibility, behaves as a plasticiser to the higher molecular mass components of the polish. Microwaxes are also used in paste polishes, their function being to impart gelling characteristics to the polish by way of their branched structures. Their relatively low DSC end of melt temperatures and molecular masses, and high penetration values mean that they will also contribute to the ease of application and buffability of the polish film (see Tables 6.1 and 6.2).

The storage modulus and penetration data show that the paraffin waxes and microwaxes are too soft to contribute to the desired mechanical and physical properties of an ink film (see section 6.1.2.3 and Table 6.1).

Paraffin waxes are universally used as candle base waxes. DSC indicates the presence of a solid-solid transition (see section 6.1.2.1 and Table 6.1). The hexagonal crystal modification lends more flexibility to a wax than the orthorhombic form. During the manufacture of drawn candles, the wax is maintained at a temperature such that it is in the hexagonal crystal form, thereby preventing the candle strand from breaking. The use of a base wax that is too hard will result in candles that are too brittle. The low oil content of the fully-refined waxes is desired, in order to avoid its bleeding onto the candle surface, as well as to allow the candle to be overdipped (see Table 6.2). Microwaxes are used as additives to improve the flexibility of the candle (see section 6.1.2.3).

The main application for the HNP waxes is in thermal transfer or solid inks. The wax acts as the carrier that facilitates the transfer of the pigment onto the printing substrate. The properties required of waxes used in the normal printing applications are therefore not relevant to this specific application. The DSC melting analyses of the HNP waxes show that their very narrow melting ranges, high fusion enthalpies and end of melt temperatures will promote rapid solidification of the ink on the substrate, and therefore avoid smudging (see Table 6.3).

6.4 REFERENCES

(1) Ullmann's Encyclopedia of Industrial Chemistry, 2000, 6th Ed., Electronic Release.

(2) ASTM D721, American Society for Testing and Materials Standard, 1997, WorldWide Standards Service Plus, Issue 00-06 v 4.0, Electronic Version.

(3) S. P. Srivastava et al, J. Phys. Chem. Solids, 1993, 54 (6), 639-670.

(4) D. S. Barmby et al, Proceedings 6th World Petroleum Congress, 1963, VI (21), 1-17.

(5) H. H. Willard et al, Instrumental Methods of Analysis, 1988, 7th Ed., Wadsworth Publishing Company, Belmont California.

(6) G. V. Webber, Schümann Sasol Internal Memorandum SW2601, 1998.

CHAPTER 7

THE NATURAL WAXES

7.1 INDUSTRIAL SYNTHESIS AND ECONOMIC SIGNIFICANCE

7.1.1 CARNAUBA

Carnauba is extracted from the leaf of the carnauba palm, *Copernica cerifera*. A yield of 5-7 g of Carnauba per leaf is expected from an 8 year old carnauba palm. The annual yield of wax per palm is ca. 150 g. About 10 000 – 16 000 t/a of Carnauba wax is available world wide. The sole exporter is Brazil. The main importers are Europe (2 000 t/a), the USA (3 000 – 4 000 t/a) and Japan. The supply of this wax is seasonal and dependent on climatic conditions and government control. Different grades of Carnauba are obtained from different parts of the palm tree and by different degrees of refining. The wax grade studied here is Carnauba Yellow, which is obtained from the youngest leaves of the Carnauba palm. This grade is considered the most superior of all the available grades. Carnauba is one of the hardest and highest melting natural waxes. It has a fine crystalline structure. The addition of a small amount of Carnauba to other waxes increases their melting and congealing points and hardness. In the case of its addition to paraffin waxes, it suppresses their tendency towards coarse crystallinity and reduces the tack of the softer waxes. The composition of Carnauba wax appears in Table 7.1. [1]

The aliphatic esters contain monocarboxylic acids of average chain length C_{26} and monohydric alcohols of average chain length C_{32}. The α-hydroxyesters present are mixtures of ca. 90% esters of α-hydroxyacids (C_{26}) and monohydric alcohols (C_{32}) and 10% esters of monocarboxylic acids (C_{28}) and α,ω-diols (C_{30}). Esters containing 4-hydroxy- and 4-methoxycinnamic acids are mainly present as oligomers and polymers. The monomer units of these are diesters of the above mentioned cinnamic acids with mono- and polyhydric alcohols and α-hydroxycarboxylic acids. The free alcohols are similar in composition to those in aliphatic esters. The wax also contains a small proportion of secondary alcohols. [1]

Table 7.1: Approximate composition of Carnauba wax [1]

Component	Weight %
Aliphatic esters	40.0
Diesters of 4-hydroxycinnamic acid	21.0
Esters of ω-hydroxycarboxylic acids	13.0
Free alcohols	12.0
Diesters of 4-methoxycinnamic acid	7.0
Free aliphatic acids	4.0
Free aromatic acids	1.0
Hydrocarbons (paraffins)	1.0
Free ω-hydroxycarboxylic acids	0.5
Triterpene diols	0.5
Unsaponifiable components	56.4
Saponifiable components	39.2
Aromatics and/or resins	4.4

Carnauba wax is approved for use in the pharmaceutical, cosmetic and food industries, as a release agent in polymer processing, and in the polish and leather industries. Carnauba has an outstanding ability to gel high concentrations of solvent, such as in a paste polish. The wax also polishes to a high gloss. [2] Many wax producers have unsuccessfully attempted to produce synthetic Carnauba alternatives with similar gelling and gloss properties.

7.1.2 CANDELILLA

The wax deposited on the stalks and leaves of the bushes or shrubs *Cerifera* and *Antisyphylitica* of the genus *Euphorbia*, which grow in the semi-deserts in southern California, south western Texas, northern Mexico and South America, is known as Candelilla wax. The purity of the wax depends on the climate, time of harvest, region and age of the harvested plants. About 800 – 1 000 t/a of Candelilla is available on the world market, of which 200 t/a is consumed by the USA. The demand for Candelilla is decreasing due to the fact that it is uneconomical to harvest and refine. [1]

Candelilla is a hard, brittle wax. The approximate composition is given in Table 7.2. Candelilla differs fundamentally from Carnauba in its high hydrocarbon content of ca. 45% and resin content of ca. 20%. [1]

Candelilla is used in cleaning preparations and polishes for furniture, car and floor applications, and in the production of candles, paper and cardboard coatings, hot melt adhesives and in polymer processing. The main use in the USA and Europe is in the production of lipstick. [2]

Table 7.2: Approximate composition of Candelilla wax [1]

Component	Weight %
Hydrocarbons (ca. 98% paraffins and 2% alkenes)	42.0
Wax + resin + sitosteroyl esters	39.0
Lactones	6.0
Free wax and resin acids	8.0
Free wax and resin alcohols (terpene alcohols)	5.0
Saponifiable components	23.0-29.0
Unsaponifiable components	71.0-77.0

7.2 ANALYSIS PROFILE

The results from the instrumental analysis of the natural waxes studied here are given in Table 7.3.

7.2.1 DSC

Figure 7.1 indicates that the DSC analyses of both Carnauba and Candelilla display melting bimodality. Table 7.3 shows that the DSC maxima are at ca. 80°C and 67°C, respectively. It is known that bimodality, due to the occurrence of a solid-solid transition, is possible if the wax melting point is <75°C. [3, 4] Carnauba's melting bimodality is therefore not as a result of the occurrence of a solid-solid transition. Visual inspection of Candelilla's DSC plot also indicates that this is not the cause of its bimodality.

Table 7.3: Analysis results of two natural waxes

Analysis	Carnauba	Candelilla
DSC		
Melt range, °C	40-84	30-72
Maxima, °C	75/80	58/63/67
Fusion enthalpy, J/g	177	145
TG		
Onset temp., °C	414	304
Temp. at 0.5% weight loss, °C	127	140
DTG maxima, °C	373/472/572	338/436/565
Rheometry		
T_{α}, °C	74	38
T_{β}, °C	-2	-40
GPC		
M_n, Daltons	600	328
M_w, Daltons	685	400
M_z, Daltons	765	462
P_d	1.14	1.22

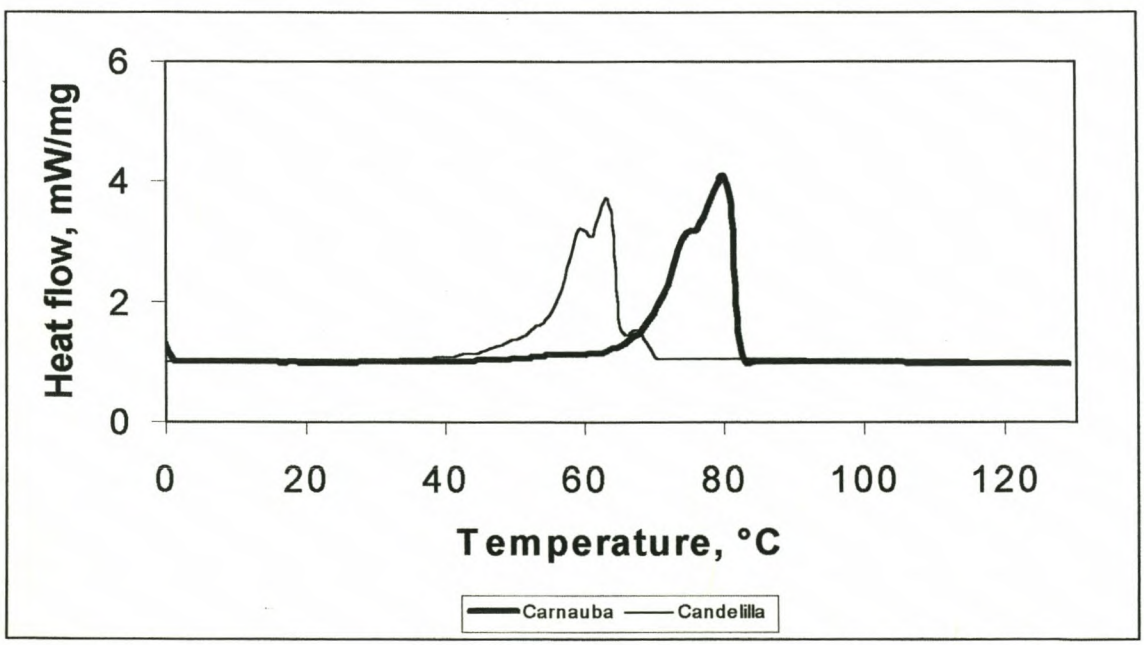

Figure 7.1: Comparison of the DSC analyses of two natural waxes

7.2.2 TG

The TG onset temperature and DTG maximum of Carnauba are significantly higher than those of Candelilla. This is to be expected, as the DSC analyses indicate that Carnauba melts at a higher temperature than Candelilla. It is therefore also to be expected that the molecular mass of the former sample will be much higher than that of the latter. The DTG profiles of both waxes display bimodality, as do their melting profiles (Figure 7.2). This usually indicates a bimodal molecular mass distribution.

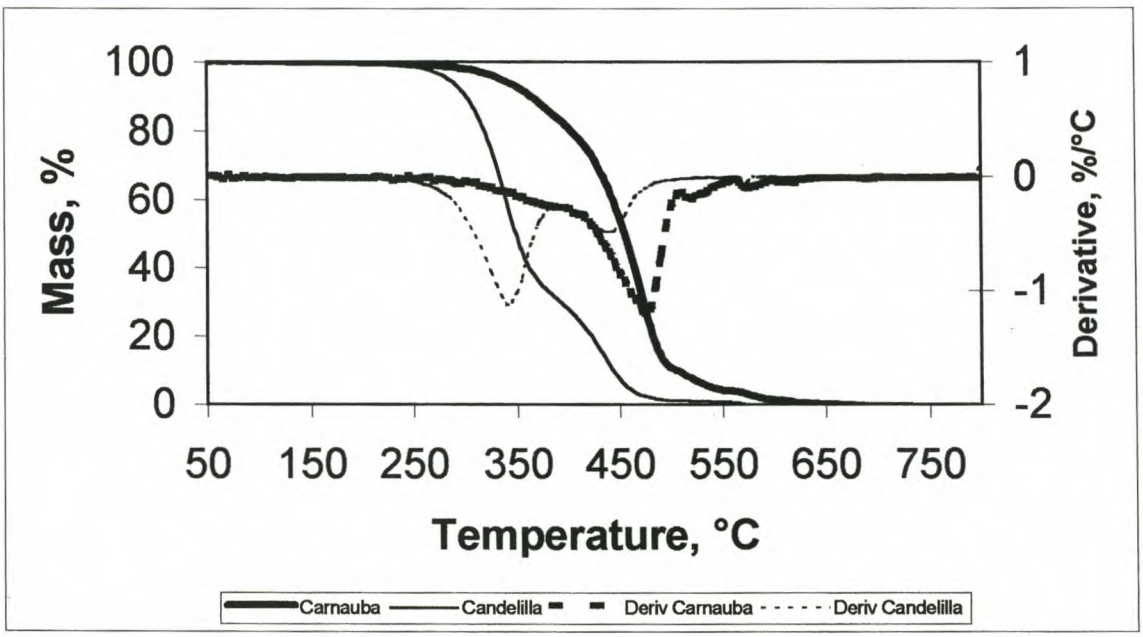

Figure 7.2: Comparison of the TG analyses of two natural waxes

7.2.3 RHEOLOGY

The storage moduli (Figure 7.3) and tan δ values (Figure 7.4) of these two natural waxes are similar. This appears to be anomalous behaviour, considering that Carnauba displays higher melting and decomposition ranges than Candelilla. The tan δ curves show that both waxes undergo both the T_α and T_β transitions (see section 3.3.1.4). The T_β transitions are as a result of oxygenate functionalities, which behave as branching. Carnauba's T_α transition is at a higher temperature than that of Candelilla's, in line with its higher molecular mass.

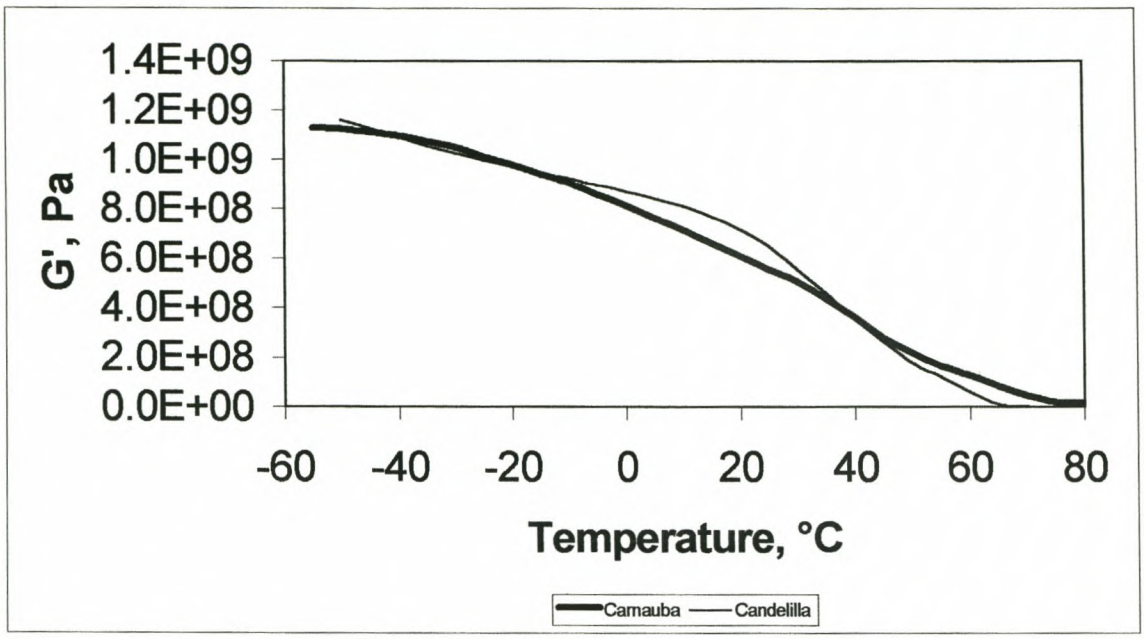

Figure 7.3: Comparison of the storage moduli of two natural waxes

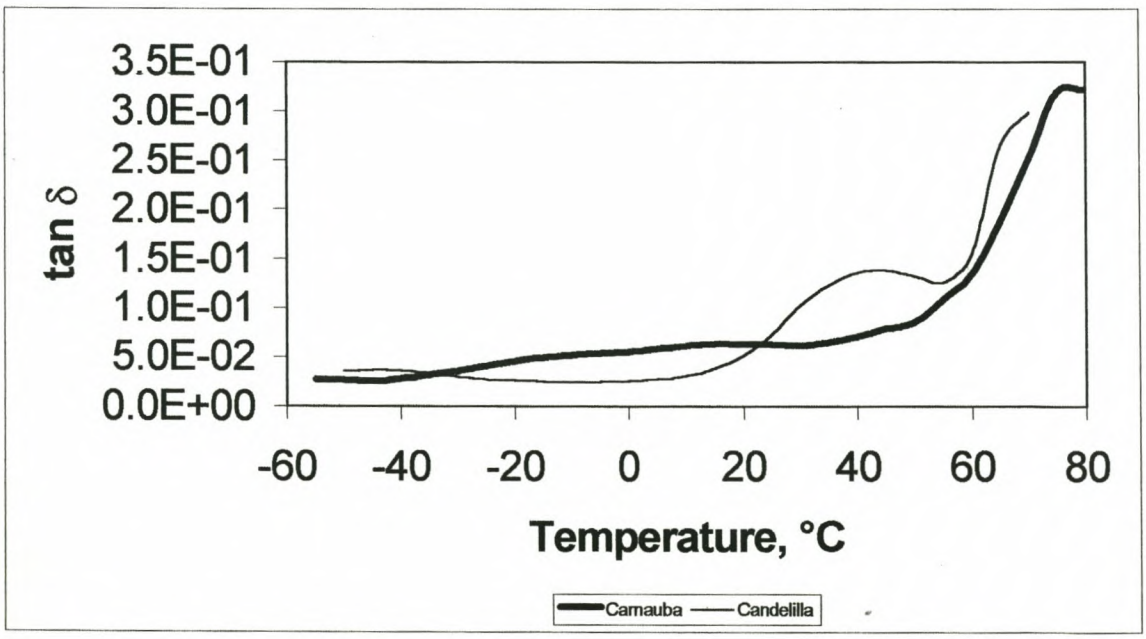

Figure 7.4: Comparison of the tan δ curves of two natural waxes

7.2.4 GPC

Carnauba and Candelilla display bimodal molecular mass distributions (Figure 7.5). According to the literature, Carnauba's first peak may be attributed to a C_{30} hydrocarbon and the second to a C_{53} ester. [5] It is also known that Carnauba contains di- and poly- esters. These analyses provide the reason for the bimodal melting and decomposition behaviours observed on their DSC and TG plots. Candelilla does not contain any oligomeric compounds, and this is therefore not the reason for its MMD bimodality. It does, however, contain a substantial amount of straight chain hydrocarbon material, as well as resin acids and alcohols. The differing melting and decomposition ranges of these compounds offer a plausible explanation for the occurrence of the DSC and DTG bimodality. It is not certain whether the melting and decomposition of the latter compounds can be assigned to the first or second DSC and DTG peaks, respectively, as not enough is known about the molecular mass of these constituents. Candelilla also has a lower MMD than Carnauba, an observation that could be made from a comparison of their DSC analyses.

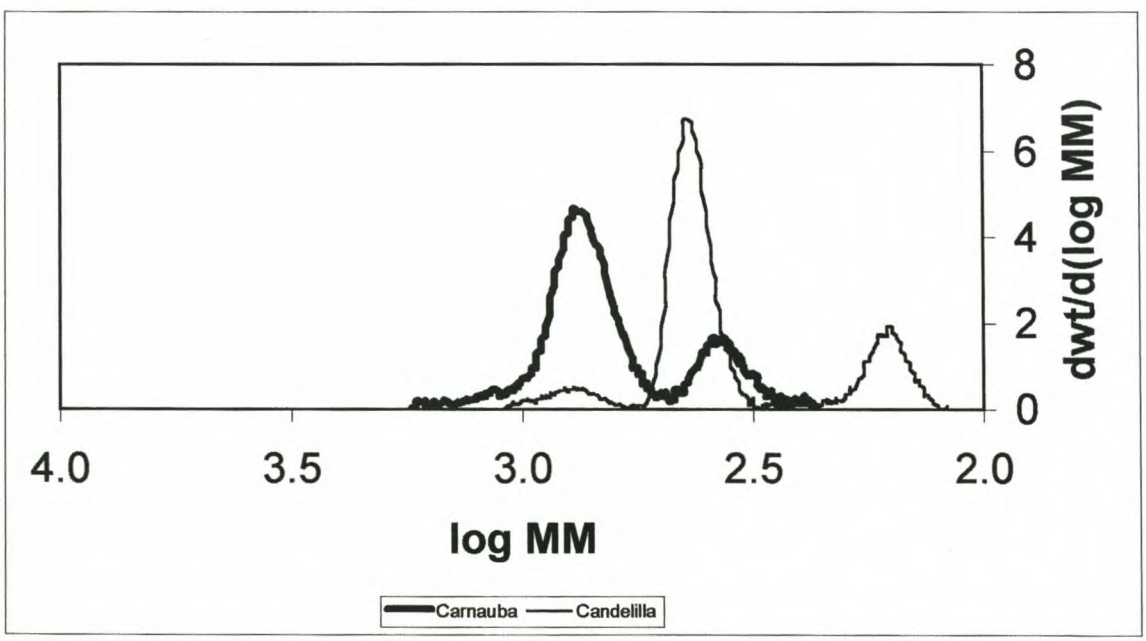

Figure 7.5: Comparison of the GPC analyses of two natural waxes

7.2.5 HTGC

The natural waxes were not analysed by HTGC, due to possible adsorption to and damage to the column stationary phase.

7.2.6 IR

In the light of the detailed chemical compositions given in Tables 7.1 and 7.2 for Carnauba and Candelilla, it can be appreciated that IR analysis serves only to give an indication of the functionalities that are present in the waxes. Both waxes display the characteristic paraffinic stretching, bending and rocking vibrations at 2900, 1400 and 720 cm^{-1}. Carnauba contains additional vibrations at 3500-3600 cm^{-1} (hydroxyl), ca. 1740 cm^{-1} (ester), ca. 1570 cm^{-1} (carboxylate COO^-) and ca. 1125 cm^{-1} (C-O stretch) (Figure 7.6). The hydroxyl band is not very strong and the corresponding carboxyl vibration, usually apparent at 1722 cm^{-1}, is not well defined. The IR analysis of Candelilla shows additional hydroxyl (3500-3600 cm^{-1}), ester, carboxyl or acetate (1736 cm^{-1}), acid carboxyl (1722 cm^{-1}), olefinic (1643 cm^{-1}) and C-O stretch (1350-1100 cm^{-1}) vibrations (Figure 7.7).

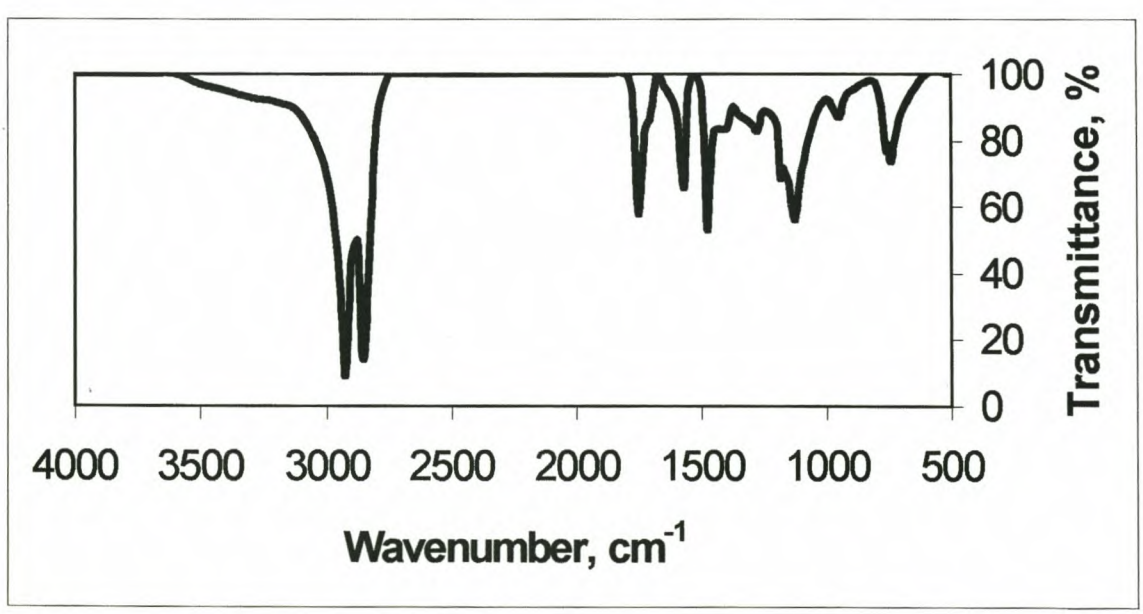

Figure 7.6: IR analysis of Carnauba

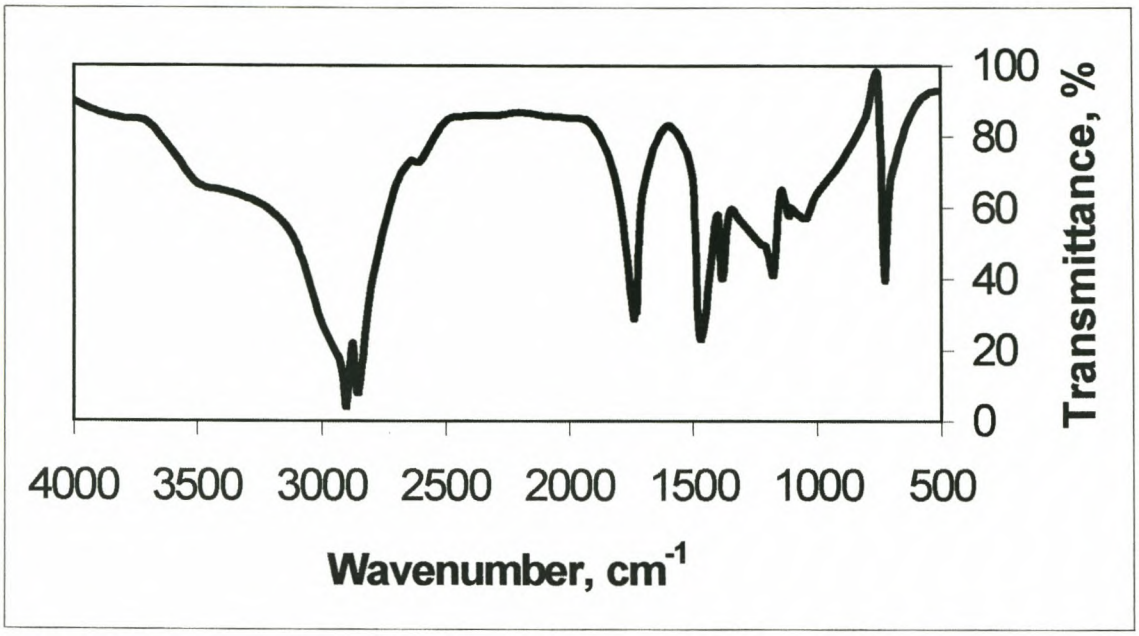

Figure 7.7: IR analysis of Candelilla

7.2.7 WET CHEMICAL ANALYSES

Carnauba's congealing and drop melting points, viscosity and penetration at 65°C, are higher than those of Candelilla (Table 7.4). This is to be expected, considering the former's higher DSC end of melt temperature, high molecular mass and more complex, polymeric-like structure (see Table 7.3). It is interesting to note that the hardness values of the waxes are similar at 25°C, where it would be expected to see a substantial difference. This is due to the fact that Candelilla contains a high percentage of resinous material. This would also explain why the rheology data for the two waxes are similar (see section 7.2.3).

Table 7.4: Physical properties of two natural waxes

Analysis	Carnauba	Candelilla
Congealing point (°C)	79	68
Drop melting point (°C)	89	73
Viscosity @135°C (cP)	15.7	6.7
Penetration @25°C (dmm)	0	<1
Penetration @65°C (dmm)	8.5	*
Density @25°C (g/cm^3)	0.80	0.80
Acid number (mgKOH/g)	10.3	17.8
Saponification number (mgKOH/g)	Too dark for analysis	54.3
MEK solubles (%)	-*	2.7

* Not possible to perform analysis due to wax properties

7.3 RELEVANCE OF THE NATURAL WAX PROPERTIES TO THEIR APPLICATIONS

The natural waxes often impart superior application performance than synthetic waxes having similar properties. They are, however, very costly, due to supply and demand factors, such as availability, seasonality and refinement difficulties. The natural waxes are not usually used in HMA, nor in ink or plastics processing applications. Carnauba wax is used extensively in paste polishes, to which it gives superior performance in terms of ease of application, buffability, durability and gloss. The reason for this lies in its bimodal melting and molecular mass profiles (see sections 7.2.1 and 7.2.4). The lower melting component will impart properties similar to those of the softer waxes, resulting in easy application and buffability. The higher melting component, with its associated hardness, will impart durability and gloss characteristics. For similar reasons, Candelilla is used as a lipstick base. The lower (softer) and higher (harder) melting components will impart ease of application and maintain the lipstick form, respectively.

7.4 REFERENCES

(1) Ullmann's Encyclopedia of Industrial Chemistry, 2000, 6th Ed., Electronic Release.

(2) H. Bennett, Industrial Waxes, 1975, 2nd Ed., Vol. 2, Chemical Publishing Company, New York.

(3) S. P. Srivastava et al, J. Phys. Chem. Solids, 1993, 54 (6), 639-670.

(3) D. S. Barmby et al, Proceedings 6th World Petroleum Congress, 1963, VI (21), 1-17.

(4) D. E. Hillman, Analytical Chemistry, July 1971, 43 (8), 1007-1013.

CHAPTER 8

IN CONCLUSION

The objectives of this work, stated in Chapter 1, were addressed as described in Chapters 4-7 and the highlights presented here.

(1) Various instrumental techniques, viz. DSC, TG, rheology, GPC, HTGC and IR (described in Chapter 3), were successfully mastered and procedures developed to efficiently characterise different waxes The various waxes were chosen to be representative of the main categories of waxes, viz. the synthetic Fischer Tropsch waxes (Chapter 4); the synthetic polymeric waxes (Chapter 5); petroleum waxes (Chapter 6); and natural waxes (Chapter 7).

(2) The data from each analytical technique, as well as from a number of wet chemical analyses, was integrated to form wax analysis profiles, not presently available in general literature, giving insight into the overall properties of waxes, as well as highlighting the differences or similarities between the various wax types.

(3) It was shown how the use of this new wax analysis profile data could be used to assess the suitability of a particular wax or waxes for each particular application (discussed in Chapter 2), i.e. aid in formulation for a given specification in the general sense.

RECOMMENDATIONS FOR FUTURE RESEARCH

A detailed study of the correlation between the instrumental analysis data and actual application test results would certainly be of worthwhile interest. The benefit of using an instrumental technique, such as rheometry, to characterise wax-containing final products, such as a HMA, polish or emulsion, would also be of value to the applications chemist.

A conclusive explanation of the cause of the melting bimodality observed on the DSC analysis of the high melting Fischer Tropsch waxes also requires investigation.